MICROVASCULAR FUNCTION AND REMODELING DUE TO CHRONIC CHANGES WITHIN THE SKELETAL MUSCLE MICROENVIRONMENT

ERIN R. MANDEL

A DISSERTATION SUBMITTED TO THE FACULTY OF GRADUATE STUDIES
IN PARTIAL FULFILLMENT OF THE REQUIREMENTS
FOR THE DEGREE OF DOCTOR OF PHILOSOPHY

GRADUATE PROGRAM IN
KINESIOLOGY AND HEALTH SCIENCE

YORK UNIVERSITY
TORONTO, ONTARIO
May 2016

Abstract:

The skeletal muscle microcirculation is a key regulator of local blood distribution, vascular resistance and overall blood pressure (BP). Arterioles and capillaries are two important components of the microcirculation, which can undergo remodeling such as arteriogenesis, angiogenesis, or capillary rarefaction. Vascular remodeling requires the coordinated action of several factors within the microenvironment. These include: matrix metalloproteinases (MMPs) and their endogenous inhibitors, tissue inhibitor of metalloproteinases (TIMPs), vascular endothelial growth factor-A (VEGF-A) and thrombospondin-1 (TSP-1). The objective of this dissertation was to examine how alterations to the microenvironment impacted the 'appropriate' microvascular remodeling responses to alterations in flow. The skeletal muscle microenvironment was altered through manipulation of TIMP1 expression or glucocorticoid (GC) levels. Furthermore, blood flow was altered via femoral artery (FA) ligation or prazosin treatment. This dissertation includes three primary hypotheses and corresponding findings to examine the importance of alterations to the microenvironment on microvascular remodeling. Firstly, the loss of TIMP1 would enhance both ischemia and flow-induced vascular remodeling by increasing MMP activity. Using TIMP1 deficient mice (*Timp1*$^{-/-}$), we demonstrated that TIMP1 is integral for vascular network maturation. Additionally, TIMP1 is required for microvascular adaptations to alterations in flow. This was proven by the absence of arteriogenesis and/or angiogenesis in *Timp1*$^{-/-}$ mice in response to elevations in flow despite an increase in both VEGF-A and eNOS mRNA. Secondly, Corticosterone (CORT) treatment would inhibit endothelial mediated shear stress signaling and subsequently, the microvascular remodeling responses to prazosin administration. Lastly,

CORT mediated hypertension and microcirculatory rarefaction would be prevented with 2 weeks of concurrent prazosin or Tempol (a ROS scavenger) administration. Endothelial cell responsiveness to shear stress was partially blunted by CORT pre-treatment. The lack of vascular remodeling (angiogenesis and arteriogenesis) and prevention of GC-mediated capillary rarefaction in CORT-prazosin animals supports this finding. The maintenance of vascular tone and skeletal muscle blood flow, more so then lowering circulating levels of ROS, was responsible for mitigating CORT-induced capillary rarefaction and hypertension. Taken together, these three studies demonstrate that perturbations of the microenvironment, due to the loss of TIMP1 or elevated GCs, results in impaired microvascular remodeling to alterations in flow. Furthermore, alterations to the skeletal muscle microcirculation can impact overall cardiovascular health.

Acknowledgments

I would like to express my sincere appreciation to my supervisor Dr. Tara Haas for her continuous support, guidance, help and patience throughout the course of my PhD, without which this work would not have been possible. I would also like to thank my committee members Dr. Michael Riddell and Dr. Robert Tsushima for all their help and insightful comments and suggestions. I would be remiss not to make a special mention to thank the members of the Haas Lab especially Emmanuel Nwadozi and Ghoncheh (Melanie) Abdifarkosh as well as Dr. Emily Dunford (formerly of Dr. Riddell's lab) for all of their help in running the experiments, and laughter on challenging days. Last but not least, I would like to thank my family; my grandparents (Oma, Bubie and Zaide), my parents, my sister Eliana and brother-in-law Sasha (and their adorable children) and of course my amazing husband Sendy. Without your love, encouragement and support I would not have been able to successfully complete my PhD.

Table of Contents:

List of abbreviations:

α1-AR: alpha 1 adrenergic receptor
Ang-1: Angiopoietin-1
AU: arbitrary units
BP: blood pressure
C:F: capillary-to-fiber ratio
CD: capillary density
CORT: corticosterone
CV: cardiovascular
ECM: extracellular matrix
EDL: extensor digitorum longus
eNOS: endothelial nitric oxide synthase
ERK: extracellular signal regulated kinase
ET-1: endothelin-1
FA: femoral artery
FITC: fluorescein isothiocyanate
FoxO: forkhead box O
GC: glucocorticoid
HIF: hypoxia inducible factor
HF: high fat
ICAM: intracellular adhesion molecule
LDL: low density lipoprotein
MAPK: mitogen activated protein kinase
MMP: matrix metalloproteinase
mRNA: messenger ribonucleic acid
MW: molecular weight
NADPH: nicotinamide adenine dinucleotide phosphate
NO: nitric oxide
NOX1, 2 or 3: NADPH oxidase 1, 2 or 3
ob/ob: mice homogenous for obese spontaneous mutation
PAD: peripheral artery disease
ROS: reactive oxygen species
SMA: smooth muscle actin
SS: shear stress
TA: tibialis anterior
TGFβ: transforming growth factor beta
TIMP: tissue inhibitor of metalloproteinase
Timp1$^{-/-}$: mice deficient in TIMP1
TSP-1: Thrombospondin-1
VCAM: vascular cell adhesion molecule
VEGF: vascular endothelial growth factor
VEGF-R: vascular endothelial growth factor receptor
VSMC: vascular smooth muscle cells
WT: wild-type
ZDF: Zucker diabetic fatty rat

List of Tables:

List of Figures:

Chapter 1: Literature Review

1.0: The cardiovascular system:

The mammalian cardiovascular (CV) system is a closed loop system comprised of a heart and blood vessels. CV health is integral for overall quality of life, health and longevity. The prevalence of CV disease is on the rise in Canada (Lovell et al., 2009); therefore understanding CV regulatory mechanisms is imperative for improvements to be made and vascular health to be maintained.

1.1 The vascular tree

The mammalian arterial system is a highly organized vascular system that ensures that all cells are within 100 to 200μm of oxygen and nutrients. This system is comprised of larger arteries, which subsequently branch into smaller arteries and smaller arterioles until reaching the smallest vessels, the capillaries. De-oxygenated nutrient poor blood will empty from the capillaries into venules as the venous system functions primarily to return blood back to the heart.

Each component of the arterial tree has distinct and important functions. For example, large peripheral arteries are responsible for transporting oxygenated blood away from the heart and towards organs/tissues. These vessels have a large diameter, thus blood is rapidly transported as it encounters very little resistance. Of interest in the current review are the structure, function and adaptability of the microcirculation.

1.1.1 The microcirculation

The microcirculation is defined as the segment of the circulation comprising small arteries, arterioles, capillaries and venules. The venule component of the microcirculation will not be discussed further. From here forward the term microcirculation will be used to describe arteries, arterioles and capillaries 150μm or smaller in diameter (Figure 1.1A). The microcirculation is the largest paracrine organ in the body, a key regulator of vascular homeostasis and an important contributor to disease pathology (Gutterman et al., 2016). In fact, alterations in microcirculatory function precedes overt signs of CV disease (Gutterman et al., 2016).

An important difference between arterioles and capillaries is that at the arteriolar level, one or more layers of smooth muscle cells and connective/elastic tissue (tunica media and externa) surround the endothelium, which is absent at the capillary level. Capillaries gain structural support from both pericytes and their basement membrane. While pericyte coverage is sporadic (Ribatti et al., 2011), they are nonetheless important in the maintenance of endothelial cell homeostasis (Gerhardt and Betsholtz, 2003; Haas et al., 2012) and play a role in vascular remodeling (Ribatti et al., 2011).

The endothelial layer of the microcirculation is an important factor in vascular and CV health. A key job of the endothelium is to detect and respond to alterations in shear stress, the frictional force exerted as blood flows past the endothelial surface, via mechanotransduction. Mechanotransduction is defined as the mechanisms through which a cell can detect a mechanical stimulus and convert it into chemical activity (Weinbaum et al., 2003; Chien, 2007). Within endothelial cells, there are a number of possible mechanosensors including: ion channels (Ando and Yamamoto, 2009), protein coupled

receptors (Kuchan et al., 1994), caveolae (Rizzo et al., 2003), adhesion proteins (Burridge and Chrzanowska-Wodnicka, 1996; Osawa et al., 2002; Tzima et al., 2005), the glycocalyx (Tarbell and Pahakis, 2006), primary cilia (Nauli et al., 2008) and tyrosine kinase receptors (Wang et al., 2002).

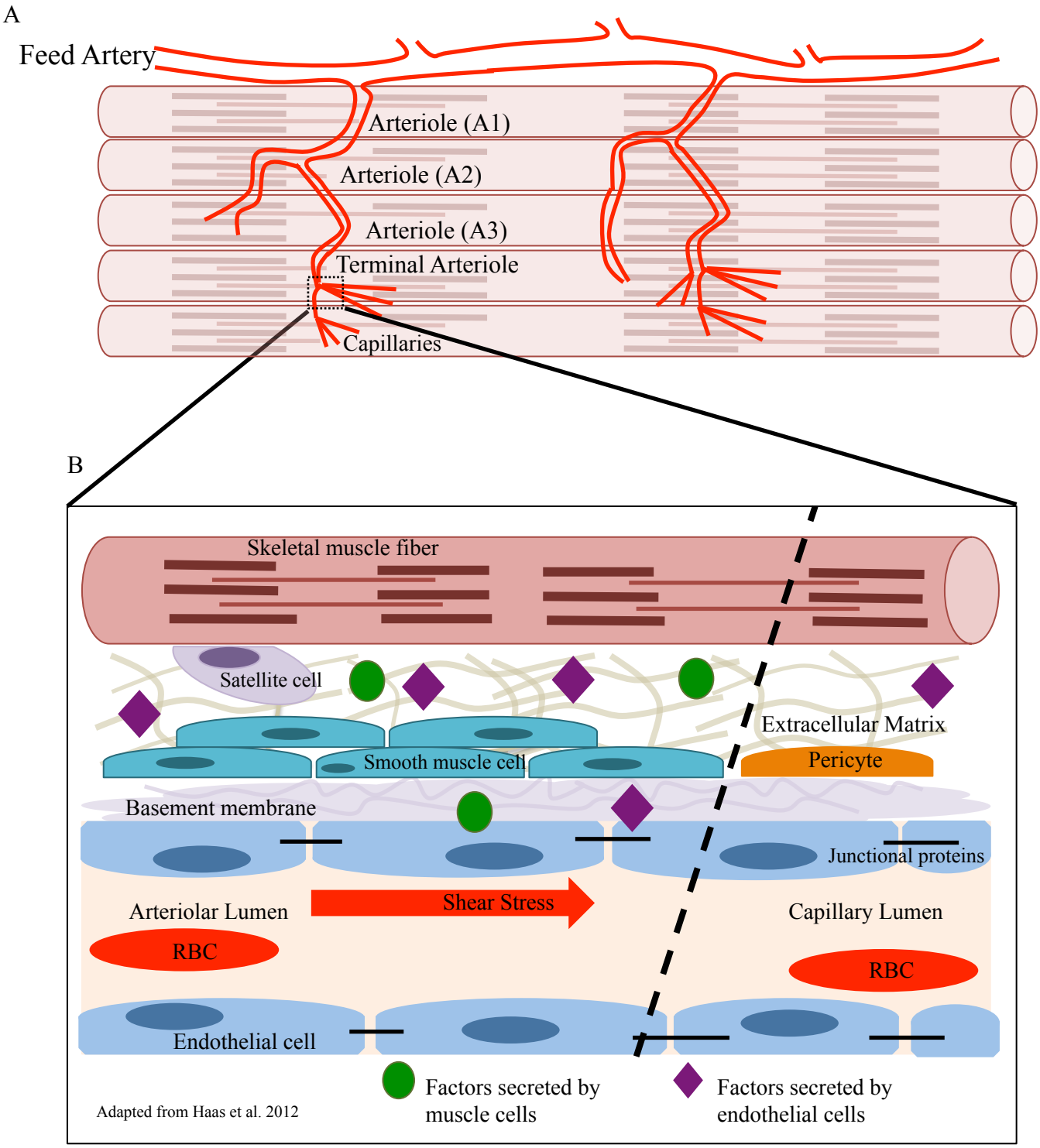

Figure 1.1: The microenvironment of the skeletal muscle microvasculature

A) Schematic representation of the skeletal muscle microcirculation. B) Closer view of the microcirculation highlighting the components of the microenvironment from the arteriolar (left side) down to the capillary (right side) level. The microenvironment consists of numerous components including: skeletal muscle cells/myocytes, smooth muscle cells, endothelial cells, pericytes, the ECM, local hemodynamics and circulating factors secreted by cells within microenvironment. All of these factors can in turn modulate changes to one or more of the cell types shown, thereby impacting vascular homeostasis and remodeling.

Once one or more mechanosensors have been activated the resulting signaling cascade modulates the expression of a variety of genes and proteins involved in the regulation of endothelial cell behavior (Chien, 2007). An alteration in blood flow/shear stress is an important stimulus for vascular remodeling. Increased blood flow elicits outward arteriolar remodeling (section 1.3.1) and splitting angiogenesis (section 1.3.2.2), whereas reduced blood flow elicits inward arterial remodeling and capillary rarefaction (1.5.1.1).

In vitro, endothelial shear stress can be simulated using a parallel plate flow chamber, which exposes a monolayer of endothelial cells to a fixed shear stress intensity (Ives et al. 1986; Milkiewicz et al. 2006). This protocol allows for the analysis of alterations in endothelial cell derived factors in response to elevated shear stress versus control cells. *In vivo* shear stress can be augmented using an $\alpha 1$ adrenergic receptor antagonist such as prazosin (for more information see section 1.5.2) (Milkiewicz et al., 2001).

The microcirculation has several important roles within skeletal muscle. One important function is the modulation of local blood flow distribution. This can be accomplished, in part, by alterations in arteriolar diameter. Diameter can be modulated by local metabolites, alterations in blood flow, temperature as well as through changes in the relative expression of vasodilatory or constriction factors (Sherwood and Kell, 2010). Additionally, capillaries play an important role in blood flow distribution due primarily to their orientation and proximity to cells. Within skeletal muscle, capillaries are oriented along the length of a muscle fiber and all cells are within 0.01cm of a capillary. These features enable easy diffusion, from the capillary to underlying tissue, thereby providing

the local microenvironment with access to oxygen and nutrients (Potter and Groom, 1983).

Another important function of the microcirculation is as a regulator of vascular resistance and blood pressure. This is due in part to the small size and large proportion of arterioles; the body contains over half a million arterioles. These features enable arterioles to offer a large amount of blood flow resistance (Mulvany and Aalkjaer, 1990; Gutterman et al., 2016). As well, the capillary network impacts vascular resistance, as seen by the finding that reductions in capillary number increases peripheral resistance and blood pressure (Greene et al., 1989; Humar et al., 2009). Additionally the microcirculation functions as a regulator of metabolic status. This was recently demonstrated by the finding that greater skeletal muscle capillary content corresponds with improved insulin sensitivity and glucose clearance (Akerstrom et al., 2014).

1.2 The cellular microenvironment

The cellular microenvironment is defined as factors that can affect the conditions surrounding a cell or group of cells thus altering their behavior, structure and/or function (Barthes et al., 2014). This encompasses the basement membrane, extracellular matrix (ECM), surrounding cells, cytokines, hormones or other bioactive agents and mechanical forces such as blood flow (Barthes et al., 2014). The current review is focused on the microenvironment of the skeletal muscle microcirculation, which is comprised of endothelial cells, basement membrane, ECM, pericytes, smooth muscle cells, skeletal muscle fibers, satellite cells, and factors secreted from all of the above mentioned cell types (Figure 1.1B). Additionally, trans-membrane proteins such as integrins are

important factors that aid in communication within the microenvironment (Chen et al., 1999).

The basement membrane is an important component of the microenvironment; the basement membrane is primarily comprised of type IV collagen and laminin. The basement membrane contains pro and anti-remodeling factors such as vascular endothelial growth factor (VEGF) and thrombospondin-1 (TSP-1) as well as pericytes at the capillary level (Hansen-Smith et al., 1996). Cellular survival is largely dependent on cell adhesion to the basement membrane. However, appropriate degradation and remodeling of the basement membrane and ECM occurs during vascular remodeling (Tronc et al., 2000; Pepper, 2001; Kuzuya and Iguchi, 2003; Haas, 2005; Haas et al., 2007) (see section 1.4.3).

The different cell types within the microenvironment must communicate with one another to ensure a normal and healthy microvasculature. For example, endothelial cells communicate with smooth muscle cells to help maintain vascular smooth muscle cells in a differentiated/contractile phenotype, a requisite for a mature, healthy and functional artery or arteriole (Powell et al., 1996; Powell et al., 1997). Furthermore, communication between skeletal myocytes and endothelial cells is important for microvascular homeostasis and remodeling, likely due to the cross talk with factors such as VEGF and nitric oxide (NO) (Uchida et al., 2015).

1.3: Microvascular Remodeling

Alterations to the microenvironment will profoundly impact the microvasculature, which is not a static structure and has the ability to adapt over time. There are three kinds of vascular remodeling; vasculogenesis, angiogenesis and arteriogenesis. Vasculogenesis is the embryonic development and formation of blood vessels (Risau and Flamme, 1995; Carmeliet, 2000), and will not be discussed further. Postnatal remodeling traditionally occurs via arteriogenesis and/or angiogenesis. Arteriogenesis is defined as the outward remodeling of an artery, and angiogenesis refers to growth of new capillaries from pre-existing ones. Arteriogenesis and/or angiogenesis can occur as a result of various stimuli such as muscle stretch or altered flow/shear stress (Zhou et al., 1998; Rivilis et al., 2002; Haas et al., 2007). This review will focus on arteriogenesis and angiogenesis within skeletal muscle.

1.3.1: Arteriogenesis of arterioles

Arteriogenesis was first identified by doctors Fulton and Baroldi in the late 1960s within the coronary circulation. Using post mortem angiograms scientists found that collateral artery remodeling allowed blood to bypass an occluded vessel thereby avoiding an infarction (Schaper, 2009). Alternatively, some define arteriogenesis as the arterialization of an existing local capillary bed, which is termed "de novo arteriogenesis" (Mac Gabhann and Peirce, 2010). Of interest in the present review is flow-mediated remodeling of existing arterioles (Figure 1.2).

Initially, elevations in blood flow will result in endothelial derived production and release of vasodilators culminating in vasodilation within small muscular arterioles. Continued elevations in shear stress will elicit outward arterial remodeling (Tronc et al.,

1996). However, flow-mediated remodeling triggers a negative feedback loop (Schaper, 2009); thus while augmented shear stress is a potent stimulus for collateralization, it is a self-limiting process. Shear stress is inversely related to arterial radius to the fourth power. Therefore as the artery remodels to a larger diameter, the magnitude of the shear stress is minimized and will no longer be a strong stimulus for continued remodeling (Schaper, 2009).

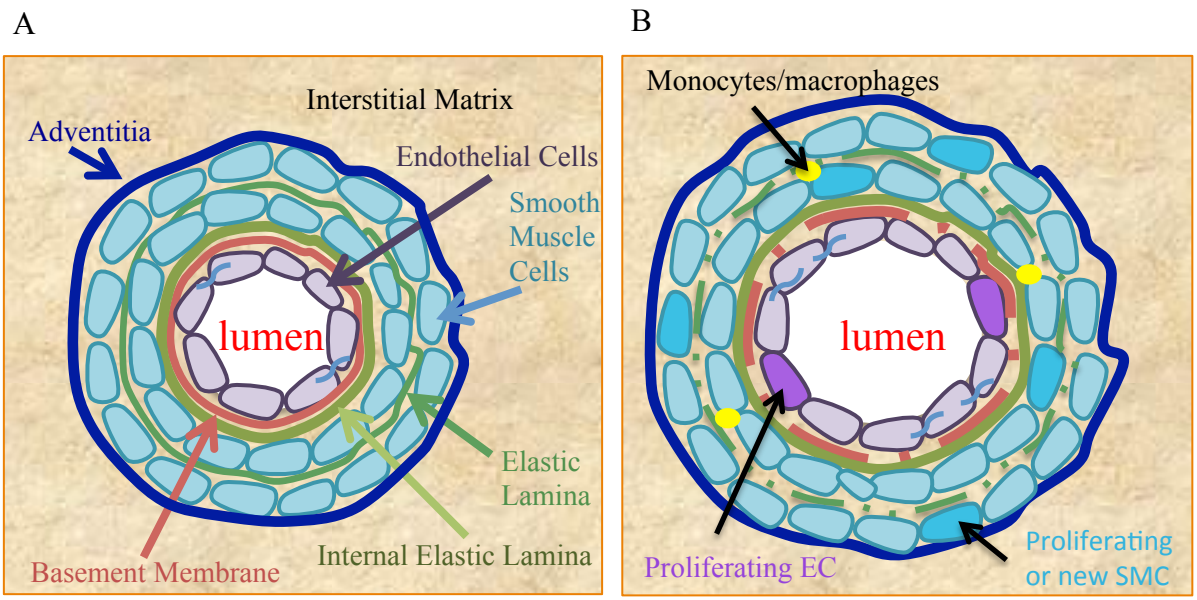

Figure 1.2: Structure and composition of an arteriole pre and post arteriogenesis

A) A quiescent arteriole characterized by a monolayer of endothelial cells surrounded by one or more layer(s) of smooth muscle cells. Muscle layers are separated from one another by elastic lamina and finally by the adventitia. B) Schematic of an arteriole post outward remodeling. The remodeling of an arteriole to a larger diameter is due to the proliferation of endothelial and smooth muscle cells.

Arteriolargenesis is commonly studied using ligation models, which blocks flow through conduit arteries thereby generating high flow conditions within neighboring collateral arterioles. As well, prazosin treatment can be used as a tool to increase skeletal muscle blood flow and study arteriogenesis within small muscular arterioles. Attention must be paid to the vessel(s) under investigation.

Under physiological conditions skeletal muscle arterioles are continuously exposed to normal flow and pressure. Conversely, collateral vessels are arteriole-arteriole anastomoses that form an alternate flow route and eventually reconnect with large adjacent conduit arteries. Under basal conditions collateral arterioles are very small in diameter and experience minimal blood flow and pressure (Helisch and Schaper, 2003). Differences exist between the impact of alterations in blood flow within skeletal muscle arterioles as compared to collateral arterioles. In response to augmented flow, skeletal muscle arterioles will experience an increase in shear stress, which will not damage the vessel. However, post ligation, collateral arterioles experience sudden large increases in blood flow and pressure, which may elicit damage and induce an inflammatory response (Tuttle et al., 2001; Tang et al., 2005; Buschmann et al., 2003). Therefore, it is preferable to specify the region and/or vessels under investigation when discussing arteriogenesis.

Arteriolar remodeling occurs through the following stages; ECM degradation, cell proliferation and migration (Heilmann, 2002; Fung and Helisch, 2012). These processes will allow small pre-existing arterioles to expand into larger, albeit still small, arterioles (Figure 1.2A & B).

The first stage, from 0 to 24 hours of high flow, is dominated by the activation of transcription factors, growth factors and other cytokines responsible for arteriogenesis.

The second stage, from 1 to 3 days post onset of high flow, is predominantly characterized by endothelial and smooth muscle cells reentering the cell cycle and undergoing proliferation (Heilmann, 2002). During the second stage and throughout the entire remodeling process, there is tightly regulated and controlled ECM breakdown via proteases, which also aids in ECM release of growth factors. Binding of these growth factors to their cell surface receptors promotes cell proliferation and migration (Lindner and Reidy, 1993). For example, the breakdown of the ECM of vascular smooth muscle cells allows for continued smooth muscle cell activation and proliferation (Arras et al., 1998). Subsequently, the vessel will enter the synthetic phase, so named for the high level of protein synthesis; this phase typically takes place from day 3 to 14 post high-flow onset. At the beginning of this stage, proliferation is still high, waning around day 7 (Couffinhal et al., 1998), and between days 10 to 14 vascular smooth muscle cells regain their contractile phenotype (Arras et al., 1998). The final phase, maturation phase, is from day 14 onward. During this phase the newly enlarged vessel begins to stabilize (Scholz et al. 2000) and smooth muscle cells continue to regain their contractile phenotype (Arras et al., 1998). The newly enlarged vessel (Figure 1.2B) is now able to transport larger volumes of blood to distal tissue. Outward arteriolar remodeling is dependent on the actions of several pro-remodeling factors including: VEGF (Chalothorn et al., 2007), placental growth factor (Pipp et al., 2003), matrix metalloproteinases (MMP) (Haas et al., 2007) and transforming growth factor-beta (TGF-β) (van Royen et al., 2002) (discussed in section 1.4).

1.3.2: Angiogenesis

Angiogenesis (Figure 1.3) is a tightly regulated process that once complete augments local tissue perfusion. It has now been well established that within adult tissue angiogenesis is seen in response to tissue growth/repair and within the female reproductive tract. Aberrant and/or excessive angiogenesis is seen in several diseases including diabetic retinopathy, cancer and rheumatoid arthritis (Folkman, 1971; Holmes and Zachary, 2005; Adair and Montani, 2011; Wang et al., 2012). Additionally, impaired or insufficient angiogenesis is a known complication of diseases including diabetes (Martin et al., 2003) and peripheral artery disease (PAD) (Haas et al., 2012). Additionally, scientists have attempted to utilize angiogenic therapies to improve the outcome of several pathologies including myocardial infarction and PAD (Adair and Montani, 2011).

Angiogenesis was first described in the late 1700s by John Hunter (Skalak, 2005). Fifty years after (mid 1800s) the initial discovery by Hunter, Meyer described the sprouting of new vessels from pre-existing vessels (Skalak, 2005). Moving forward to the early 1900s, Clark first described flow-induced microvessel remodeling, within the tadpole tail. As reviewed by Skalak (2005), the work of Dr. Folkman spearheaded our understanding of the role of angiogenesis in cancer progression. Furthermore, Dr. Hudlicka pioneered the field of skeletal muscle microvascular remodeling (Skalak, 2005).

Both sprouting and splitting angiogenesis will be discussed in greater detail, as they are the two main forms of angiogenesis within adult tissue (Figure 1.3B & C).

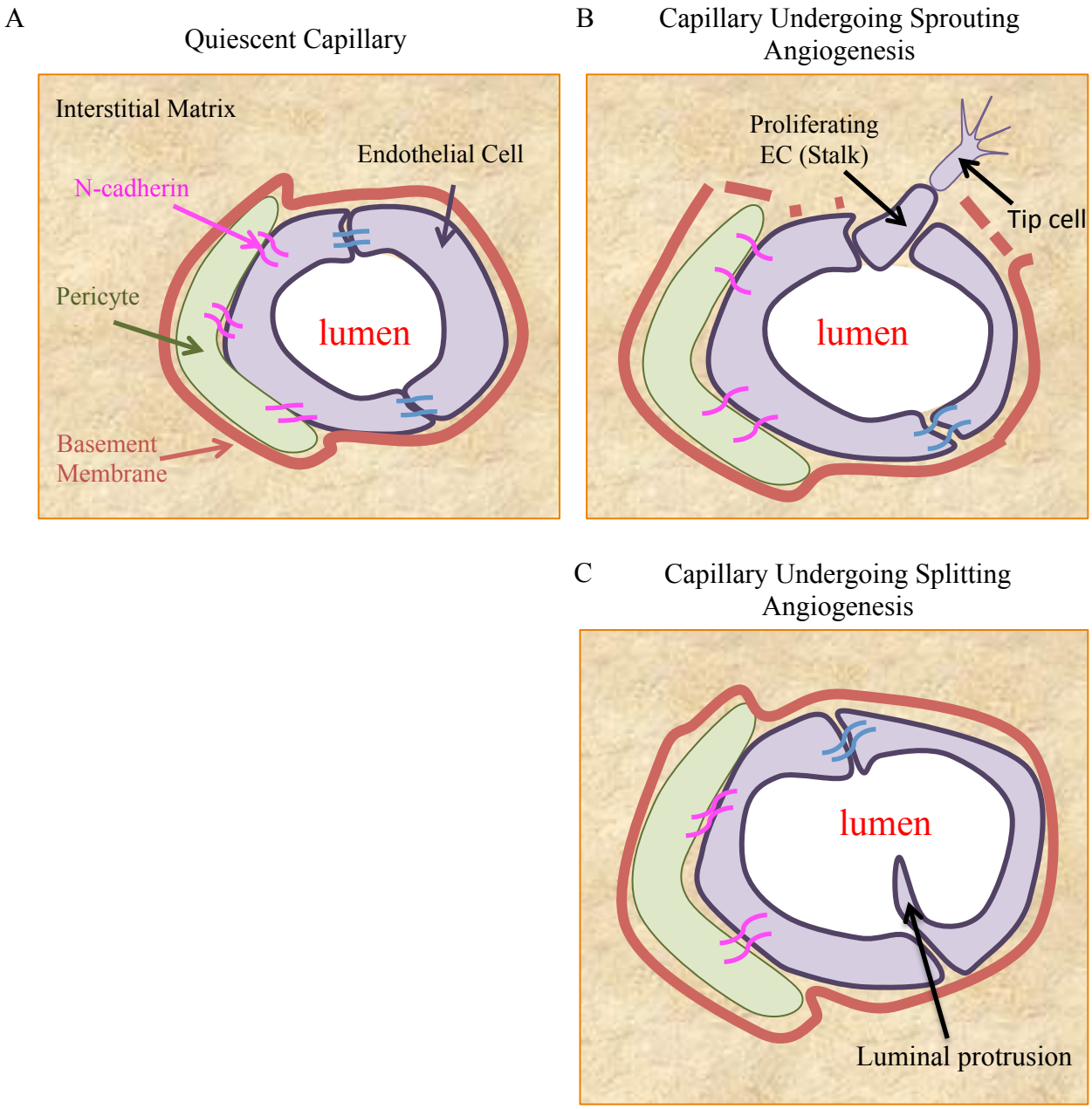

Figure 1.3: Structure and composition of a skeletal muscle capillary pre and post angiogenesis

A) Schematic representation of the composition of a normal capillary, as characterized by quiescent endothelial cell(s) connected by junctional proteins such as VE-Cadherin. The endothelial cells are surrounded by a basement membrane within which the pericyte(s) are located.
B) Schematic representation of a capillary undergoing sprouting angiogenesis. This form of angiogenesis is characterized by basement membrane degradation as well as by stalk/ proliferating endothelial cells and tip/migratory cells.
C) Schematic representation of vessels undergoing splitting angiogenesis. This form of angiogenesis is characterized by the presence of luminal protrusions.

1.3.2.1: Sprouting angiogenesis

Sprouting angiogenesis is defined as the budding of endothelial cells from the abluminal side of the capillary to form a new capillary (See figure 1.3B). This new "bud" will eventually result in the connection of two existing capillaries. Sprouting angiogenesis occurs through the following stages: endothelial cell activation, proliferation, proteolysis of the basement membrane, migration and formation of a new capillary with an intact basement membrane (Pepper, 1997).

Endothelial cell activation is the alteration in morphology from a quiescent phenotype to one ready to undergo proliferation; proliferation refers to the increase in endothelial cell number. Proteolysis of the endothelial cell basement membrane is due to proteases such as MMPs (Haas 2002) allowing endothelial cells to pass through the basement membrane and migrate. Lastly, the formation of a stable new capillary is aided by the return of endothelial cell pericyte coverage (Egginton et al. 2000). Sprouting angiogenesis is thought to be the primary form of angiogenesis seen in response to exercise training (Haas, 2002; Roudier et al., 2009; Slopack et al., 2014), muscle stretch (Egginton et al., 1998; Milkiewicz et al., 2007; Gorman et al., 2014) and potentially hypoxia (Deveci et al., 2001).

Asides from exercising an animal, stretch induced angiogenesis can be examined *in vivo* by extirpating an agonist muscle, such as the tibialis anterior (TA). This in turn exposes the extensor digitorum longus (EDL) muscle to overload induced muscle stretch which culminates in angiogenesis (Egginton et al., 1998; Milkiewicz et al., 2007; Gorman et al., 2014). Sprouting angiogenesis is mediated by several pro-remodeling factors including VEGF, MMPs (Rivilis et al., 2002) and hypoxia inducible factor (HIF)

(Milkiewicz et al., 2007). Sprouting angiogenesis is a rapid process in rodents, with increases in C:F evident after as little as 7 days of muscle overload (Gorman et al., 2014) or two weeks of treadmill training (Slopack et al., 2014).

1.3.2.2: Splitting angiogenesis

Splitting angiogenesis is the division of an existing "parent" capillary into two "daughter" vessels (Figure 1.3C) (Egginton and Gerritsen, 2003). This form of angiogenesis is known to occur in response to sustained elevations in blood flow/shear stress (see review Hudlicka & Brown 2009). Sustained elevation in shear stress stimulates an endothelial filiform-like process which transverses the "parent" capillary (Figure 1.3C), to create two "daughter" vessels. Rodents treated with prazosin (50mg/L) will undergo splitting angiogenesis within 7 to 14 days (Ziada et al., 1989; Zhou et al., 1998; Milkiewicz et al., 2006; Milkiewicz et al., 2007).

Splitting angiogenesis requires the coordinated alteration in multiple factors. Splitting angiogenesis is known to elicit an increase in VEGF-A expression (Milkiewicz et al., 2007) and activity of MAPKs JNK and p38 (Uchida et al., 2008; Gee et al., 2010). There is no change in MMP activity with shear stress induced angiogenesis (Milkiewicz et al., 2006), which is linked with the apparent lack of basement membrane degradation (Egginton et al., 2001). Additionally, shear stress induces an increase in ETS-1 expression through ERK1/2 dependent signaling (Milkiewicz et al., 2008). Elevated ETS-1 expression contributes to shear stress dependent increases in the expression of protease inhibitors. The shear induced increase in plasminogen activator inhibitor-1 and tissue inhibitor of metalloproteinase (TIMP) 1 and 3 in response to elevated shear stress is thought to be an important contributor to the lack of migration and proliferation seen with

splitting angiogenesis (Milkiewicz et al., 2008). Prazosin cannot exert its pro-angiogenic effects in eNOS deficient mice or mice concurrently treated with a NO inhibitor, which highlights the importance of NO in shear stress induced angiogenesis (Williams et al. 2006).

1.3.2.3: Comparison of splitting and sprouting angiogenesis

There are several notable differences between splitting and sprouting angiogenesis; splitting angiogenesis is thought to have several advantages over sprouting angiogenesis. Computational modeling has suggested greater improvement of tissue oxygenation with splitting angiogenesis (Ji et al., 2006). As well, splitting angiogenesis is more energy efficient than sprouting angiogenesis because splitting angiogenesis does not require endothelial cell proliferation, basement membrane degradation or endothelial cell migration (Egginton et al., 2001). While the balance between pro and anti angiogenic factors as well as between proteases and their inhibitors is essential for both forms of angiogenesis (Bode et al., 1999; Olfert and Birot, 2011), there are several notable differences. Both splitting and sprouting angiogenesis are associated with increased VEGF expression (Milkiewicz et al., 2001; Rivilis et al., 2002; Milkiewicz et al., 2007), however only sprouting angiogenesis is associated with increased MMP activity (Rivilis et al., 2002). As well, HIF-1α, which has been shown to be important for sprouting angiogenesis, is not required for splitting angiogenesis (Milkiewicz et al., 2007). Alterations in other growth factors will be discussed in greater detail below (see section 1.4).

Although the pericytes will not be discussed in further detail, it is worthy to mention that pericytes play a role in the regulation of angiogenesis (Egginton et al.,

2000). Pericytes have been proposed to have a role in sensing an angiogenic stimulus (Gerhardt and Betsholtz, 2003). As well, research has suggested that pericytes aid in ECM production or degradation, regulate endothelial cell proliferation and/or differentiation and play a role in endothelial cell-cell signaling (Gerhardt and Betsholtz, 2003).

1.4: Factors associated with vascular remodeling

The microvasculature responds to changes within its local microenvironment, such as alterations in blood flow, muscle stretch or hypoxia via the modulation of pro-remodeling and anti-remodeling factors (Pepper, 2001). This tight regulation of the microenvironment is required for the appropriate amount of microvascular remodeling to occur. A few key regulators secreted by one or more cell types within the microenvironment, which are known to be relevant to vascular remodeling, will be discussed below in more detail.

1.4.1: Vascular endothelial growth factor

VEGF is one of the thoroughly researched pro-angiogenic factors. Although first discovered under the name vascular permeability factor (Senger et al., 1983), the name VEGF was established shortly thereafter (Ferrara and Henzel, 1989) and became the commonly used name.

It is now known that there are 7 members of the VEGF family: VEGF-A, B, C, D, E, F and placental growth factor (Hoeben et al., 2004). VEGF-A is best described for its pro-angiogenic functions, therefore it will be the focus in the current review. For the remainder of this dissertation the term VEGF will refer to VEGF-A. VEGF-A can undergo exon splicing to create multiple splice variants. In humans, this results in the

production of VEGF-A121, 145, 165, 183, 189 and 206. Mouse splice variants retain the same functional and biological functions, however they are 1 amino acid smaller (Vempati et al., 2014). These variants all contains exons 1 to 5 and 8, the splicing takes place on exons 6 and 7 (Holmes and Zachary, 2005). There are several differences between the different VEGF-A isoforms. For example, VEGF-A isoform 121 is soluble and easily diffusible, while 165 contains both soluble and cell bound properties (Dehghanian et al., 2014). The ECM attachment of the larger isoforms of VEGF is due to heparin binding (Houck et al., 1992). Proteases, such as MMPs or plasmin, cleave matrix bound VEGF isoforms and release soluble fragments that are able to exert pro-angiogenic effects (Lee et al., 2005).

Since its initial discovery, a substantial amount of research has been geared towards understanding the important role(s) of VEGF. VEGF is indispensible for vascular development and survival; animal studies have proven this point by demonstrating that global VEGF deletion in mice is embryonically lethal (Carmeliet et al., 1996; Ferrara et al., 1996). VEGF is well known for its ability to increase permeability, cell proliferation, migration and survival (Ferrara, 2004) making VEGF integral for post-natal angiogenesis (Milkiewicz et al., 2001; Williams et al., 2006; Uchida et al., 2015). Williams and colleagues demonstrated that both prazosin and stretch induced angiogenesis are abrogated by preventing the actions of VEGF via the VEGF-Trap (Williams et al. 2006). Additionally, recent work by Haas and colleagues demonstrated that a significant decrease in VEGF within the skeletal muscle microenvironment abolishes prazosin-induced angiogenesis (Uchida et al., 2015). Taken

together these studies demonstrate that VEGF is important for prenatal vascular growth and development as well as postnatal remodeling.

For VEGF to exert its pro-angiogenic effects it must bind to one of its cell surface receptors. To date, three VEGF tyrosine kinase receptors (VEGF-R) have been identified: fms-like tyrosine kinase-1 or VEGF-R1, fetal liver kinase-1 or VEGF-R2 and fms-like tyrosine kinase-4 or VEGF-R3 (Ortega et al., 1999). VEGF-R3 is predominantly located within lymphatic endothelial cells (Holmes and Zachary, 2005) and thus will not be discussed further. VEGF-R1 and VEGF-R2 are both predominantly expressed on vascular endothelial cells (Quinn et al., 1993; Neufeld et al., 1999; Ferrara et al., 2003) and to a lesser extent on smooth muscle cells (Ortega et al., 1999; Ishida et al., 2001). VEGF-R1 and R2 and are known to be integral for VEGF mediated angiogenesis (Ferrara et al., 2003). These two receptors were discovered in the early 1990's by de Vries and Terman respectively (de Vries et al., 1992; Terman et al., 1992). Interestingly, VEGF has a greater affinity for VEGF-R1 than VEGF-R2 (Terman et al., 1992; Quinn et al., 1993). However, it is VEGF binding to VEGF-R2 that triggers an angiogenic response (Ferrara, 2004). Within endothelial cells, VEGF-R1 is known to be weakly phosphorylated which suggests that this receptor acts as a "decoy" receptor, to prevent angiogenic signaling through VEGF-R2 (Lee et al., 2007) (Figure 1.4).

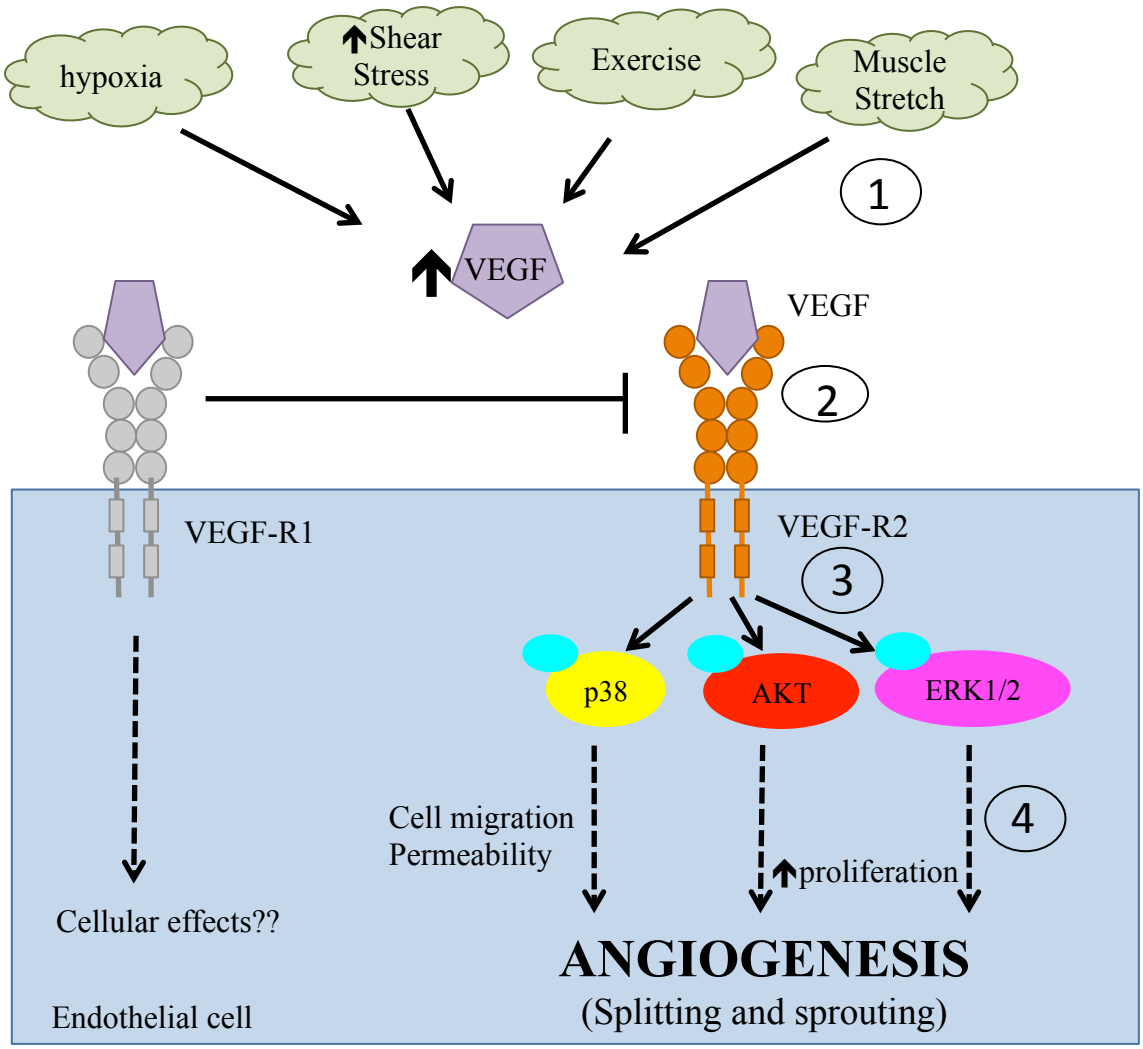

Figure 1.4: Schematic representation of endothelial cell VEGF signaling

Schematic representation of endothelial VEGF signaling. 1) VEGF levels can be increased due to a variety of stimuli including hypoxia, augmented shear stress, exercise and muscle stretch. 2)This increase in VEGF will increase VEGF binding to VEGF-R1 and R2. Binding to VEGF-R1 is thought to reduce binding to VEGF-R2, furthermore the cellular actions of VEGF binding to VEGF-R1 are not well characterized. Binding of VEGF to VEGF-R2 will elicit receptor dimerization. 3) Receptor autophosphorylation is required for the subsequent activation of pro-survival and pro-angiogenic factors. This will, for example, elicit the phosphorylation of p38. AKT and ERK1/2. 4) Activation of theses, and other pro-survival and pro-angiogenic factors, will augment cell survival and angiogenesis through several actions including increased cell adhesion, alterations in permeability and proliferation.

Binding of VEGF to VEGF-R2 will induce receptor dimerization (Mac Gabhann and Popel, 2007) (Figure 1.4), which is accompanied by autophosphorylation of several tyrosine resides (Wu, 2000). Receptor dimerization is required for its activation (Mac Gabhann and Popel, 2007), while autophosphorylation allows for the activation of downstream signaling pathways (Olsson et al., 2006). VEGF activation and signaling is complex and thus in the present review only a few downstream factors will be discussed (Figure 1.4). Autophosphorylation of Tyr1175 will result in activation of the ERK pathway (Arsham et al., 2002), which is known to be important for a variety of pro-remodeling actions including proliferation, transcription and cell adhesion (Roskoski, 2012). Furthermore, a common downstream target of VEGF binding to VEGF-R2 is the activation of Akt (Byzova et al., 2000). Akt activation/phosphorylation can play a role in a variety of functions integral for angiogenesis including cell growth and proliferation (Manning and Cantley, 2007). As well, the MAPK p38, is a downstream target activated by VEGF binding toVEGF-R2 (Olsson et al., 2006; Lamalice et al., 2007; Gee et al., 2010). Furthermore, p38 is required for splitting angiogenesis (Gee et al., 2010) and exerts several pro-angiogenic functions including cellular migration via stress fiber formation (Lamalice et al., 2007) and increased vascular permeability (Olsson et al., 2006).

Within the skeletal muscle microcirculation, VEGF expression is known to be increased in response to a variety of stimuli: exercise (Gustafsson et al., 2001), muscle overload (Rivilis et al. 2002; Williams et al. 2006), elevated shear stress (Milkiewicz et al., 2001; Rivilis et al., 2002) and hypoxia (Forsythe et al., 1996; Brown et al., 2003;

Breen et al., 2008). Below, hypoxia and shear stress stimuli will be discussed in greater detail.

Hypoxia is a potent stimulus for increased VEGF expression (Breen et al., 2008). The VEGF gene contains a hypoxic response element within its promoter region to which HIF1α and HIF1β bind, allowing for increased VEGF transcription (Forsythe et al., 1996). Briefly, HIF1α is rapidly degraded under normoxic conditions but becomes stabilized under hypoxic conditions (Kallio et al., 1999). Additionally, hypoxia will result in the generation of reactive oxygen species (ROS) as well as MMP9, both of which will increase VEGF mRNA (Arbiser et al., 2002). It is through these signaling pathways that hypoxia is thought to alter the microvascular microenvironment and create a pro-angiogenic environment subsequently resulting in capillary growth (Breen et al., 2008). Augmented blood flow or shear stress induces an increase in VEGF (Milkiewicz et al. 2001; Williams et al. 2006), which occurs alongside an increase in NO (Milkiewicz et al., 2001). NO, a potent vasodilator, is important in VEGF signaling (Papapetropoulos et al., 1997). Augmented VEGF-A expression in response to hypoxia or increased flow is integral for the maintenance of vascular health and/or remodeling.

Elevated VEGF levels are integral for the process of vascular remodeling. Research has shown that the peak increase in VEGF precedes the increase in C:F (Rivilis et al., 2002; Milkiewicz et al., 2007). VEGF mRNA and protein analyzed from whole muscle lysates post prazosin treatment revealed that the increase in VEGF was seen after 2 days while no increase in C:F is seen till day 7 (Rivilis et al., 2002). In response to muscle stretch, a tool used to elicit and examine sprouting angiogenesis, VEGF

expression is increased by day 7 but no increase in C:F is seen until day 14 (Milkiewicz et al., 2007).

Within the microenvironment of the microcirculation, VEGF can be produced by several different cell types including: myocytes, vascular smooth muscle cells, endothelial cells, or pericytes (Milkiewicz et al., 2001; Darland et al., 2003). Alterations in VEGF production, from one or more of the above cell types, will impact the microenvironment and subsequently microcirculatory health and function. In recent years researchers have been interested in uncovering which cell type or types within the microenvironment is/are primarily responsible for VEGF production required for vascular remodeling. This was explored using inducible models of endothelial or smooth muscle cell specific VEGF deletion. Interestingly, recent studies have suggested that it is skeletal muscle cell derived VEGF (Olfert et al., 2010; Delavar et al., 2014; Uchida et al., 2015) and not endothelial derived VEGF (Lee et al., 2007) that is responsible for both sprouting and splitting angiogenesis (Olfert et al., 2010; Delavar et al., 2014; Uchida et al., 2015). Endothelial cells will detect alterations in flow and respond by increasing NO production and secretion, which will subsequently stimulate myocyte production and release of VEGF. In turn, myocyte derived VEGF will be secreted into the microenvironment, stimulate endothelial cells finally resulting in angiogenesis (Uchida et al., 2015). These findings highlight the complexity of cellular communication within the microenvironment regulating vascular remodeling.

VEGF also plays a role in other forms of vascular remodeling including arteriogenesis and capillary rarefaction. Arteriogenesis requires VEGF as shown by the fact that the lower levels of VEGF in BalB/c mice is responsible for their decreased

collateralization, as compared to C57Bl/6 mice which have higher VEGF levels (Chalothorn et al., 2007). Additionally, VEGF-R antagonism will inhibit collateral vessel arteriogenesis (Lloyd et al., 2005), and newly formed/remodeled vessels will not mature and will be pruned away if VEGF levels are low (Hanahan, 1997). Some reports have shown that capillary regression is the result of a decrease in VEGF (Bey et al., 2003) or VEGF-R2 (Wagatsuma, 2008; Roudier et al., 2010) protein levels. Taken together these studies highlight the importance of VEGF in multiple different forms of skeletal muscle microvascular remodeling.

1.4.2: Thrombospondin-1

TSP-1 is a large matrix glycoprotein (MW 450kDa), which was first isolated from the human placenta in a study concluded in 1978 (Lawler et al., 1978). Within 10 to 12 years of its initial discovery, TSP-1 was the first protein to be classified as an endogenous inhibitor of angiogenesis (Good et al., 1990). While TSP-1 is not the only anti-angiogenic factor, it remains the most commonly investigated one (Malek and Olfert, 2009). Within the microenvironment TSP-1 can be produced by vascular smooth muscle, endothelial cells and is found within the extracellular matrix of skeletal muscle (Mosher, 1990). TSP-1 has been shown to inhibit angiogenesis as well as modulate endothelial cell survival through VEGF-dependent and independent mechanisms.

TSP-1 can inhibit angiogenesis by altering VEGF-A expression and/or actions. This can occur by TSP-1 directed inhibition of proteolytic enzymes (Hogg, 1994) such as MMPs, thus minimizing VEGF release from the ECM (Lee et al., 2005). As well, TSP-1 can bind directly to VEGF, thereby controlling VEGF removal from the microenvironment and limiting its pro-angiogenic actions (Greenaway et al., 2007). TSP-

1 can bind and activate the cell surface receptor CD36, which subsequently reduces VEGF-A function by altering VEGF-R2 and/or p38 MAPK phosphorylation (Primo et al., 2005). Furthermore, TSP-1 can counter regulate the pro-angiogenic actions of VEGF-A through activation of FAS ligand, a pro-apoptotic cytokine (Yano et al., 2003). Taken together, these studies highlight the roles of TSP-1 in inhibiting VEGF-A expression and function within the microenvironment.

TSP-1 can inhibit angiogenesis independently of VEGF. TSP-1 can inhibit cell cycle progression through interactions with CD36, resulting in cell arrest at the G_0/G_1 phase (Armstrong et al., 2002) and thus decreasing endothelial cell proliferation (Bagavandoss and Wilks, 1990). TSP-1 may impair cell cycle progression via reduced Akt expression/activation (Oganesian et al., 2008), which could reduce several types of microvascular remodeling that are dependent on cell proliferation (arteriogenesis, sprouting angiogenesis). TSP-1 can also decrease cell adhesion (Murphy-Ullrich and Höök, 1989) and endothelial cell migration, through the cell surface receptor CD36 (Simantov and Silverstein, 2003). Furthermore, TSP-1 has been shown to directly block the pro-angiogenic actions of NO, through interactions with CD36 or CD47 (Roberts et al., 2007). TSP-1 may be inhibiting the pro-angiogenic actions of NO through myristic acid (Isenberg et al., 2007), a fatty acid thought to be important for nitric oxide synthase (NOS) activation and therefore NO signaling (Zhu and Smart, 2005). TSP-1 has been shown to play a role in regulating endothelial cell apoptosis, independent of VEGF signaling (Jiménez et al., 2000). These pro-apoptotic effects are thought to occur through alterations in c-Jun N terminal kinase, commonly referred to as JNK, expression (Jiménez et al., 2001). TSP-1 can also mediate apoptosis via increasing Bax, an apoptosis

promoter, expression while concurrently reducing Bcl-2, a apoptosis inhibitor, expression (Nör et al., 2000). The anti-angiogenic and pro-apoptotic functions of TSP-1 has generated interest in using TSP-1 therapies as a treatment option for various types of cancers (Zhang and Lawler, 2007).

Alterations in TSP-1 expression are linked with changes in vascularity. Increased TSP-1 expression is seen in type I diabetes (Kivelä et al., 2006), PAD (Roudier et al., 2013) and with elevated GCs (Logie et al., 2010), all of which are associated with reduced vascularity. As well, TSP-1 null mice have been shown to have increased skeletal muscle capillarization, as compared to wild-type (WT) controls (Malek and Olfert, 2009). The contrasting pro and anti-angiogenic roles of VEGF and TSP-1 are summarized in Figure 1.5.

VEGF-A	**TSP1**
Increase C:F	Decrease C:F
Cell survival and proliferation - Activation of Akt	Cell apoptosis - Inhibition of Akt
Increase nitric oxide	Reduced nitric oxide
Activation of MMP2 and 9	Inhibition of MMP9

Figure 1.5: Summary of the effects of VEGF-A and TSP-1 on the microvasculature

VEGF-A is the most commonly examined pro-angiogenic and arteriogenic factor. VEGF-A can exert a variety of pro-survival and remodeling actions within the microenvironment. Conversely, TSP-1 is the best-characterized anti-angiogenic factor, known to impede remodeling and cell survival. (See text for complete details and references)

1.4.3: Matrix Metalloproteinases and tissue inhibitor of metalloproteinases

The MMP family consists of over 20 zinc and calcium-dependent proteases. MMPs were first described to be involved in the process of basement membrane degradation in the early 1980s (Kalebic et al., 1983). It is now known that MMPs are secreted as latent enzymes (pro-MMPs), which are activated by the cleavage of their amino terminal pro-peptide. MMPs are classified as matrilysins, collagenases, stromelysins, membrane type and gelatinases. Overall, MMPs are important for endothelial cell attachment, migration, invasion, proliferation and apoptosis (Haas 2002). This review will specifically focus on gelatinases, MMP2 and MMP9, which have been found to be especially important for vascular remodeling.

MMPs are produced by a variety of cells within the microenvironment of the microcirculation including endothelial cells (Haas et al. 1998), smooth muscle cells (Shofuda et al. 2001) and monocytes/macrophages (Haug et al., 2004). Additionally, other pro-remodeling factors, including NO (Wang et al., 2004) and ERK 1/2 (Boyd et al., 2005) can regulate MMP2 levels.

Correct alteration in MMP expression and activity are important for various forms of vascular remodeling. Increased expression and activity of MMPs is a requisite for sprouting angiogenesis (Haas et al., 2000; Rivilis et al., 2002) allowing for basement membrane degradation (Pepper, 2001). Additionally, increased MMP activity will permit the release of ECM anchored VEGF (Haas, 2002) and other growth factors such as basic fibroblast growth factor (Pepper, 2001). The importance of MMPs in sprouting angiogenesis was validated by the finding that GM6001 administration, a broad spectrum MMP inhibitor, prevented muscle stimulation mediated angiogenesis (Haas et al., 2000).

Conversely, with splitting angiogenesis MMP2 expression and activity is not upregulated by augmented shear stress (Rivilis et al., 2002) due in part to the shear stress induced increase in NO (Milkiewicz et al., 2006) or potentially TIMP1 (Milkiewicz et al., 2008; Uchida and Haas, 2014). Lastly, arteriogenesis requires increased MMP activity; inhibition of MMP activity via doxycycline treatment inhibits outward arterial remodeling (Haas et al., 2007). Furthermore, MMP2 or MMP9 deficient mice have reduced arteriogenesis (Cheng et al., 2007; Huang et al., 2009). These studies highlight the importance of regulating MMP expression and activity for appropriate vascular remodeling.

TIMPs are the endogenous inhibitors of the proteolytic activity of MMPs (Brew et al., 2000; Snoek-van Beurden and Von den Hoff, 2005; Ries, 2014). There are four known TIMPs, TIMP1, 2, 3 and 4. TIMPs differ from one another in several regards: their interaction and/or activation of pro-MMPs, solubility and expression. TIMP2, 3 and 4 can cleave the pro-domain of MMP2, while TIMP1 and 3 can cleave and activate pro-MMP9 (Brew and Nagase, 2010). With regards to solubility, TIMPs 1, 2 and 4 are soluble while TIMP3 is not and is found bound to the ECM. Other important differences include the fact that TIMP2 and 3 can inhibit membrane type MMPs and TIMP1 and 3 can inhibit the actions of ADAMs (a disintegrin and metalloproteinase, a sister enzyme to MMPs) (Lambert et al., 2004). The present dissertation will focus on the role of TIMP1 within the microvasculature.

The MMP dependent functions of TIMPs classify them as inhibitors of angiogenesis/vascular remodeling; however the story is far more complex. The ratio of TIMPs to MMPs is thought to be important for the regulation of basement membrane

proteolysis (Chirco et al., 2006). Greater MMP activation, relative to TIMPs, results in excessive proteolysis; this would impede vascular remodeling as the necessary scaffolding for cellular movement is absent (Montesano et al., 1990). Conversely, insufficient proteolysis will inhibit cell invasion and subsequent new vessel lumen formation (Pepper et al., 1990). Furthermore, overproduction of MMPs is known to cause tissue destruction associated with inflammatory disease (Konttinen et al., 1999; Tetlow et al., 2001) and many human cancers (Galis and Khatri, 2002; Creemers et al., 2001). These findings emphasize that TIMPs are not simply anti-angiogenic, rather they are important regulators of relative MMP expression and activity. The appropriate balance between TIMPs and MMPs insures appropriate vascular remodeling responses to a given stimulus.

It should be noted that TIMPs may exert MMP independent functions on various cellular processes (reviewed in, Ries 2014). For example, within myeloid cells, TIMP1 has been shown to promote cell survival and proliferation through MAPK and Akt pathways (Lambert et al., 2004). Interaction of TIMP1 with the cell surface receptor CD63 is linked with suppression of apoptosis (Liu et al., 2005). Conversely, TIMP1 has been reported to induce cell cycle arrest in epithelial cells by decreasing cyclin D1 and increasing p27 (Taube et al., 2006).

1.5: Research models to manipulate the microvascular microenvironment

The microenvironment is recognized as being important, however little is currently known regarding the impact of changes to the microenvironment on the microvasculature. My dissertation involves utilizing multiple methods to manipulate the microenvironment and subsequently examine the consequences on the microvasculature. Flow is an integral physiological stimulus that can be used to assess normal endothelial cell responses required for remodeling. I have chosen to study the influence of changes in skeletal muscle blood flow through either femoral artery (FA) ligation or continuous prazosin treatment in rodents. The microenvironment will be manipulated via the deletion of TIMP1 or GC excess. The deletion of TIMP1 will be used to assess the impact of manipulating the proteolytic balance within the microenvironment. Lastly, sustained elevations in circulating corticosterone (CORT), a synthetic GC, will be used due to its known rarefactory effects on the microvasculature (Shikatani et al., 2012). These models each provide distinct and important information regarding microvascular health and overall cardiovascular health.

1.5.1 Femoral artery ligation: A model of high and low flow

Conduit artery ligation is an experimental tool used to mimic PAD (Lotfi et al., 2013; Krishna et al., 2016). In humans, PAD develops as a result of atherosclerotic plaque formation within large conduit arteries. The most commonly affected vessels are those of the lower limb, such as the popliteal, femoral or iliac arteries. As well, PAD is a common secondary complication of other diseases such as type-2 diabetes (Ziegler et al. 2010).

Ligation studies are typically performed on small mammals such as rodents and rabbits. Currently numerous different strategies are employed to generate hind-limb ischemia. Some research groups utilize a single ligation of the femoral or iliac artery, leaving the venous circulation and nervous tissue undisturbed (Brevetti et al., 2001; Milkiewicz et al., 2011; Roudier et al., 2013), which is proposed to represent intermittent claudication (Lotfi et al., 2013). Others have used excision of the FA (Murohara et al., 1998; Cheng et al., 2007; Huang et al., 2009), which is thought to more closely mimic human critical limb ischemia (Lotfi et al., 2013). Using the single ligation model is beneficial as it does not result in an inflammatory response or tissue necrosis (Hudlicka et al., 1994; Milkiewicz et al., 2006), and thus it was used in the current project.

FA ligation generates two distinct areas (Figure 1.6); below the ligation site is a low flow region, while parallel to the ligation area is a non-ischemic region of elevated flow (Shireman and Quinones, 2005). Different forms of vascular remodeling are proposed to occur within each of these regions.

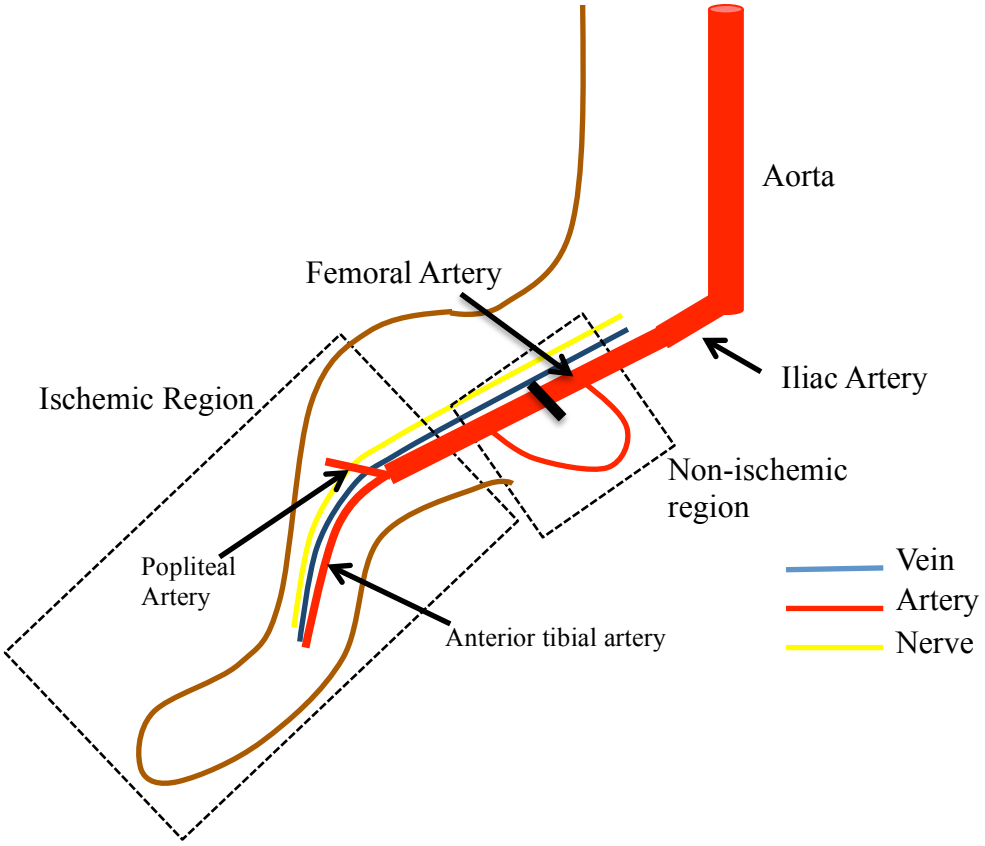

Figure 1.6: Schematic of rodent lower limb vasculature and the impact of femoral artery ligation

Ligation of the femoral artery will create two distinct zones. Parallel to the site of ligation, there is a non-ischemic region, which encompasses the collateral vessels. Distal to the site of ligation is the hypoxic/ischemic region.

1.5.1.1: Microvascular responses distal to the site of ligation: reduced flow

The region distal to the site of obstruction exhibits reductions in blood flow as well as increased metabolic and hypoxic stress. Sustained reduction in blood flow/shear stress is known to result in microvascular rarefaction (Triantafyllou et al., 2015). At the arteriolar level, reduced blood flow elicits a decrease in luminal diameter; the consequence of which is a chronic increase in resistance and an overall reduction in downstream/distal perfusion (Pourageaud and De Mey, 1997). At the capillary level, insufficiently perfused capillary beds will result in capillary rarefaction, or the loss of

existing capillaries. Capillary rarefaction is seen in several diseases including diabetes (Benedict et al., 2011) and hypertension (Vogt and Schmid-Schobein, 2001). Microvascular rarefaction may be due to a decrease in pro-angiogenic factors such as VEGF (Bonner et al., 2013) and angiopoietin-1 (Ang-1) (Wagatsuma, 2008) or an increase in anti-angiogenic factors such as TSP-1 (Olfert, 2015).

The loss of skeletal muscle microvasculature will decrease oxygen and nutrient delivery to the muscle, thereby effecting exercise ability (Haas et al., 2012) and potentially insulin sensitivity (Akerstrom et al., 2014). Microvascular rarefaction has been shown to play a key role in the pathophysiology of hypertension (Humar et al., 2009). This situation elicits a vicious circle; microvascular rarefaction increases peripheral resistance (Greene et al., 1989) thereby further reducing blood flow and elevating systemic blood pressure (Humar et al., 2009). Additionally, hypertension is a potent stimulus for capillary rarefaction (Hansen-Smith et al., 1996).

Hypoxia is likely present distal to the site of occlusion, which generates a potent angiogenic stimulus (Westvik et al. 2009). Although a pro-angiogenic environment is present within the microcirculation, the occurrence of an angiogenic response remains controversial. Some studies have shown angiogenic adaptations to hind-limb ischemia (Ito et al. 1997; Couffinhal et al. 1998; Westvik et al. 2009), while others have not (Scholz et al., 2002; Milkiewicz et al., 2011; Roudier et al., 2013). These different reports could be due to methodological differences within the studies. Some studies reported C:F and others reported capillary density (CD) as measurements of angiogenesis. However, CD may be an inaccurate inference of angiogenesis because it can be confounded by changes in muscle fiber cross-sectional area as well (Roudier et al., 2010). Secondly, the

various studies reported used different species or strains for experimentation. This needs to be accounted for, as there are species/strain differences in the size and quantity of existing collateral routes. Lastly, we must consider whether the ligation model used will elicit an inflammatory response, which is a potent stimulator of angiogenesis (Zhuang et al., 2011). As well, angiogenesis may be inhibited due the increased expression of the anti-angiogenic factor FoxO1 in response to ischemia (Milkiewicz et al., 2011).

1.5.1.2: Microvascular responses parallel to the site of ligation: elevated flow

Adjacent to the ligation site is a normoxic region (Figure 1.6) in which arteriogenesis occurs (Shireman and Quinones, 2005). Due to the blockage of the conduit vessel, blood is diverted through collateral routes; this increase in blood flow through the collateral arterioles is a potent arteriogenic stimulus (Ziegler et al., 2010) (Figure 1.7A & B). Collateralization is thought to be the primary method of restoring blood flow to an ischemic area (Scholz et al. 2002). Alterations in pro-remodeling factors/signaling pathways mediates adaptive collateralization; altered factors/pathways include: NO (Dai and Faber, 2010), ERK (Lanahan et al., 2010) and PI3K/Akt and Src (Tzima et al., 2005), see section 1.3.1 for further details. As well, it should be reiterated that there is the possibility of immune cells contributing to collateralization (see section 1.3.1) (Tuttle et al., 2001; Buschmann et al., 2003; Fung and Helisch, 2012). *In vivo*, arteriogenesis can be examined directly through angiography or corrosion casting, or indirectly via laser Doppler flow assessments.

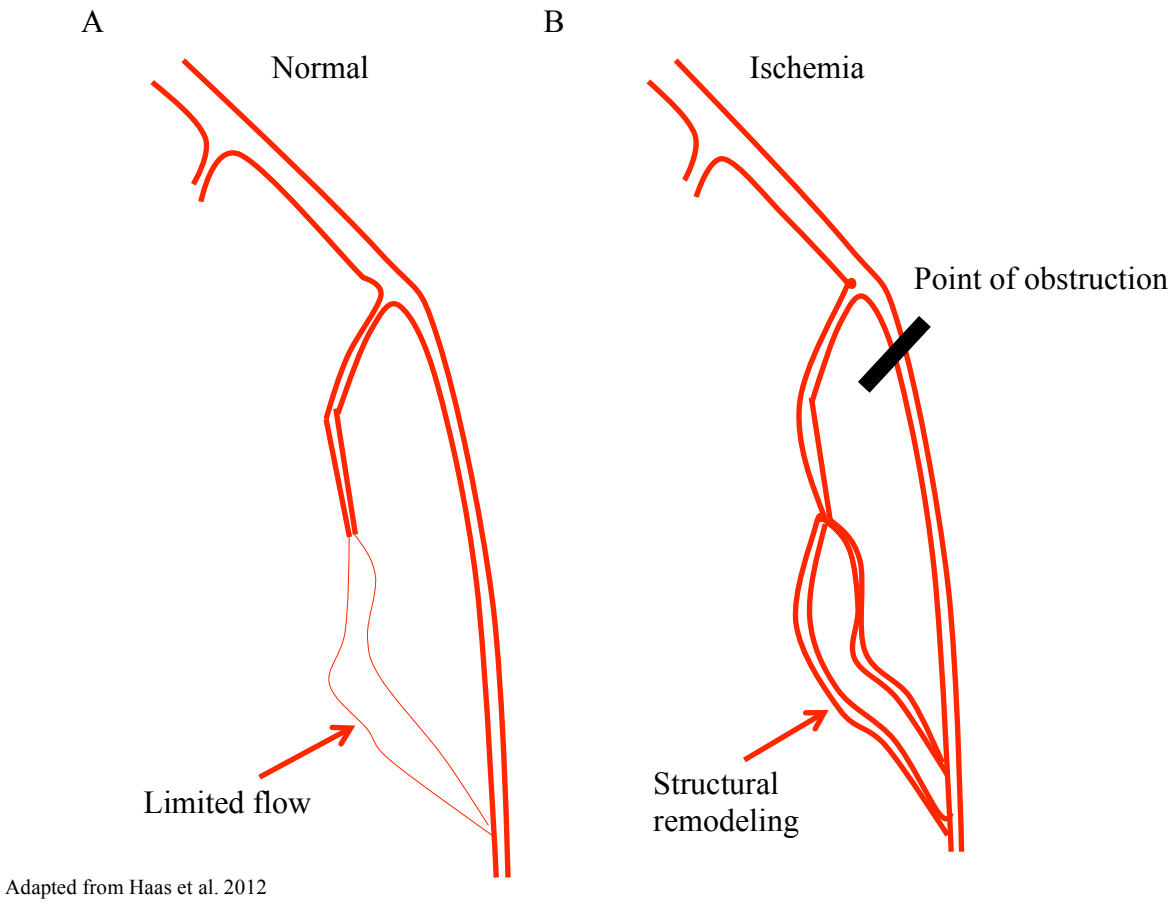

Adapted from Haas et al. 2012

Figure 1.7: Schematic representation of collateral vessel remodeling in response to femoral artery ligation

Collateral arteriogenesis is proposed to occur within the normoxic region of animals that underwent femoral artery ligation. This allows previously small and minimally perfused vessels (A) to remodel to a larger diameter (B) and therefore provide a route for blood to bypass the occlusion and reach the distal hypoxic tissue.

In the current project, unilateral FA ligation was performed in both WT and TIMP1 deficient mice (*Timp1*$^{-/-}$). We chose *Timp1*$^{-/-}$ mice because this should in theory shift the balance between proteases (MMPs) and their inhibitors (TIMPs) within the microenvironment of the microcirculation. This method provides a tool to examine the importance of TIMP1 and the proteolytic balances on vascular remodeling to both reduced and elevated blood flow.

1.5.2: Prazosin- a model of elevated skeletal muscle blood flow

Prazosin is an α-1 adrenergic receptor (α1-AR) antagonist that first came on to the market in the 1970's as a treatment for hypertension. α1-ARs are a class of G-protein coupled receptors known to modulate responses to the actions of catecholamines and are primarily located at the arteriolar level of the vascular tree. Resting skeletal muscle vasculature is generally constricted due the release of norepinephrine from sympathetic neurons, which binds to α1-ARs. The blockade of this system by prazosin elicits vascular dilation, primarily within the skeletal muscle vasculature, due to the high prevalence of α1-AR on smooth muscle cells of this microcirculation (Piascik et al., 1990). It should also be noted that prazosin has been shown to have beneficial roles in lowering total serum cholesterol, LDL and total triglycerides (Leren, 1984). As well, human studies have demonstrated that prazosin treatment may help improve insulin resistance (Pollare et al., 1988; Swistocki et al., 1989).

Animal studies have calculated that resting skeletal muscle capillary shear stress is around 5 dynes/cm^2, which increases roughly threefold to 15 dynes/cm^2 with prazosin treatment (Milkiewicz et al., 2001). While prazosin induces skeletal muscle vasodilation, no significant reductions in mean arterial pressure were noted (Milkiewicz et al., 2001). Animal studies traditionally administer prazosin via dissolution in the drinking water, which insures continuous drug delivery, as prazosin has a relatively short half-life of around 2.5 hours (Jaillon, 1980).

In my dissertation I used prazosin treatment, which is a useful tool to assess alterations to shear mediated signaling pathways. Prazosin treatment was used in conjunction with TIMP1 deletion or elevated GCs, as a tool to evoke flow-induced

remodeling, as has been well established to occur in healthy animals (Ziada et al., 1989; Zhou et al., 1998; Milkiewicz et al., 2007; Uchida and Haas, 2014).

1.5.3: Glucocorticoids

GCs are a class of cholesterol derived steroid hormone secreted by the adrenal glands and are essential for survival. Within humans, the primary GC is known as cortisol while in rodents it is called CORT. GCs are regulated by both a circadian rhythm and are produced in response to stress. Typically, GCs (natural and synthetic) transduce their effects through binding to the glucocorticoid receptor (GR) (Figure 1.8).

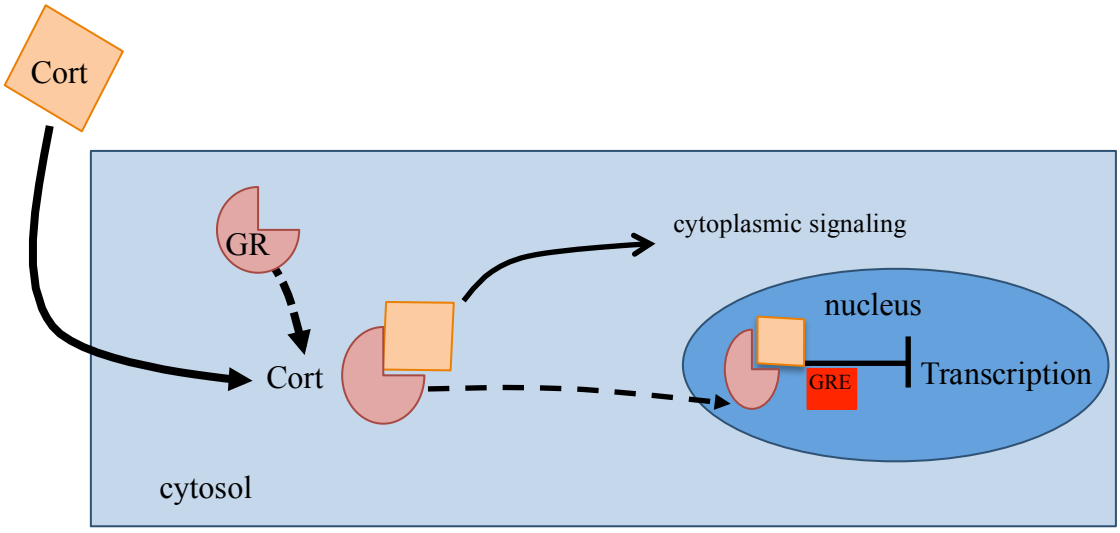

Figure 1.8: Local cellular effects of glucocorticoids

Schematic representation of the cellular effects of GCs. GC will diffuse easily into a cell, due to their lipophilic nature. Once in the cytosol, GC will bind to the GC-receptor (GR) after which the complex will translocate to the nucleus to exert transcriptional effects via binding to the glucocorticoid response element. Additionally, GC can remain in the cytoplasm to exert additional affects.

Once GC bind to the GR, the complex will translocate to the nucleus where GCs can exert their genomic effects such as transcriptional activation or repression, on a vast array of target genes (Oakley and Cidlowski, 2011). These actions are the result of binding to glucocorticoid response elements found within the promoter or intragenic region of GC target genes (Kadmiel and Cidlowski, 2013).

GCs are known to impact angiogenesis within various tissues, including bone (Weinstein et al., 2010), aortic ring preparations (Small et al., 2005) and skeletal muscle (Shikatani et al., 2012). In the current project, pathophysiological levels of GCs were used as a tool to examine skeletal muscle microvascular responsiveness to pro-remodeling cues within the microenvironment.

Several studies have provided insight into potential mechanisms underlying GC-mediated inhibition of angiogenesis and induction of capillary rarefaction. For example, sustained exposure to a pathophysiological level (600nM) of CORT was shown to inhibit endothelial cell proliferation and migration, key cellular events in the process of angiogenesis (Small et al., 2005; Shikatani et al., 2012). CORT has been shown to reduce VEGF mRNA levels (Shikatani et al., 2012; Ullian, 1999), NO bioavailability (Ullian, 1999; Rogers et al., 2002) and other pro-angiogenic factors including MMP2, RhoA and phospho-ERK1/2 (Shikatani et al., 2012). Furthermore, GCs may augment the expression of potent anti-angiogenic factors such as FoxO1 (Shikatani et al., 2012) and TSP-1 (Barclay et al., 2016).

There is evidence to suggest that ROS levels may be elevated due to GC-treatment (Zhang et al., 2004). ROS are produced by a variety of cellular processes including, mitochondrial respiration (Han et al., 2001), NADPH oxidase (Nauseef, 2008),

xanthine oxidase (Garattini et al., 2003), as well as via eNOS uncoupling (Marchesi et al., 2009). Within the vasculature, there is a physiological role for moderate levels of ROS on the regulation of vascular tone (Zhang and Gutterman, 2007) and angiogenesis (Abid et al., 2007; Frey et al., 2009). However, excessive levels of ROS has been shown to play a pivotal role in the development of hypertension (Montezano and Touyz, 2014) and insulin resistance (Anderson et al., 2009; Houstis et al., 2006; Furukawa et al., 2004; Haber et al., 2003). *In vivo*, circulating ROS levels can be reduced with Tempol treatment. Briefly, Tempol is a stable, cell permeant piperidine nitroxide that acts as a superoxide dismutase mimetic (Wilcox and Pearlman, 2008). Tempol has been shown to reduce blood pressure and to protect lipids and proteins from oxidative damage (Schnackenberg et al., 1998; Schnackenberg and Wilcox, 1999; Damiani et al., 2000).

Recently our laboratory has shown that GC excess results in skeletal muscle capillary rarefaction (Shikatani et al., 2012); however, the precise mechanisms responsible for the phenotype are currently unknown. Capillary rarefaction may in turn be an important contributor of GC induced hypertension (Staiculescu et al., 2014). Additionally, recent research has reported a link between capillary content and skeletal muscle insulin and glucose handling (Akerstrom et al., 2014). Therefore, it stands to reason that GC-mediated rarefaction may impact insulin sensitivity. Lastly, sustained elevations in circulating GC levels results in dysfunctional glucose handling, whole body insulin resistance and skeletal muscle atrophy (Shpilberg et al., 2012; Yuen et al., 2013). The rodent model of elevated GC levels significantly impacts the microcirculation (Shikatani et al., 2012) as well as mimics the phenotype of metabolic syndrome and/or type-2 diabetes (Shpilberg et al., 2012).

1.6: Scope of the dissertation

The current studies used several different models to assess how pathological alterations to the microenvironment will impact microvascular content and flow-induced remodeling (Figure 1.9). TIMP1 deletion and GC excess are the two different perturbations used to alter the microenvironment, which were used in conjunction with prazosin or FA ligation. Examining alterations to the microenvironment in response to FA ligation is of interest for researchers hoping to gain preclinical information on important signaling pathways and mechanisms to be considered. Both prazosin and FA ligation modulate hind-limb blood flow thereby providing a tool to examining how alterations in TIMP1 expression or GC levels within the microenvironment will subsequently affect the microvasculature's ability to remodel in response to physiological signaling (Table 1).

Table 1.1: Models used to alter flow both *in vivo* and *in vitro*

Models used to Increase flow		**Models used to lower flow**
Duration of Treatment		
Prazosin Treatment	1 to 2 weeks	
Femoral artery ligation	4,7, 14, or 21 days	Femoral artery ligation: ischemic region
In vitro: Shear stress	2 or 24 hours	*In Vitro*: low shear stress
	1 to 2 weeks	Glucocorticoid treatment

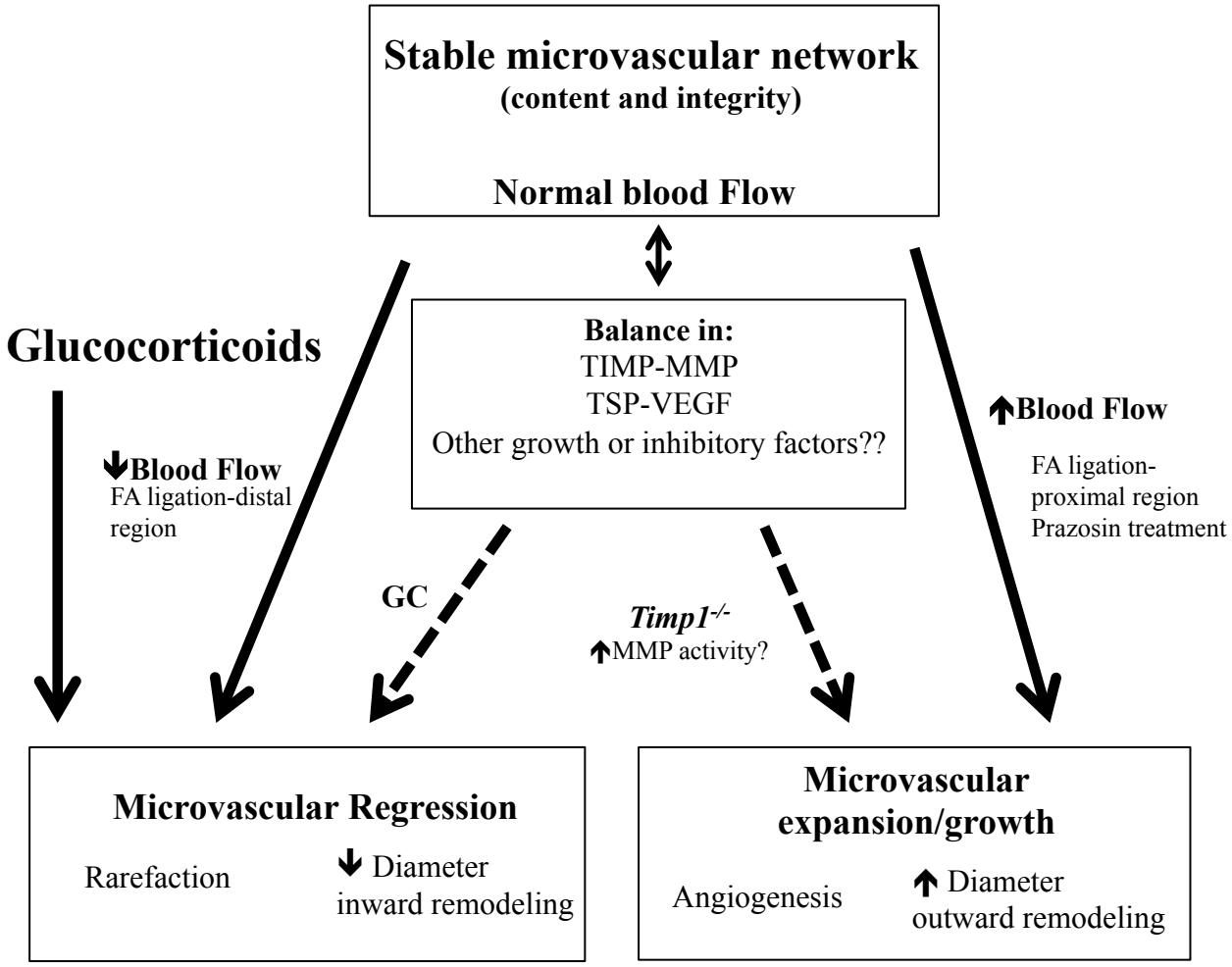

Figure 1.9: Schematic representation of the scope of the dissertation

A stable microvascular network requires a balance in pro-survival/angiogenic factors and pro-apoptotic/anti-angiogenic factors. Alterations in blood flow is known to result in microvascular remodeling (solid black lines). Increased blood flow, as seen in response to FA ligation or prazosin treatment will elicit arteriogenesis and angiogenesis. Conversely, a reduction in flow will elicit microvascular rarefaction. The current study will examine how elevated GC levels or a loss of TIMP1 (dashed lines) will impact the microvasculature and its responses to alterations in blood flow.

The first study was aimed at uncovering the importance of TIMP1 expression on vascular remodeling. TIMP1 regulates proteases activity within the microenvironment and flow induced remodeling requires the tight regulation of proteolysis. Therefore, WT and *Timp1*$^{-/-}$ animals were subjected to prazosin treatment or FA ligation to examine how alterations in TIMP1 expression affect microvascular remodeling. Cell culture models were also employed to more closely examine endothelial cell specific alterations in TIMP and/or MMP expression in response to alterations in shear stress. Lastly, I aimed to identify mechanisms through which sustained elevations in GC negatively impact the microenvironment and subsequently blood pressure. Co-treatment with prazosin was used to study endothelial cell shear responsiveness under the negative effects of CORT (Figure 1.9). Although *Timp1*$^{-/-}$ and GC excess are very different models, they each provide a unique manipulation of microvasculature. These manipulations will provide further insight into the intricacies of the microenvironment and the subsequent impact on peripheral microvascular health and adaptability. Alterations to the skeletal muscle microcirculation can in turn affect CV health, making this an important area of research.

Chapter 2:

Tissue inhibitor of metalloproteinase 1 influences vascular adaptations to chronic alterations in blood flow

Erin R Mandel[1], Cassandra Uchida[1], Emmanuel Nwadozi[1] and Tara L Haas[1*]

[1] School of Kinesiology and Health Science and Muscle Health Research Centre, York University, Toronto ON Canada

Figures:7

Tables:1

Submitted to: Journal of Cell Physiology

I performed all the experiments pertaining to femoral artery ligation in WT and *Timp1*$^{-/-}$ mice (Figures 2.1-2.4). As well, I performed all of the mRNA analysis from the prazosin treatment component of the study (Figures 2.6B & C, 2.7B & C). The prazosin-experiments were performed by Cassandra Uchida with the help of Emmanuel Nwadozi (Table 2.1, Figures 2.5, 2.6A, 2.7A, D & E).

Chapter Summary:

Remodeling of the skeletal muscle microvasculature involves the coordinated actions of matrix metalloproteinases (MMPs) and their endogenous inhibitors, tissue inhibitor of metalloproteinases (TIMPs). We hypothesized that the loss of TIMP1 would enhance both ischemia and flow-induced vascular remodeling by increasing MMP activity. TIMP1 deficient (*Timp1*$^{-/-}$) and wild-type (WT) C57BL/6 mice underwent unilateral femoral artery (FA) ligation or were treated with prazosin, an alpha-1 adrenergic receptor antagonist, in order to investigate vascular remodeling to altered flow. Under basal conditions, *Timp1*$^{-/-}$ mice had reduced microvascular content as compared to WT mice. Furthermore, vascular remodeling was impaired in *Timp1*$^{-/-}$ mice. *Timp1*$^{-/-}$ mice displayed reduced blood flow recovery in response to FA ligation and no arteriogenic response to prazosin treatment. *Timp1*$^{-/-}$ mice failed to undergo angiogenesis in response to ischemia or prazosin, despite maintaining the capacity to increase VEGF-A and eNOS mRNA. Vascular permeability was increased in muscles of *Timp1*$^{-/-}$ mice in response to both prazosin treatment and FA ligation, but this was not accompanied by greater MMP activity. This study highlights a previously undescribed integral role for TIMP1 in both vascular network maturation and adaptations to ischemia or alterations in flow.

Introduction:

Tissue inhibitors of metalloproteinases (TIMPs) play an integral role in regulating extracellular matrix (ECM) turnover (Ries, 2014). Their functional effects are primarily thought to occur via inhibition of matrix metalloproteinase (MMP) activity (Brew et al., 2000; Snoek-van Beurden and Von den Hoff, 2005; Ries, 2014). Appropriately controlled increases in expression/activity of MMPs relative to TIMPs facilitate normal ECM turnover, which is considered to be an important aspect of vascular remodeling processes (Chirco et al., 2006). However, excessive MMP activity may result in a disproportionate extent of ECM proteolysis, having pathological consequences (Chirco et al., 2006). Mice deficient in TIMP1 exhibit several cardiovascular-associated phenotypes suggestive of excessive proteolysis, including a propensity to develop aneurysms, altered myocardial remodeling after infarction, and increased vascular permeability and inflammation in the lungs in response to injury (Kim et al., 2005; Eskandari et al., 2005; Ikonomidis et al., 2005).

The vasculature adapts to sustained alterations in blood flow. At the arterial level, sustained reductions in flow results in inward arterial remodeling (Sullivan and Hoying, 2002; Dumont et al., 2014). Conversely, arteries and arterioles respond to a sustained augmentation in blood flow via arteriogenesis, or outward remodeling, to increase lumen diameter (Langille, 1996; De Mey et al., 2005; Heil et al., 2006). MMP activity is required for flow-induced outward remodeling of mesenteric arteries (Haas et al., 2007). Likewise, the deletion of MMP2 or 9 impairs the process of collateral artery remodeling in response to femoral artery (FA) ligation (Cheng et al., 2007; Huang et al., 2009). These

findings highlight the importance of appropriate MMP levels for flow-induced artery remodeling.

At the capillary level, a sustained reduction in flow results in capillary rarefaction (Triantafyllou et al., 2015), while a chronic increase in flow evokes splitting, or intussusceptive, angiogenesis (Ziada et al., 1989; Zhou et al., 1998; Rivilis et al., 2002; Milkiewicz et al., 2006; Milkiewicz et al., 2007; Hudlicka and Brown, 2009; Gee et al., 2010). Splitting angiogenesis occurs via internal division of capillary segments and is not characterized by basement membrane degradation (Zhou et al. 1998). Flow stimulation of endothelial cells reduces the production of MMP2 while increasing TIMP1 (Rivilis et al., 2002; Milkiewicz et al., 2008; Uchida and Haas, 2014) suggesting that restraint of MMP activity may facilitate splitting angiogenesis, by inhibiting the proteolytic processes associated with abluminal sprouting.

We therefore hypothesized that the loss of TIMP1 would enhance MMP activity thereby augmenting arterial remodeling in response to alterations in flow and promoting sprouting angiogenesis in response to high flow or ischemic conditions.

Material and Methods:

Ethical Approval

All animal experiments were approved by the York University Animal Care Committee and conducted in accordance with the Canadian Council for Animal Care Guidelines.

Animals

B6.129S4-Timp1^{tm1Pds}, which harbor mutated *Timp1* alleles (in-frame stop codon within exon 3), were purchased from Jackson Laboratories (Bar Harbor, ME, USA). Because *Timp1* is located on the X chromosome, the female genotype is *Timp1$^{-/-}$* while the male genotype is *Timp1$^{-/0}$*. For simplicity, we will refer to them all as *Timp1$^{-/-}$*. The *Timp1$^{-/-}$* genotype was confirmed by PCR analysis of DNA extracted from ear punches utilizing the REDExtract-N-Amp Tissue PCR kit (Sigma) and primers for the mutated upstream (5'GCTATCAGGACATAGCGTTGG3') and non-mutated downstream (5'AACCAGGCCCTTTTCCTTTA3') (Invitrogen, Burlington, ON) sites within exon 3 of *Timp1*. Age matched *C57BL/6* mice were purchased from Charles River Laboratories (Sherbrooke, QC) and used as wild-type (WT) controls. Equal numbers of males and females aged 8 to 11 weeks were used for all experiments. Mice were housed in the York University Vivarium in 12 hour light-dark cycle and fed a standard chow diet *ad libitum*.

Femoral Artery Ligation

The FA ligation model was used to evoke: a) ischemia-induced remodeling within lower limb muscle microvessels, and b) flow-induced remodeling in response to a sustained increase in flow through preexisting collateral arteries. Mice were randomly assigned to sham or ligation groups. Under inhaled isoflurane anesthesia, the right FA was dissected away from the vein and nerve distal to the epigastric artery. The artery was ligated with

6-0 suture (ligation group) or remained un-ligated (sham) and incisions were closed with 5-0 suture. Animals were administered buprenorphine (0.15mg/10g BW), at the time of surgery, for pain management. Prior to surgery (Pre), immediately post-surgery (D0) and on days 4, 7, 14 and 21 (D4, D7, D14 or D21) post-surgery, hind-limb blood flow was assessed non-invasively by laser Doppler imager (PeriMed, Stockholm, Sweden) while animals were maintained under isoflurane anesthesia, with body temperature maintained at 37°C using a warming pad. A minimum of 2 scans was captured for each animal, using a constant scanning area (7.5 x 3.7 cm) and working distance (21.2 cm). Using PIMSoft software (PeriMed), regions of interest (ROI) were drawn to encase the knee to foot region in the surgery and control legs and average mean pixel intensity within each region was determined. Intensities were represented as the ratio of mean pixel intensity of the surgical limb to the non-surgical limb. On days 14 and 21 post surgery, FA collateral blood flow was assessed more directly using a needle laser Doppler probe (mooreVMS-LDF2 laser Doppler monitor, Moor Instruments, Delaware USA) while animals were under isoflurane anesthesia, with body temperature maintained at 37°C using a warming pad. An incision was made through skin to expose the underlying tissue and to allow direct positioning of the needle probe over each artery location. More specifically, the needle probe was positioned over a collateral route, 3 vessels that have previously been described to bypass the FA (Hoefer, 2001). Flow was recorded for one minute at each location. Subsequently, flow through each vessel was normalized (surgery: control) and subsequently, the flow ratios of all three vessels were averaged to obtain an average collateral flow ratio per animal.

Prazosin Treatment

To induce a chronic increase in blood flow within the skeletal muscle microvascular network, mice were treated with the α1-adrenergic inhibitor prazosin (50 mg/L; P7791, Sigma), which was administered in the drinking water for 2, 4, 7, 14 or 21 days (Dawson and Hudlická, 1989; Ichioka et al., 1998). Based on an average daily water consumption of 6 ml per mouse, mice ingested approximately 0.3 mg prazosin/day. Control animals were provided with tap water *ad-libitum*.

Tissue Isolation

Animals were anesthetized with inhaled isoflurane on day 4, 7, 14, or 21 and muscles were removed, weighed and snap frozen in liquid nitrogen or liquid nitrogen-cooled isopentane for further analysis.

Muscle Histology

10 to12μm thick cryosections from the belly of the EDL muscle were fixed and stained with fluorescein isothiocyanate-conjugated *Griffonia simplicifolia* isolectin B4 (1:100; Vector Laboratories, Burlington ON, Canada) and anti-smooth muscle actin-Cy3 (1:300; C6198, Sigma Aldrich, Oakville ON, Canada) as described previously (Uchida et al., 2015). Sections were viewed using a Zeiss M200 inverted microscope with 20x objective. Images were captured using a cooled CCD camera controlled with MetaMorph imaging software. Capillary-to-fiber (C:F) counts were averaged from 3 to 4 independent fields of view per mouse by a blinded observer. The number of smooth muscle actin-positive (SMA^+) vessels was counted for each field of view and their perimeters measured using MetaMorph software. Where a lumen could not be seen, perimeter was estimated by measuring the vessel diameter and using the formula $P=2\pi r$. Analysis of average SMA^+

vessels was performed on vessels 20μm and smaller as these vessels are within the range of newly formed arterioles.

Electron Microscopy

The *extensor hallucis proprius* (EHP) muscle of animals from the prazosin experiments were fixed *in situ*, then post-fixed and processed for transmission electron microscopy using standard protocols. This muscle is thin, enabling the rapid post-fixation that is ideal for electron microscopy). Ultrathin sections were viewed using a Philips EM201 electron microscope at 20,000X magnification. Images were taken using a cooled CCD digital camera (L-3, Scientific Instruments and Applications, Duluth, GA, USA).

Protein Extraction and Matrix Metalloproteinase Activity

Protein was extracted from TA muscle using RIPA buffer including protease inhibitors and phosphoSTOP (Roche, Indianapolis IN) as described previously (Milkiewicz et al., 2011). Protein extracts were quantified using a bicinchoninic acid assay (Pierce, Fischer Thermoscientific). 5μg of protein per muscle was used to assess overall MMP activity within EDL muscle homogenates using the Amplite ^{TM} fluorimetric universal MMP activity assay kit (#13510; AAT Bioquest, California, USA).

Measurements of Vascular Permeability

A subset of *Timp1*$^{-/-}$ and WT mice at the 4 day time point post-prazosin or FA ligation were injected with Evans Blue dye (3% in 0.9% saline *i.p,* at a dose of 1 or 2ml/kg of body weight; E2129, Sigma: Oakville, ON, Canada), and were anesthetized after 20 minutes for tissue extraction. A section of liver (50 to 90mg) and both EDL and soleus muscles were removed, weighed and placed in formamide at 56°C overnight to extract the dye. Sample absorbance at 560 nm was assessed using a microplate reader

(Cytation™ 3, Biotek, Vermont USA and compared to a standard curve of known concentrations of Evans blue dye in formamide. The amount of dye in each sample was calculated relative to tissue weight (ng dye/mg EDL or liver). In the ligation study, the amount of dye in the EDL from the ligated leg was expressed as a ratio to that of the non-ligated leg. In the prazosin study, the dye amount in the EDL was expressed as a ratio to liver.

RNA Analysis by Real Time qPCR

RNA was isolated from TA muscle using the Qiagen RNeasy Fibrous Tissue Mini Kit (74704, Qiagen, Toronto, ON Canada) as per the manufacturer's instructions. RNA was reverse transcribed using MMLV reverse transcriptase (New England Biolabs, Whitby ON Canada). cDNA were analyzed by qPCR using TaqMan® Fast Advanced Master Mix (4444963; Invitrogen Canada; Burlington, ON Canada) and TaqMan® probes for HPRT1 (Mm00446968_m1), GAPDH (Mm004308313_m1), MMP2 (Mm00439498_m1), TIMP1 (Mm00441818_m1), TIMP2 (Mm00441825_m1), TIMP3 (Mm00441826_m1), TIMP4 (Mm01184417_m1), VEGFA (Mm00437306_m1), ICAM-1 (Mn00516023_m1), VCAM (Mn01320970_m1) or eNOS (Mn00435217_m1) and detected using the ABI 7500 Fast PCR system (Invitrogen Canada). The comparative Ct ($2^{-\Delta Ct}$) method was used to determine mRNA expression of the target genes relative to the housekeeping genes HPRT1 or GAPDH.

Cell culture and shear stress stimulation

Skeletal muscle microvascular endothelial cells were isolated from tibialis anterior muscle of male Sprague Dawley rats as described previously (Han et al., 2003). Cells were cultured with Dulbecco's Modified Eagle Medium (Invitrogen) supplemented with

10% heat denatured FBS, 1mM sodium pyruvate, 1mM Glutamax (Invitrogen), 50 units penicillin, 0.5mg/ml streptomycin and 1.25μg/ml fungizone (Gibco). Cells were used between passages 4 to 7. Shear stress experiments were conducted as previously described (Milkiewicz et al., 2006). Briefly, for shear stress experiments, endothelial cells were plated on gelatin coated glass cover slips. Cells were subjected to 5 dynes/cm^2 shear stress for 24 hours using parallel plate flow systems (Bioptechs). This shear stress was utilized because it is comparable to the reported normal/resting capillary shear stress within skeletal muscle (Hudlicka et al., 2006).

Statistical analysis

Results were expressed as mean $\pm$ SEM and analyzed via two-tailed students t-test, one-way ANOVA, or a two-way ANOVA with subsequent Tukey or Bonferroni post hoc tests (Prism4; Graphpad software Inc; La Jolla, CA, USA). In all cases, $P < 0.05$ was considered statistically significant.

Results:

Characteristics of the skeletal muscle microvascular network in *Timp1*$^{-/-}$ mice

Under basal conditions, the EDL microvascular network within *Timp1*$^{-/-}$ mice was characterized by a significantly lower C:F and reduced density of small arterioles (SMA^+ vessels <20 μm diameter) compared to WT animals (Table 2.1). We considered that the phenotype of *Timp1*$^{-/-}$ mice might exhibit sexual dimorphism, because the *Timp1* gene is located on the X chromosome. However, C:F and arteriole density did not differ between male and female mice of WT or *Timp1*$^{-/-}$ mice (Table 2.1). Both plantaris and gastrocnemius were proportionately smaller in the *Timp1*$^{-/-}$ mice compared to WT mice of the same sex, but this influence was not detected in other muscles (Table 2.1). As no sex differences were evident with respect to C:F or SMA^+ vessel density, male and females were grouped together for all subsequent analyses. Despite the reduced number of microvessels, there was no evidence of apoptosis in the EDL of *Timp1*$^{-/-}$ mice, as assessed by cleaved caspase 3 staining (data not shown).

Impaired microvascular remodeling within the ischemic limb of *Timp1*$^{-/-}$ mice

The angiogenic response within chronically ischemic muscle is minimal despite the generation of a pro-angiogenic environment, which may be a consequence both of reduced shear stress signaling and an upregulation of anti-angiogenic factors (Scholz et al., 2002; Milkiewicz et al., 2011; Roudier et al., 2013). A significant increase in TIMP1 mRNA was detectable in the ischemic muscle of WT mice 4 days after FA ligation (Figure 2.1A), suggestive of a potential anti-angiogenic role for TIMP1.

As expected, C:F did not increase within the ischemic muscle in response to FA ligation in WT mice, similar to previous reports (Scholz et al., 2002; Milkiewicz et al.,

2011; Roudier et al., 2013). However, ischemia-induced angiogenesis did not occur in *Timp1*$^{-/-}$ mice (Figure 2.1B & C), despite the presence of a pro-angiogenic stimulus, as evident by a significant increase in VEGF-A mRNA (Figure 2.1D). The average diameter of SMA^{+} vessels was unaffected by genotype or ischemia (data not shown). The density of small arterioles was significantly reduced in *Timp1*$^{-/-}$ mice, but was unaffected by ischemia (Figure 2.1E). These findings suggest that endogenous TIMP1 does not act to restrain angiogenesis or arteriolar remodeling within the ischemic muscle.

Effects of ischemia and *Timp1*$^{-/-}$ on TIMP and MMP expression

To further explore the mechanism(s) mediating the lack of alteration in vascular remodeling in *Timp1*$^{-/-}$ mice, the expression of MMPs and the other TIMPs was examined. TIMP1 deletion did not influence the basal expression of MMP2 or MMP9 (Figure 2.2A & B). MMP2, but not MMP9, mRNA was significantly increased within the ischemic skeletal muscle of both WT and *Timp1*$^{-/-}$ mice (Figure 2.2A & B). TIMP2, 3 and 4 were increased significantly in *Timp1*$^{-/-}$ vs. WT mice under ligation and basal conditions (Figure 2.2C- E). Microvascular permeability of the EDL, as assessed by extravasation of Evans blue dye, was examined as a potential downstream effect of excess proteolysis. Basal permeability was unaffected by the loss of TIMP1, but permeability increased within the ischemic EDL muscle of *Timp1*$^{-/-}$ mice (Figure 2.2F). Global MMP activity was not altered in *Timp1*$^{-/-}$ compared to WT mice (Figure 2.2G). Together, these data suggest that MMP activity is maintained by compensatory increases in other TIMPs and that the augmented vascular permeability within the ischemic muscle of *Timp1*$^{-/-}$ mice may be a consequence of other structural alterations to the microvasculature.

Because changes in gene expression within ischemic muscle are impacted by mild hypoxia/metabolic stress as well as reduced flow, we also examined cultured microvascular endothelial cells maintained under normal flow or no flow conditions. TIMP1 mRNA was substantially lower under no-flow (~ 0 dynes/cm^2) compared to normal flow conditions (~5 dynes/cm^2) (Figure 2.3A). Conversely, mRNA levels of TIMP3 and MMP2 did not differ between normal and no-flow conditions (Figure 2.3B & C respectively). Thus, the reduction of blood flow within ischemic muscle may act to down-regulate endothelial TIMP1 expression within endothelial cells, but this appears to be counter-balanced by the hypoxic/metabolic stress, resulting in an overall increase in TIMP1 expression within the ischemic microenvironment.

***Timp1*$^{-/-}$ mice exhibit impaired blood flow recovery post-ligation**

The FA ligation model also was used to examine the role of TIMP1 in flow-induced collateral artery remodeling. FA ligation causes diversion of blood flow through smaller collateral pathways, which induces outward remodeling of the collateral arteries (Cai et al., 2004). Collateral dependent recovery of hind-limb blood flow, as assessed by laser Doppler imaging, was restored to pre-ligation values by day 14 in WT mice (Figure 2.4A). However, blood flow in the ligated limb of *Timp1*$^{-/-}$ mice remained significantly lower than that of the non-ligated limb even after 21 days of recovery (Figure 2.4A &B). Similarly, collateral vessel blood flow, as assessed by Doppler needle probe, increased significantly in WT but not *Timp1*$^{-/-}$ mice after 14 days of recovery (Figure 2.4C). After both 14 and 21 days post-ligation, average collateral blood flow was greater in WT than *Timp1*$^{-/-}$ mice (Figure 2.4C). These findings suggest an impaired collateral artery remodeling response within *Timp1*$^{-/-}$ mice.

Timp1$^{-/-}$ mice have reduced microvascular remodeling with prazosin treatment

We utilized chronic prazosin treatment to further evaluate microvascular remodeling in *Timp1*$^{-/-}$ mice in response to elevated flow. Previously, we reported that high shear stress (15 dynes/cm^2) reduced MMP2 and increased TIMP1 expression (Milkiewicz et al., 2006; Uchida and Haas, 2014), suggesting a role for TIMP1 in promoting splitting rather than sprouting angiogenesis. C:F increased in WT mice after 21 days of prazosin treatment, but not in the *Timp1*$^{-/-}$ animals, whose C:F ratio was significantly lower than WT animals at every time point (Figure 2.5A & B). SMA$^+$ vessel density was increased significantly in WT mice after 7 days of prazosin treatment, but was significantly lower in *Timp1*$^{-/-}$ mice at all time points (Figure 2.5C).

Examination of capillary ultrastructure by electron microscopy revealed activation of endothelial cells in response to 7 and 14 days of prazosin treatment in WT mice only. This was evidenced by membrane ruffling and protrusions of the endothelial cells into the capillary lumen (Figure 2.6A, indicated by arrows). However, these indicators of endothelial cell activation were not observed in the *Timp1*$^{-/-}$ mice at any time point (Figure 2.6A). Luminal protrusions consistent with splitting angiogenesis were detected in WT mice only. Abluminal protrusions were not detected in capillaries from WT or *Timp1*$^{-/-}$ mice.

VEGF-A and nitric oxide are critical mediators of flow induced angiogenesis (Williams et al., 2006). Thus, we postulated that the impaired remodeling responses in *Timp1*$^{-/-}$ mice may be caused by reduced expression of VEGF-A or eNOS. However, the prazosin induced increases in VEGF-A and eNOS mRNA were not different between WT and *Timp1*$^{-/-}$ mice (Figure 2.6B & C respectively).

Prazosin increases microvascular permeability in *Timp1*$^{-/-}$ mice

Electron microscopy images also showed evidence of cells within the vascular compartment that were adherent to, or in the process of migrating through, the capillary wall in muscles from *Timp1*$^{-/-}$ mice (Figure 2.7A). This phenomenon was not detected in any of the samples from WT mice. These images suggested alterations in vascular permeability and/or a potential increase in inflammation within *Timp1*$^{-/-}$ mice. VCAM-1 and ICAM-1 mRNA, two endothelial pro-inflammatory adhesion molecules (Jublanc et al., 2011), were assessed. No significant differences were noted in VCAM-1 expression (Figure 2.7B). ICAM-1 mRNA expression was significantly increased by prazosin treatment in the *Timp1*$^{-/-}$ mice (Figure 2.7C). Evans Blue dye extravasation indicated a significant increase in permeability after 4 days of prazosin treatment in the EDL muscles *Timp1*$^{-/-}$ but not in WT mice (Figure 2.7D). A similar influence on permeability also was detected in the oxidative soleus muscles of 4 day prazosin-treated *Timp1*$^{-/-}$ mice compared to their time matched WT controls (0.77 ± 0.05 vs. 0.50 ± 0.05 ng/mg muscle, respectively; $P<0.05$). However, the augmentation in permeability was not associated with increased MMP activity, as there was no influence of *Timp1*$^{-/-}$ on global MMP activity (Figure 2.7E).

Table 2.1: Baseline animal characteristics of WT and *Timp1*$^{-/-}$ mice.

	WT		***Timp1*$^{-/-}$**	
	Male (n=12)	**Female (n=24)**	**Male (n=23)**	**Female (n=25)**
Body mass (g) [a,c]	24.1±0.60	19.2±0.20	26.9±0.60[b]	21.1±0.40[b]
Soleus mass (g) [c]	8.7±0.30	7.1±0.20	9.1±0.20	7.6±0.10
Soleus mass:body mass [ns]	0.36±0.01	0.36±0.01	0.34±0.01	0.35±0.01
Plantaris mass (g) [c]	16.8±0.50	12.1±0.20	17.2±0.50	12.8±0.40
Plantaris mass:body mass [d]	0.70±0.01	0.63±0.01	0.64±0.01[e]	0.61±0.02
Gastrocnemius (g) [c]	119.7±2.1	88.3±1.2	119.5±3.20	88.6±1.90
Gastrocnemius mass:body mass [d]	5.0±0.08	4.6±0.04	4.4±0.07[e]	4.2±0.08[e]
TA (g) [c]	44.6±0.70	35.2±0.50	48.5±1.30	38.3±0.80
TA mass:body mass [ns]	1.9±0.03	1.8±0.01	1.8±0.04	1.8±0.04
EDL mass (g) [c]	11.3±0.20	8.4±0.20	11.8±0.40	8.9±0.20
EDL mass:body mass [ns]	0.47±0.01	0.44±0.01	0.44±0.01	0.43±0.01
EDL capillary-to-fiber ratio [a]	1.4±0.04	1.3±0.2	1.0±0.04[e]	1.0±0.05[f]
EDL SMA^+ vessel density (#/mm^2) [g]	22.7±1.10	23.7±1.60	11.9±1.20[h]	14.3±1.90

All data are presented as means ± standard error of measurement
a, 2 way ANOVA genotype effect, $P<0.0001$
b, post hoc significant difference compared to respective WT gender matched group, $P<0.01$
c, 2 way ANOVA gender effect $P<0.0001$
d, 2 way ANOVA genotype and gender effects, $P<0.01$ and $P<0.001$, respectively
e, *post hoc* significant difference compared respective WT of same sex, $P<0.0001$
f, *post hoc* significant difference compared respective WT of same sex, $P<0.05$
g, 2 way ANOVA genotype effect, $P<0.01$
h, *post hoc* significant difference compared respective WT of same sex, $P<0.01$
ns, non significant

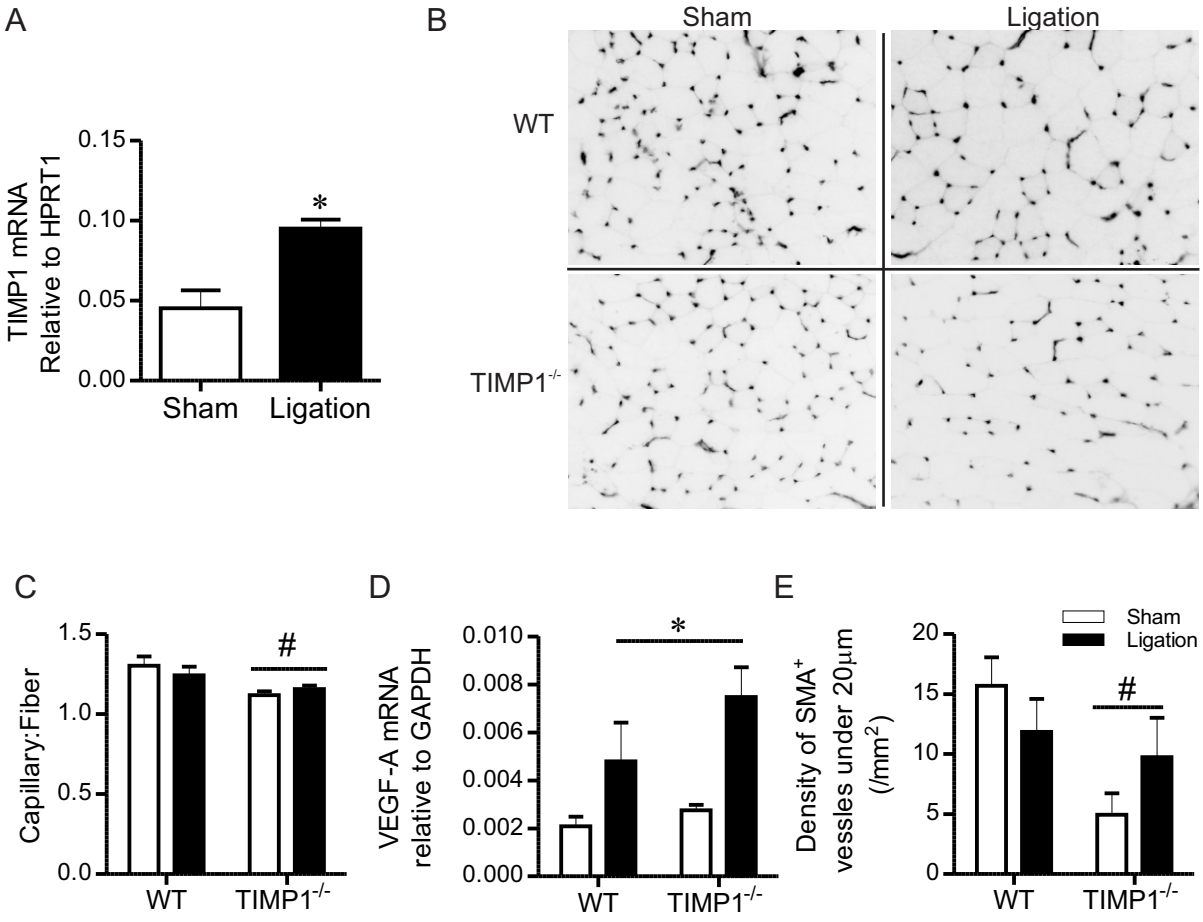

Figure 2.1: Impact of the loss of TIMP1 on vascular remodeling in response to ischemia

A) RNA was isolated from the TA muscle, reverse transcribed and underwent qRT-PCR 4 days post sham or femoral artery ligation to examine TIMP1 expression. Data was analyzed via students unpaired t-test (n=4-5). * P <0.05 compared to sham.
B) Representative images of EDL muscle stained to visualize capillaries and SMA^+ vessels 21 days after sham or ligation surgery. C) Capillary-to-fiber ratio from 3-4 non-overlapping fields of view per mouse analyzed D) VEGF-A mRNA E) SMA^+ vessel density (for vessels under 20µm in diameter). Data analyzed via two way ANOVA and post hoc test. # P<0.05, indicated an overall genotype effect, * P<0.05 compared to sham group (n=4-8).

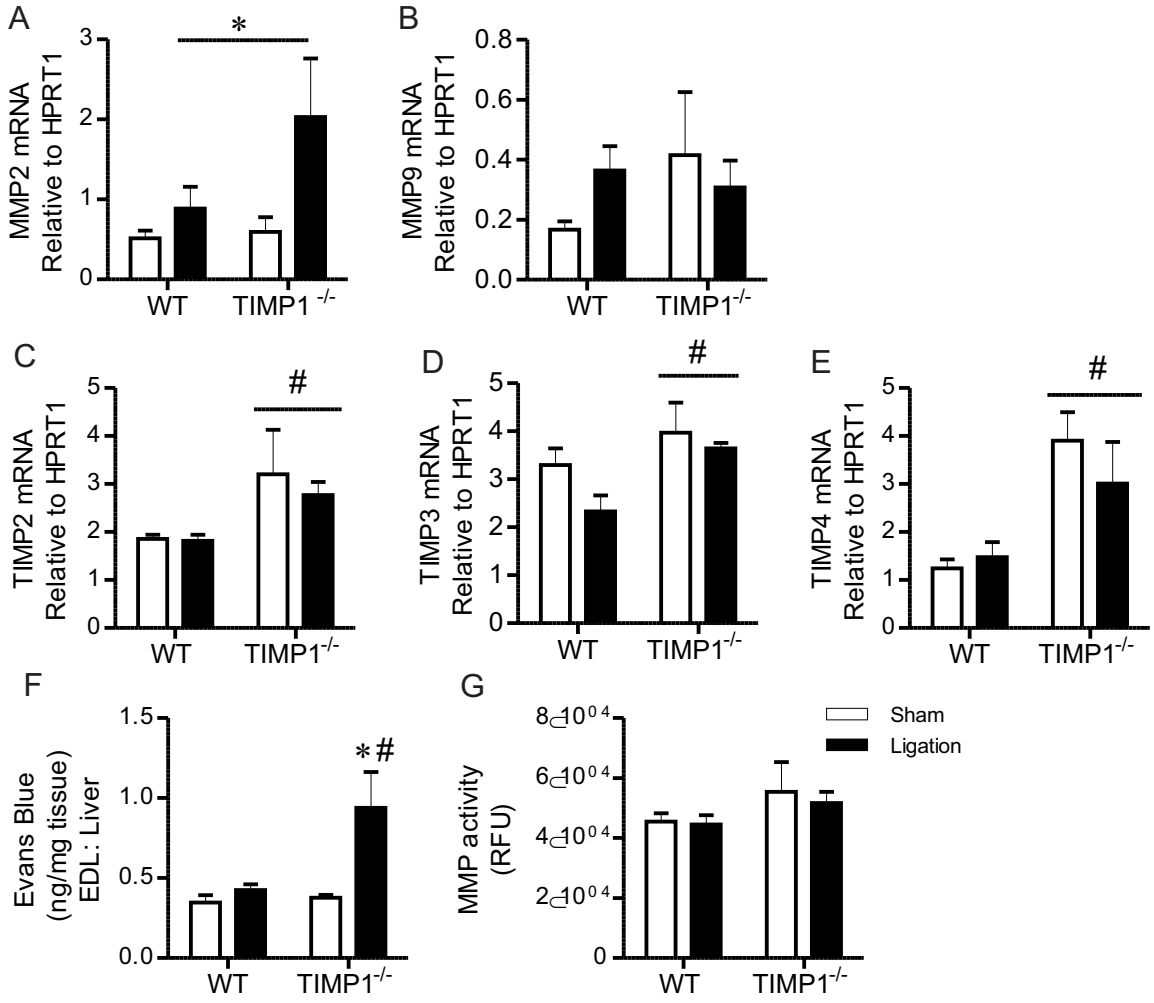

Figure 2.2: Influence of ischemia on the expression of MMPs, TIMPs and vascular permeability in wild type and *Timp1*$^{-/-}$ mice

RNA was isolated from the TA muscle, reverse transcribed and underwent qRT-PCR 4-days post sham or femoral artery ligation. Gene of interest was normalized to the housekeeping gene HPRT1. Two way ANOVA and subsequent Bonferroni post hoc test was used to assess the data. A) MMP2 B) MMP9 C) TIMP2 D) TIMP3 E) TIMP4. * P<0.05 compared to respective sham group; #P <0.05 compared to corresponding WT group (n=4-8).
F) Evans blue dye leakage from the EDL muscle was measured (Abs= 560) as a marker of vascular permeability 4-days post ligation. * P<0.05 compared to respective sham group; # P<0.05 compared to respective WT group. G) Protein was isolated from the TA to assess overall MMP activity (MMP1-14), via a fluorometric kit 4 days post ligation (P>0.05, n=4-6)**.**

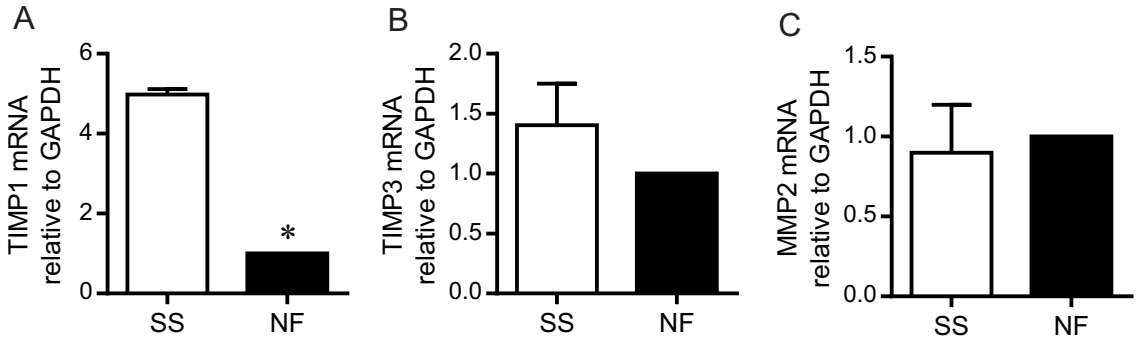

Figure 2.3: Influence of reduced flow on TIMP and MMP mRNA in cultured endothelial cells

Skeletal muscle endothelial cells were exposed to normal capillary flow at 5 dynes/cm^2 (SS) or to no flow (NF) conditions for 24 hours. mRNA was subsequently isolated and quantified by Taqman qPCR and expressed as $2^{-\Delta\Delta Ct}$ to analyze TIMP1 (A), TIMP3 (B) and MMP2 (C) expression via paired students t-test. * $P<0.05$ compared to SS condition (n=3-5).

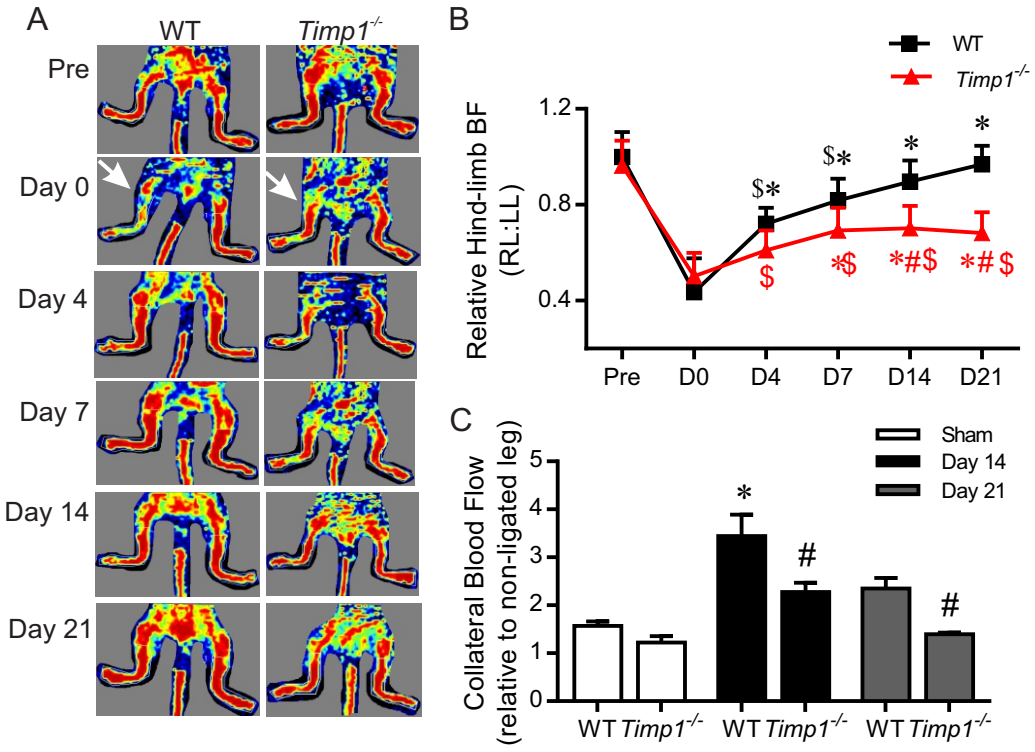

Figure 2.4: Hind-limb blood flow recovery post femoral artery ligation in wild type and *Timp1*$^{-/-}$ mice

A) Representative laser Doppler images from the hind-limb of WT and *Timp1*$^{-/-}$ mice over the time course of femoral artery ligation recovery. B) Quantification of hind-limb blood flow at all time points, which is a ratio of perfusion in the right (operated) to the left (control) leg. Data analyzed via two-way ANOVA and post hoc test. $ $P<0.05$ compared to respective pre condition, * $P<0.05$ compared to respective D0, # $P<0.05$ compared to respective WT group (n=9-30). C) Flow was assessed via the Moore needle probe on femoral artery collateral arteries of both the operated (right) and control (left) limbs 14 and 21 days post unilateral sham or ligation surgery. * $P<0.05$ compared to respective sham group, # $P<0.05$ compared to respective WT group (n= 4-11).

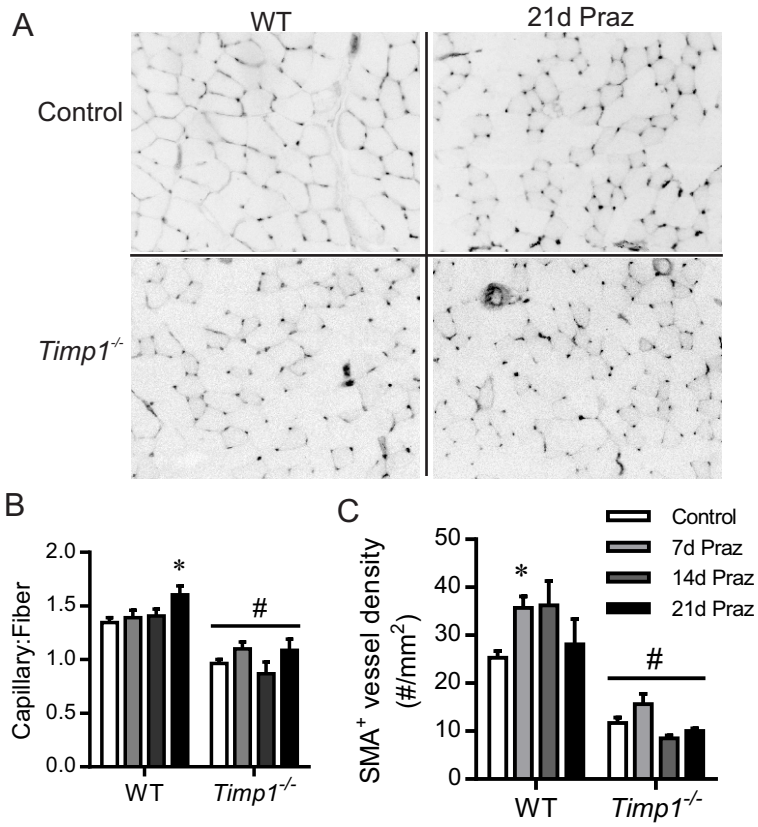

Figure 2.5: *Timp1*$^{-/-}$ mice have a blunted microvascular remodeling in response to elevated blood flow.

A) Representative images of isolectin staining and Cy3-anti- smooth muscle actin to visualize capillaries and SMA^{+} within the EDL muscle of control and prazosin (Praz) treated mice. Two-way ANOVA was used to assess B) Capillary-to-fiber ratio from 3-4 separate (non-overlapping) fields of view per mouse C) SMA^{+} density * P<0.05 compared to respective control group, # P<0.05 compared to WT animals (n=6).

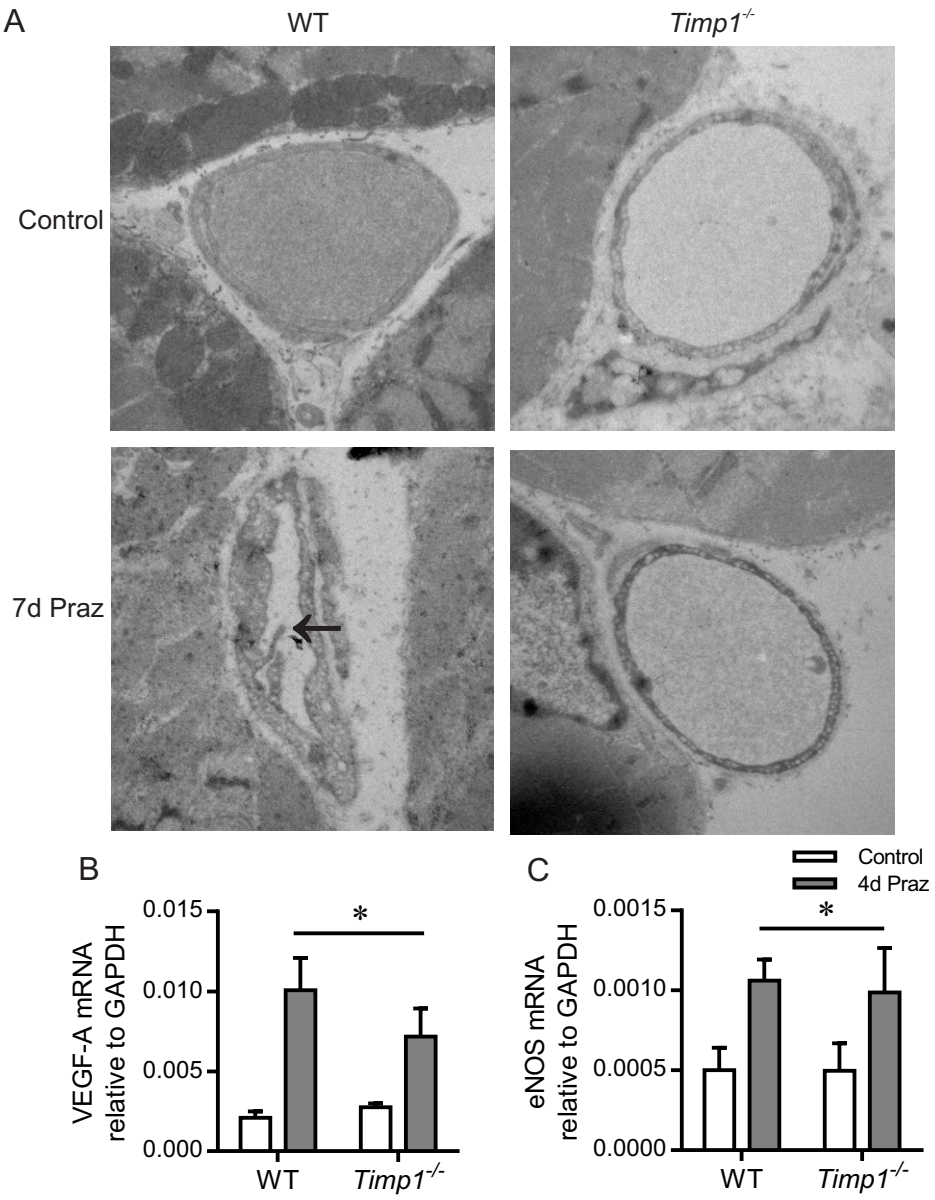

Figure 2.6: *Timp1*$^{-/-}$ mice lack prazosin-induced endothelial cell activation despite a pro-angiogenic environment.

A) *Timp1*$^{-/-}$ and WT mice were treated with prazosin (Praz) for 7 days. The extensor hallucis proprius was removed, cross-sectioned and visualized by electron microscopy. Note the presence of luminal protrusions and endothelial cell ruffling only in the WT mice treated with prazosin, as indicated by arrows.
RNA was isolated from the plantaris muscle of mice treated with prazosin for 4 days. RNA was reverse transcribed and underwent qRT-PCR to analyze VEGF-A (B) and eNOS (C) mRNA and assessed via two way ANOVA and post hoc test (*P<0.05 compared to respective control group, (n=4-12).

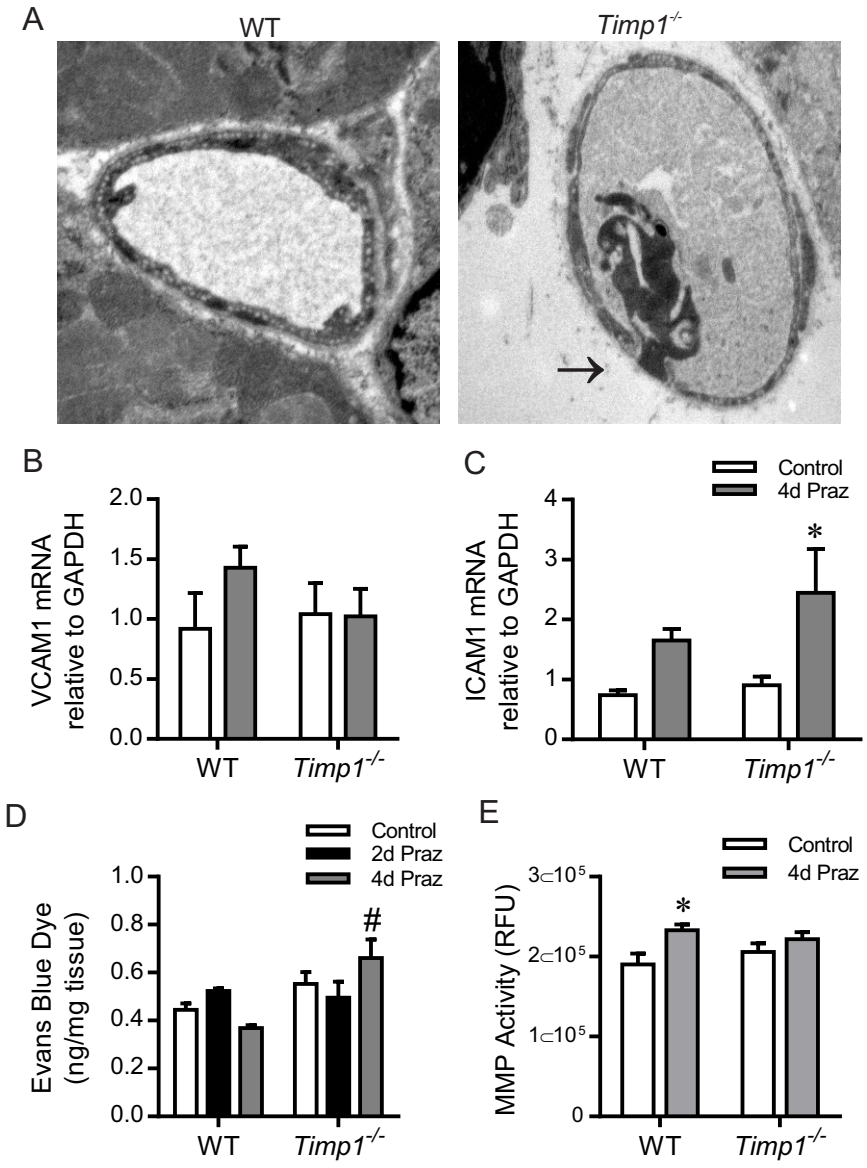

Figure 2.7: Capillary permeability in response to prazosin treatment

A) Electron microscopy images taken of the extensor hallucis proprius after 4 days of prazosin treatment indicated cells adherent to or transmigrating the capillary wall in the vessels of the knockout mice treated with prazosin; this was not observed in WT counterparts. RNA was isolated from the plantaris muscle, reverse transcribed and underwent qRT-PCR 4-days post commencement of prazosin treatment to analyze VCAM (B) and ICAM (C) mRNA expression ($2^{-\Delta\Delta CT}$). mRNA was assessed via two way ANOVA and post hoc test (* $P<0.05$ compared to respective control group, n=4-6). D) Vascular permeability was assessed in EDL via quantification of Evans Blue dye extravasation and assessed via two-way ANOVA. #$P<0.05$ compared to respective WT group by post-hoc analysis (n=6-9 per group) E) Muscle homogenates of the TA were obtained and MMP activity in the muscle was measured using a fluorescent activity assay. Two-way ANOVA indicated a main effect of prazosin (Praz) ($P=0.02$), which a Bonferroni post hoc analysis revealed was only significant in WT controls (*$P<0.05$,n=6).

Discussion:

This study demonstrated that the loss of TIMP1 was associated with a constitutive reduction in the skeletal muscle microvascular network, as evidenced by a lower C:F ratio and reduced density of small SMA^+ vessels. Vascular remodeling in response to alterations in blood flow was impaired by the loss of TIMP1. The loss of TIMP1 did not elicit an angiogenic response to hind-limb ischemia. Furthermore, in response to hind-limb ischemia, collateral artery flow and whole limb blood flow recovery were blunted by the deletion of TIMP1. Angiogenesis and arteriolar remodeling in response to prazosin induced increases in flow were also abrogated in *Timp1*$^{-/-}$ mice, despite increases in VEGF-A and eNOS mRNA equivalent to those of WT mice.

The reduction in skeletal muscle microvascular content in untreated *Timp1*$^{-/-}$ mice suggests that TIMP1 plays an unexpected and previously unreported role in establishing a mature microvascular network. This effect was sex independent. Furthermore, it should be noted that TIMP1 does not play a critical role in early vascular development as *Timp1*$^{-/-}$ pups are viable and mature *Timp1*$^{-/-}$ mice are fertile. Considering that maturation, branching and pruning of the microvascular network itself is highly dependent on blood flow (Lenard et al., 2015), it is possible that the reductions in C:F and arteriole density in *Timp1*$^{-/-}$ mice under resting conditions reflects a generalized failure of appropriate flow-mediated remodeling processes.

The influence of *Timp1*$^{-/-}$ on vascular remodeling was assessed using FA ligation and prazosin treatment as experimental tools to manipulate oxygen levels and blood flow through the skeletal muscle circulation. In contrast to the initial hypothesis that loss of

TIMP1 would enhance remodeling, we observed a failure to undergo adaptive angiogenesis and arteriogenesis in *Timp1*$^{-/-}$ mice.

The microvascular response to low oxygen and low blood flow was examined *in vivo* via FA ligation. Hypoxia is a potent stimulus for increased VEGF production (Shweiki et al., 1992). However, the increase in VEGF-A does not result in angiogenesis within ischemic muscle (Scholz et al., 2002; Milkiewicz et al., 2011; Roudier et al., 2013). The increase in TIMP1 within ischemic muscle suggested that it might restrain sprouting angiogenesis due to inhibition of MMP activity. However, TIMP1 deletion did not elicit ischemia induced angiogenesis. Neither the basal or stimulus induced level of VEGF-A or MMP expression was altered within muscles of *Timp1*$^{-/-}$ mice. Thus, the loss of TIMP1 is unable to alter the microenvironment to allow for ischemia induced vascular remodeling to occur.

Vascular remodeling in response to elevated blood flow was not detected within the collateral zone generated by FA ligation of *Timp1*$^{-/-}$ mice, based on analysis of hind limb blood flow recovery and collateral artery flow. Likewise, shear stress induced angiogenesis and arteriogenesis did not occur within the skeletal muscle microvasculature of *Timp1*$^{-/-}$ mice following prazosin administration. Both eNOS and VEGF-A play critical roles in flow induced angiogenesis and arteriogenesis (Rudic et al. 1998; Hudlicka et al. 2006; Williams et al. 2006). However, neither basal levels nor flow induced increases in VEGF-A or eNOS mRNA were altered in *Timp1*$^{-/-}$ mice, indicating that the signal pathways that control the expression of these important factors are not disrupted by TIMP1 deletion. Nonetheless, the lack of prazosin-induced endothelial cell activation and luminal protrusions within capillaries of *Timp1*$^{-/-}$ mice suggests that the

loss of TIMP1 impairs downstream cellular processes associated with flow induced angiogenesis and arteriogenesis.

Previously, shear induced expression of TIMP1 was postulated to limit proteolysis and to prevent abluminal sprouting (Milkiewicz et al., 2008; Uchida and Haas, 2014), thus implying that deletion of TIMP1 would provoke an abluminal sprouting response to elevated flow. However, there was no evidence of abluminal sprouting in capillaries of prazosin-treated *Timp1*$^{-/-}$ mice. Furthermore, we did not find evidence of augmented MMP activity within skeletal muscle of *Timp1*$^{-/-}$ mice under any conditions. The compensatory increases in TIMP2, 3 and 4 mRNA observed in the current study may explain the lack of increase in overall MMP activity, as they may have prevented excessive proteolysis and minimized increases in vascular permeability. Similar compensatory increases in TIMP2 (Ikonomidis et al., 2005) and TIMP3 (Kim et al., 2001) have been detected within cardiac muscle and kidney tissue of *Timp1*$^{-/-}$ mice.

Timp1$^{-/-}$ mice exhibited increased vascular permeability under 'stress' conditions (ischemia or elevated flow), indicating a failure to maintain vascular integrity. Capillary permeability is strictly maintained by adherens and tight junctions (Dejana, 2004). While increased capillary permeability may occur as a consequence of increased MMP-mediated cleavage of junctional proteins (Alexander and Elrod, 2002), we do not have evidence that this occurred in *Timp1*$^{-/-}$ mice. However, we cannot exclude the possibility of localized peri-capillary increases in proteolysis that were not detectable by the analysis of whole muscle global MMP activity. Excessive permeability also occurs as a consequence of inflammation (Cotran and Majno, 1964; Chistiakov et al., 2015). *Timp1*$^{-/-}$ (but not *Timp2*$^{-/-}$) mice were previously reported to have increased vascular permeability

and inflammation within the lung (Kim et al., 2005). In the current study, ICAM1 mRNA was significantly elevated in *Timp1*$^{-/-}$ mice in response to prazosin treatment. The increase in ICAM1 may contribute to the increased membrane permeability and cellular infiltration within *Timp1*$^{-/-}$ capillaries, as it has been reported that ICAM1 activation induces intracellular signals that result in enhanced endothelial solute permeability (Sumagin et al., 2011).

The phenotype of *Timp1*$^{-/-}$ and concurrent lack of alteration in MMP activity raises the possibility that TIMP1 impacts the vasculature in an MMP-independent mechanism. It has been reported that TIMP1 exerts MMP-independent functions that influence cell survival and proliferation (reviewed in, Ries 2014); however, these studies were conducted on myeloid and epithelial cells rather than endothelial cells. Our laboratory found that recombinant TIMP1 did not impact survival of cultured endothelial cells (Mandel et al., 2013). This, together with a lack of detectable apoptosis in *Timp1*$^{-/-}$ muscle in the current study, suggests that TIMP1 deletion does not impact endothelial cell survival.

The current study demonstrates that TIMP1 plays an important role in the maturation and expansion of the skeletal muscle microvascular network. While TIMP1 does not act to constrain ischemia induced angiogenesis, our study indicates that it is required for appropriate flow induced angiogenesis and arteriogenesis. The cellular actions of TIMP1 that result in the impaired vascular remodeling responses exhibited by *Timp1*$^{-/-}$ mice remain to be identified. While there was no evident increase in MMP activity in *Timp1*$^{-/-}$ mice, the increased vascular permeability observed in response to prazosin or ischemia is indicative of a failure to maintain vascular integrity. This study

demonstrates that TIMP1 does not act as an anti-angiogenic factor within the skeletal muscle microvasculature, providing evidence of a critical permissive function of TIMP1 in the processes associated with flow induced vascular remodeling.

Chapter 3:

Elevated skeletal muscle blood flow can prevent glucocorticoid mediated capillary rarefaction

Erin R Mandel[1], Emily C. Dunford[1], Anastassia Trifonova[2], Ghoncheh Abdifarkosh[1], Trevor Tiech[1], Michael C. Riddell[1] and Tara L. Haas[1,2#]

School of Kinesiology and Health Science and Muscle Health Research Centre[1], Department of Biology[2], York University, Toronto, ON Canada

Figures: 5
Tables: 2

Submitted to: American journal of physiology. Regulatory, integrative and comparative physiology

I collected all the data within the current manuscript except for Figures 3.5A-E (Anastassia Trifonova) and Figures 3.2 B-C, 3.3F, which were collected by Ghoncheh Abdifarkosh. Emily C. Dunford assisted with the study design and data collection.

Chapter Summary:

Glucocorticoids (GC) are angiostatic and elicit capillary rarefaction within skeletal muscle, which can subsequently impair blood distribution and muscle function. Conversely, skeletal muscle angiogenesis can be induced by treatment with the alpha-1 adrenergic receptor inhibitor prazosin due to augmented skeletal muscle blood flow. We hypothesized that corticosterone (CORT) treatment would inhibit endothelial mediated shear stress signaling and subsequently the angiogenic response to prazosin administration. CORT pellets were implanted subcutaneously (400 mg/rat) for 1 or 2 weeks in male Sprague Dawley rats, with or without concurrent prazosin treatment (50mg/L in drinking water). The CORT-induced reduction in capillary-to-fiber ratio (C:F) corresponds with reduced Angiopoietin-1 mRNA. Rarefaction was prevented with concurrent prazosin administration; however, no angiogenesis or arteriogenesis occurred in CORT-treated animals. The shear induced increase in pSer473 Akt was impaired by 2W CORT treatment. In 2W CORT animals, VEGF-A protein was increased significantly by concurrent prazosin treatment. However, prazosin did not rescue CORT-induced reductions in TGFβ or MMP2 mRNA. Shear stress dependent signaling was assessed in cultured rat skeletal muscle endothelial cells pre-treated with CORT (600nM) for 48 hours, then exposed to 15 dynes/cm^2 shear stress or maintained with no flow. CORT blunted the shear stress induced increases in pSer473 Akt, VEGF and TGFβ mRNA, while MAPK phosphorylation or nitric oxide (NO) production were unaffected. This study demonstrates that the maintenance of MAPK, NO and VEGF responsiveness to augmented shear stress contributes to the prevention of CORT-mediated rarefaction, but is unable to elicit an angiogenic or arteriogenic responses.

Introduction:

Endothelial cells are continuously exposed to the physical force of blood flow, which generates shear stress. Shear stress activates a diverse array of intracellular signaling networks within endothelial cells predominantly those involved in promoting cell survival and maintenance of a healthy vasculature (Sessa, 2004). Shear stress activates endothelial nitric oxide synthase (eNOS), increasing nitric oxide (NO) production (Kuchan and Frangos, 1994), along with vascular endothelial growth factor (VEGF) (Milkiewicz et al., 2001). Both NO and VEGF-A are imperative for survival and angiogenic signaling (Williams et al. 2006; Williams et al. 2006b). Animal models have demonstrated that sustained increases in shear stress within the skeletal muscle capillary network stimulates angiogenesis via luminal splitting (Ziada et al., 1989; Zhou et al., 1998; Gee et al., 2010). Shear stress stimulates VEGF-A production by both endothelial cells and the surrounding skeletal myocytes, which is essential for shear stress induced angiogenesis (Milkiewicz et al. 2001; Williams et al. 2006; Gee et al. 2010; Uchida et al. 2015). Conversely, shear stress has been reported to repress production of the anti-angiogenic matrix protein thrombospondin-1 (TSP-1) (Bongrazio et al., 2008). Furthermore, augmented shear stress is a potent stimulus for arteriogenesis or the outward remodeling of arteries and/or arterioles (Skalak, 2005; Cai and Schaper, 2008). Arteriogenesis will result in more large vessels thereby normalizing the augmented shear response and reducing the angiogenic stimulus (Schaper, 2009).

Elevated levels of glucocorticoids (GC) are observed in individuals with poorly controlled diabetes, metabolic syndrome, or Cushing syndrome (Lansang and Hustak, 2011; Beaudry and Riddell, 2012). The prolonged pathophysiological increase in GC

causes the loss (rarefaction) of preexisting capillaries within skeletal muscle (Shikatani et al., 2012). Loss of skeletal muscle capillaries is associated with poor skeletal muscle, metabolic and cardiovascular health (Nascimento et al., 2013; Triantafyllou et al., 2015), likely due to reduced access to hormones and nutrients such as insulin and glucose (Bonner et al., 2013). The mechanisms through which GC excess elicits the loss of skeletal muscle capillaries have not been established. Research utilizing cultured cells has suggested that GC can exert an anti-angiogenic influence through inhibiting endothelial cell proliferation, matrix proteolysis, sprouting and migration (Folkman et al., 1983; Small et al., 2005; Shikatani et al., 2012); however, evidence is lacking regarding a direct influence of GCs on endothelial cell apoptosis. GC excess has been reported to reduce the production of VEGF (Ullian, 1999; Shikatani et al., 2012) and inhibit eNOS-dependent production of NO (Ullian, 1999). These influences suggest that GC may impair physiological shear stress signaling, which could impair survival signaling and flow-induced vascular remodeling.

The effects of sustained increases in microvascular blood flow can be modeled within skeletal muscle by the administration of prazosin, an alpha-1 (α1) adrenergic receptor antagonist. A significant increase in skeletal muscle capillary-to-fiber ratio (C:F), indicative of an angiogenic response, is detectable after 7 to 14 days of prazosin treatment (Ziada et al., 1989; Zhou et al., 1998; Rivilis et al., 2002). Thus, in the current study, we utilized the model of sustained prazosin treatment and shear stress stimulation of cultured endothelial cells to test the hypothesis that elevated levels of CORT would inhibit shear stress signaling and restrain the angiogenic response to prazosin administration.

Materials and Methods:

All animal experiments were approved by York University Animal Care Committee (approval number 2013-5) and conducted in accordance with the Canadian Council for Animal Care Guidelines.

Animal Protocol

Male Sprague Dawley rats (N=48; initial weight 200-250g) were purchased from Charles River Laboratories (Montreal, QC, Canada). Rats were housed in the York University Vivarium in a12 hour light-dark cycle. After 7 days acclimation, animals were assigned randomly to one of four groups: corticosterone-treated or wax-treated (control), with either regular drinking water (CORT-water and control-water), or drinking water containing prazosin hydrochloride (50 mg/L; P7791, Sigma Aldrich Canada) (CORT-prazosin and control-prazosin). All animals were fed a standard rodent chow diet (14% fat, 54% carbohydrate, 32% fat; 3.0 calories/g) ad libitum.

100mg wax or CORT pellets were made and on Day 0, four pellets were implanted subcutaneously in the mid-scapular region of each rat, under isoflurane anesthesia, as described previously (Shpilberg et al., 2012). Subsequently, rodents recovered in individual cages and were given ampicillin (20mg/Kg body weight) in their drinking water. On day 2, rats were continued with regular water or commenced with prazosin-treated water for 7 or 14 days. These groups will be referred to as 1W and 2W control or CORT- water or -prazosin.

Plasma Corticosterone Analysis

Blood was collected via saphenous vein puncture at 8am on days 0, 7 and 14. Plasma CORT was measured by radio-immunoassay (07-120102, MP Biomedicals; Solon, OH) according to manufacturer's instructions.

Tissue Isolation

At the end point of each study, animals were anesthetized with inhaled isoflurane muscles were removed, weighed and snap frozen in liquid nitrogen or liquid nitrogen-cooled isopentane for further analysis, and animals were euthanized by exsanguination.

Cell culture and shear stress stimulation

Skeletal muscle microvascular endothelial cells were isolated from the *extensor digitorum longus* (EDL) muscle of male Sprague Dawley rats as described previously (Han et al., 2003). Cells were cultured with Dulbecco's Modified Eagle Medium (Invitrogen) supplemented with 10% heat denatured FBS, 1mM sodium pyruvate, 1mM Glutamax (Invitrogen), 50 units penicillin, 0.5mg/ml streptomycin and 1.25μg/ml fungizone. Cells were used for experiments between passages 4 to 7. Endothelial cells were plated on 35mm dishes or gelatin coated glass cover slips and pretreated with 600 nM CORT for 48 hours, a dose that previously was shown to inhibit angiogenic behavior (Small et al., 2005; Shikatani et al., 2012). Shear stress experiments were conducted as previously described (Milkiewicz et al., 2006). Briefly, cells were subjected to 15 dynes/cm^2 shear stress for 2 hours using a parallel plate flow system (Bioptechs), to provide a stimulus comparable to reported capillary shear stress within skeletal muscle of prazosin-treated rats (Milkiewicz et al., 2001).

Protein Extraction and Analysis via Western Blotting or ELISA

For western blots, protein was extracted from the *tibialis anterior* (TA) muscle or cultured endothelial cells in RIPA buffer including protease inhibitors and phosphoSTOP (Roche, Indianapolis IN). Muscle extracts were processed using a tissue lyser (MM400, Retsch GmbH, Haan, Germany). Protein extracts were quantified by bicinchoic acid assay (Pierce, Fisher Thermoscientific). 20 to 40 μg of total proteins were separated through 8% or 10% SDS-polyacrylamide gels under reducing conditions. Proteins were transferred to PVDF membrane (Immobilon-P, Millipore) using wet transfer (Biorad trans-blot) and membranes were blocked for 1hr with 5% milk in TBS- 0.05% Tween (TTBS). Membranes were incubated overnight at 4°C with antibodies for phospho Akt Ser473, Thr308 (#4058 & 9275, Cell Signaling), phospho ERK1/2 (# 9101, Cell Signaling), phospho-p38 (#9211, Cell Signaling) or TSP-1 (#MA5-13398, Thermo Scientific) in 5% BSA -TTBS. Secondary antibodies (rabbit IgG-HRP) were detected by enhanced chemiluminescence (Pierce WestPico, Fisher Thermoscientific). Membranes were stripped and re-probed for total AKT (# 9272, Cell Signaling), total p38 (#9272, Cell Signaling) or anti-β-actin (1:5000, Santa Cruz Biotechnology, Santa Cruz CA) for normalization. Blots were quantified and analyzed using Carestream software.

For the VEGF-A ELISA, *gastrocnemius* muscle was solubilized in PBS and processed by tissue lyser. On the same day, 100μg of protein per sample was assayed by ELISA (R&D systems, #RRV00), as per the manufacturer's instructions.

RNA extraction and Real Time qPCR

RNA was isolated from TA muscle using the Qiagen RNeasy Fibrous Tissue Mini Kit (74704, Qiagen, Toronto, ON Canada) as per the manufacturer's instructions. RNA was

reverse transcribed using MMLV reverse transcriptase (New England Biolabs, Whitby ON Canada). cDNA were analyzed by Taqman qPCR using qPCR mastermix (#4444963; Invitrogen Canada) and Taqman probes for rat HPRT (Rn01527840), VEGF-A (Rn00582935), TSP-1 (Rn01513693), Ang1 (Rn01504818), MMP2 (Mm00439498), TIMP1 (Rn00587558) and TGFβ1 (Rn99999016) using the ABI 7500 Fast PCR system (Invitrogen Canada). For each sample, the comparative Ct method ($2^{-\Delta Ct}$) was used to determine relative mRNA expression of target genes compared to the housekeeping gene HPRT.

Muscle Histology and cell staining

10μm cryosections of TA muscle were fixed with 3.7% paraformaldehyde and stained with fluorescein isothiocyanate-conjugated *Griffonia simplicifolia* isolectin B4 (1:100; Vector Laboratories, Burlington ON, Canada) and anti-smooth muscle actin-Cy3 (1:300; C6198, Sigma Aldrich, Oakville ON, Canada). Sections were viewed using a Zeiss M200 inverted microscope with 20x objective and images were captured using a cooled CCD camera using Metamorph imaging software. C:F counts were averaged from 3 to 4 independent fields of view per rat by a blinded observer. The density and diameters of smooth muscle actin (SMA) positive vessels were calculated.

Statistical Analysis

Results were expressed as mean ± SEM and analyzed by one-way or two-way ANOVA with subsequent Bonferroni post hoc tests where appropriate (Prism4; Graphpad software Inc; La Jolla, CA, USA). $P < 0.05$ was considered statistically significant.

Results:

Plasma CORT was significantly elevated above control after both 1W and 2W of exogenous CORT pellet treatment, but was unaffected by prazosin administration (Table 3.1). For complete animal characteristics see Supplementary Table 3.1.

CORT-induced reduction in skeletal muscle capillarization is abrogated with prazosin treatment

Both 1W and 2W CORT significantly reduced skeletal muscle C:F as compared to time-matched control animals (Figure 3.1A-C). C:F was elevated in 2W con-prazosin treated animals (Figure 3.1A & C), consistent with previous literature (Ziada et al., 1989; Zhou et al., 1998; Milkiewicz et al., 2007). The CORT-dependent reduction in C:F was prevented by 2 weeks of concurrent prazosin treatment; nonetheless, C:F remained significantly lower in muscles of CORT-prazosin compared to control-prazosin rats (Figure 3.1A & C).

Factors associated with Corticosterone-mediated capillary rarefaction

We assessed factors associated with endothelial cell survival and angiogenesis to delineate potential mediators of CORT-induced capillary rarefaction, and the preventative influence of prazosin. The mRNA level of Angiopoietin-1 (Ang-1) was assessed due to its established role as a vascular stabilization and cell survival factor (Asahara et al., 1998; Fukuhara et al., 2010). Ang-1 mRNA was not altered in cultured endothelial cells exposed to 48 hours of elevated CORT (Figure 3.2A). However, Ang-1 mRNA in whole muscle lysates was significantly decreased after both 1 and 2 weeks of CORT treatment (Figure 3.2B & C). Prazosin diminished the impact of CORT treatment, as Ang-1 levels in 2W prazosin-treated CORT rats were no longer different from control levels (Figure

3.2C). Akt is important for cell survival (Manning and Cantley, 2007) and is a downstream effector of Ang-1/Tie2 signaling (Daly et al., 2006). However, 1W CORT did not significantly alter basal phosphorylation of Akt at Ser473 or Thr308 (Figure 3.2D & E). Of note, the prazosin-induced increase in pAkt Ser473 seen in wax animals was absent in CORT-treated animals (Figure 3.2D). No changes in Akt phosphorylation (Ser473 or Thr308) were detectable in the 2W treated muscles (data not shown).

VEGF-A acts as a pro-survival as well as pro-angiogenic factor (Zachary, 2003). However, neither 1W or 2W CORT treatment reduced VEGF-A mRNA (Figure 3.3A & B). VEGF-A mRNA levels increased significantly in the 2W CORT-prazosin compared with CORT-water muscles (Figure 3.3B). Similarly, VEGF-A protein was significantly elevated at the 2W time point in CORT-prazosin compared to CORT-water treated rats ($P<0.05$, Figure 3C).

TSP-1 can induce endothelial cell apoptosis and prevent angiogenesis (Iruela-Arispe et al., 1999; Zhang and Lawler, 2007), and thus could contribute to CORT-induced capillary rarefaction. However, TSP-1 mRNA was not altered by 1W or 2W of CORT-treatment or by prazosin treatment (Figure 3.3D, E). 2W of CORT treatment elicited a small reduction in TSP-1 protein level, with no effect of concurrent prazosin treatment (Figure 3.3F). Taken together, our results indicate that the alteration in Ang-1, rather than VEGF-A or TSP-1, may best explain the CORT-induced capillary rarefaction. However, the increase in VEGF-A in CORT-prazosin muscles may contribute to the prevention of rarefaction.

Prazosin-induced arteriolar remodeling is impaired in skeletal muscle of CORT-treated rats

Prazosin also induces arteriolar remodeling (Skalak, 2005), analogous to the outward remodeling that occurs in larger arteries exposed to elevated shear stress (Pipp, 2004). While SMA^+ blood vessel density was unaltered by 2 weeks of prazosin or CORT treatment (Figure 3.4A), SMA^+ vessel diameter was augmented by prazosin-treatment within control animals only (Figure 3.4B). Shear stress stimulated outward remodeling of blood vessels can be promoted by TGFβ1 signaling (van Royen et al., 2002) and MMP activity (Haas et al., 2007). 1W CORT treatment significantly blunted the level of TGFβ1 mRNA; however, this influence was not detected after 2 weeks of treatment (Figure 3.4C & D). We previously reported that CORT treatment repressed MMP2 expression in cultured endothelial cells (Shikatani et al., 2012). In the current experiment, we observed that MMP2 mRNA was reduced significantly within the skeletal muscle of CORT treated rats and was not affected by concomitant prazosin treatment (Figure 3.4E). TIMP1 mRNA, an endogenous inhibitor of MMP proteolytic activity, was not altered by CORT or prazosin in 2W treated animals (Figure 3.4F). Thus, the repression of TGFβ1 and MMP2 with CORT treatment is consistent with the impaired arteriolar remodeling in response to increased blood flow.

CORT-dependent regulation of pro-survival and angiogenic factors in endothelial cells

Due to the impairment of normal blood flow remodeling responses in CORT-treated animals, we used cultured endothelial cells to more specifically assess the influence of CORT on endothelial cell shear stress dependent signaling. Shear stress stimulates endothelial cell phosphorylation of ERK1/2 and p38 MAPK (Gee et al., 2010)

and Akt (Dimmeler et al., 1998). CORT did not attenuate the shear stress stimulated phosphorylation of ERK1/2 or p38 MAPK (Figure 3.5A & B). Interestingly, CORT treatment abolished the shear stress mediated phosphorylation of Akt at Ser473 while phosphorylation at Thr308 was unaffected (Figure 3.5C & D). The shear stress induced increase in nitrite levels, a measure of NO production, was not altered by CORT (Figure 3.5E). Elevated shear stress significantly increased VEGF-A mRNA in untreated cells, but this effect was blunted in CORT-treated cells (Figure 3.5F). TSP-1 mRNA level was not influenced by shear stress nor CORT treatment of endothelial cells (Figure 3.5G). TGFβ1 mRNA was significantly reduced by CORT-treatment; however, the shear stress induced increase in TGFβ1 expression was maintained in CORT-treated cells (Figure 3.5H).

Table 3.1: Animal plasma CORT concentration

		1 Week		
Plasma corticosterone (ng/ml)	**Control-Water (n=5)**	**Control-Prazosin (n=5)**	**CORT-Water (n=5)**	**CORT-Prazosin (n=5)**
	17.54±1.4	18.94±5.5	583.1±39.8#	485.5±72.3#
		2 Weeks		
Plasma corticosterone (ng/ml)	**Control-Water (n=5)**	**Control-Prazosin (n=5)**	**CORT-Water (n=9)**	**CORT-Prazosin (n=6)**
	16.21± 6.5	9.6 ±0.6	296.3±34.4#	284.7±34.2#

Values are expressed as mean ± standard error
#, Significant difference compared to respective control group, as determined by two-way ANOVA and Bonferroni post hoc analysis.

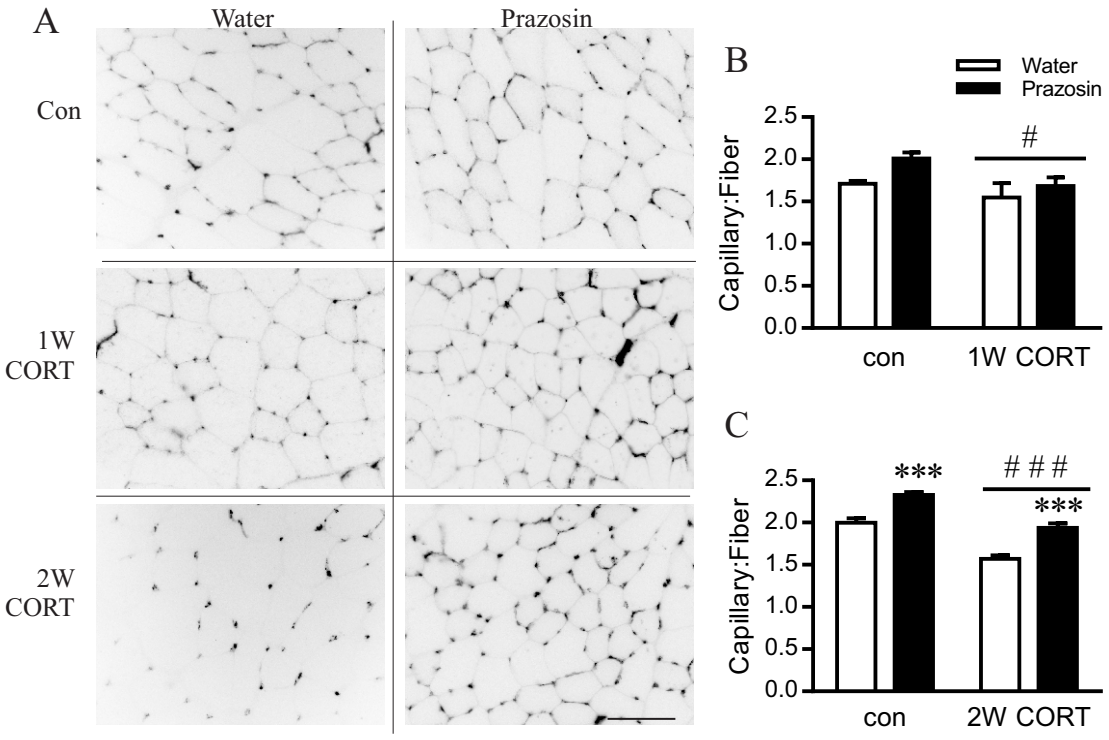

Figure 3.1: Corticosterone-induced capillary rarefaction is abrogated by continuous prazosin treatment

The TA muscle was sectioned and stained for capillaries using Griffonia Simplicifolia isolectin-fluorescein and Cy3-anti-a smooth muscle actin. A) Representative images of isolectin staining after 1W and 2W of CORT-treatment. Inverted grey scale images of isolectin staining are displayed to enhance visualization of individual muscle fibers. Line represents 100μm. B) C:F at the 1W time point calculated from the average of 5 non overlapping fields of view, # $P<0.05$ vs. corresponding control group. C) C:F at the 2W time-point was calculated as the average from 5 non-overlapping fields of view per rat,. ***, ### $P<0.001$ vs. corresponding water or control group respectively, n=6-9.

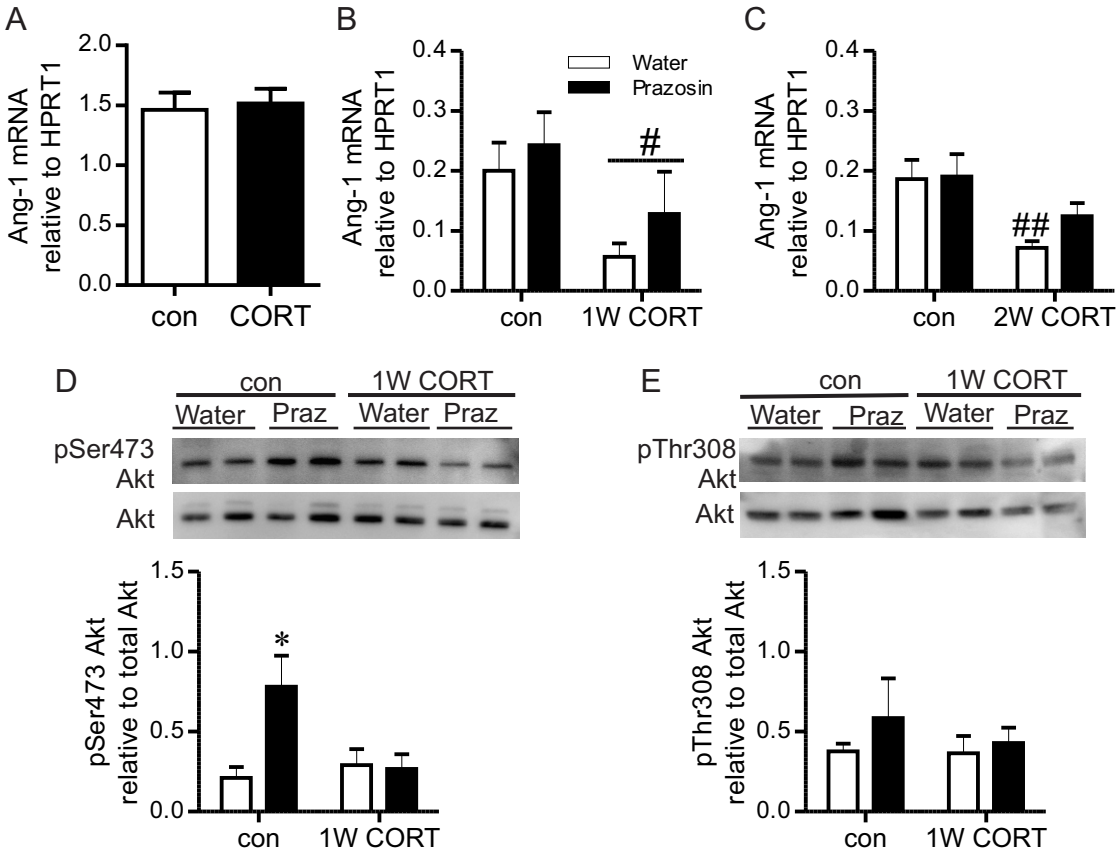

Figure 3.2: Causes of Cort-mediated capillary rarefaction

RNA was isolated from the endothelial cell extracts after 48 hours of CORT-treatment or from the TA muscle after 1W or 2W of CORT treatment with or without the consumption of prazosin. Taqman qPCR was used to assess the expression of Ang-1 as analyzed by $2^{-\Delta ct}$. A) Ang-1 mRNA was unaltered within cultured endothelial cells after 48hours of CORT-treatment and analyzed via paired t-test (P=0.85, n=5).
B) Two-way ANOVA and post hoc test was used to asssess Ang-1 mRNA after both 1 and 2W of CORT treatment with or without concurrent prazsoin administration (n=4-8). B) Ang-1 was significantly reduced with 1W CORT-treatment regardless of prazosin co-treatment (# P=0.02). C) Ang-1 mRNA was significantly reduced with 2W of CORT-treatment (## P<0.05).
Protein was extracted from the TA muscle of control or 1W CORT treated rats. Changes in phospho Ser473-Akt (D) and Thr308-Akt (E) were assessed using Western blot and normalized to levels of total Akt. D) A significant interaction between prazosin and CORT treatment was detected for pSer473-Akt. Post hoc analysis further indicated a significant difference between water and prazosin in the control-treated animals (* P<0.05). E) No significant changes occurred with regards to pThr308-Akt (n=4-5).

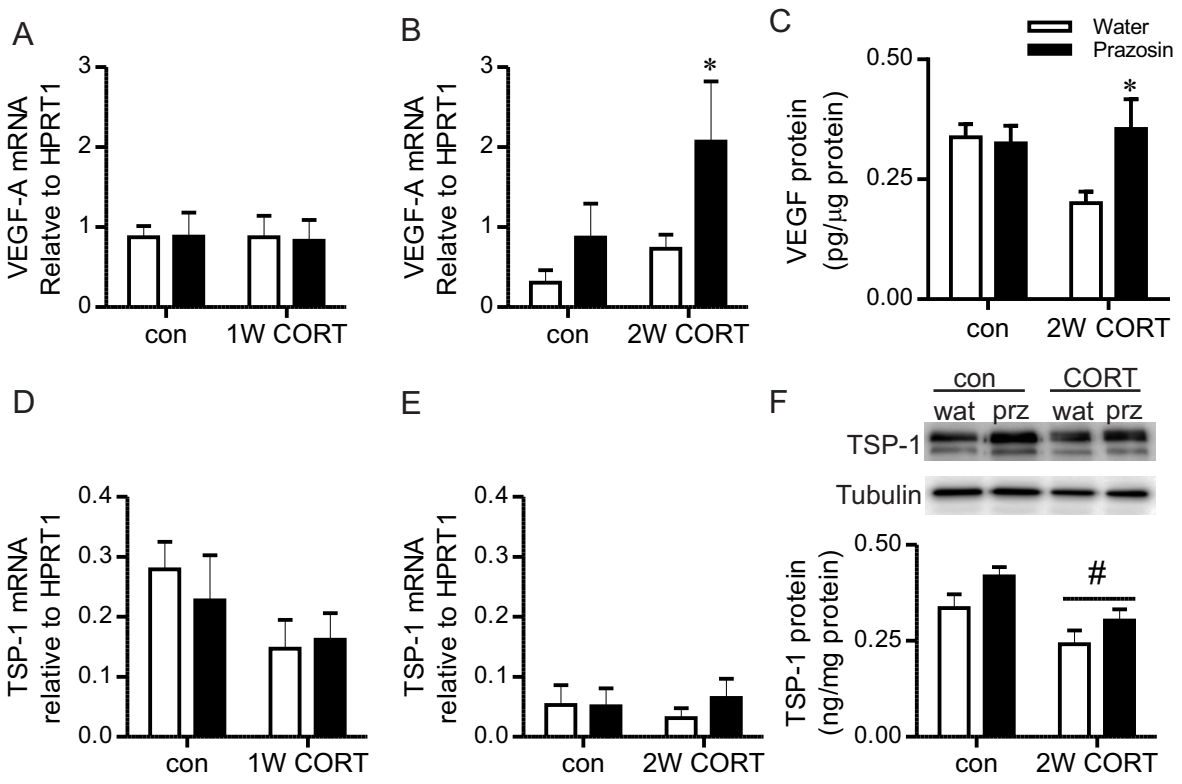

Figure 3.3: Alterations to VEGF-A and TSP-1 with elevated corticosterone with or without prazosin treatment

RNA or protein was isolated from the TA muscle after 1W or 2W of CORT treatment with or without the consumption of prazosin. Data was analyzed via two-way ANOVA and post hoc analysis. Taqman qPCR was used to assess the expression of VEGF-A (A & B), TSP-1 (D & E), which A) 1W did not significantly alter VEGF mRNA in response to CORT and/or prazosin. B) No significant effect of CORT was seen (P=0.08), while a significant prazosin effect was seen within the CORT group (* P<0.05). C) At the protein level, VEGF expression showed a trend towards a CORT effect (P=0.08), while expression was significantly increased in the CORT-prazosin cohort, compared to water matched CORT animals (* P<0.05). D) There was no significant Cort and/or prazosin effect on TSP-1 mRNA. E) TSP-1 mRNA after 2W showed no CORT or prazosin effect were noted. F) TSP-1 protein expression was significantly reduced with CORT treatment (# P<0.05), and there was a trend (P=0.086) for an increase in TSP-1 after 2W of prazosin treatment within control animals (n=4-9).

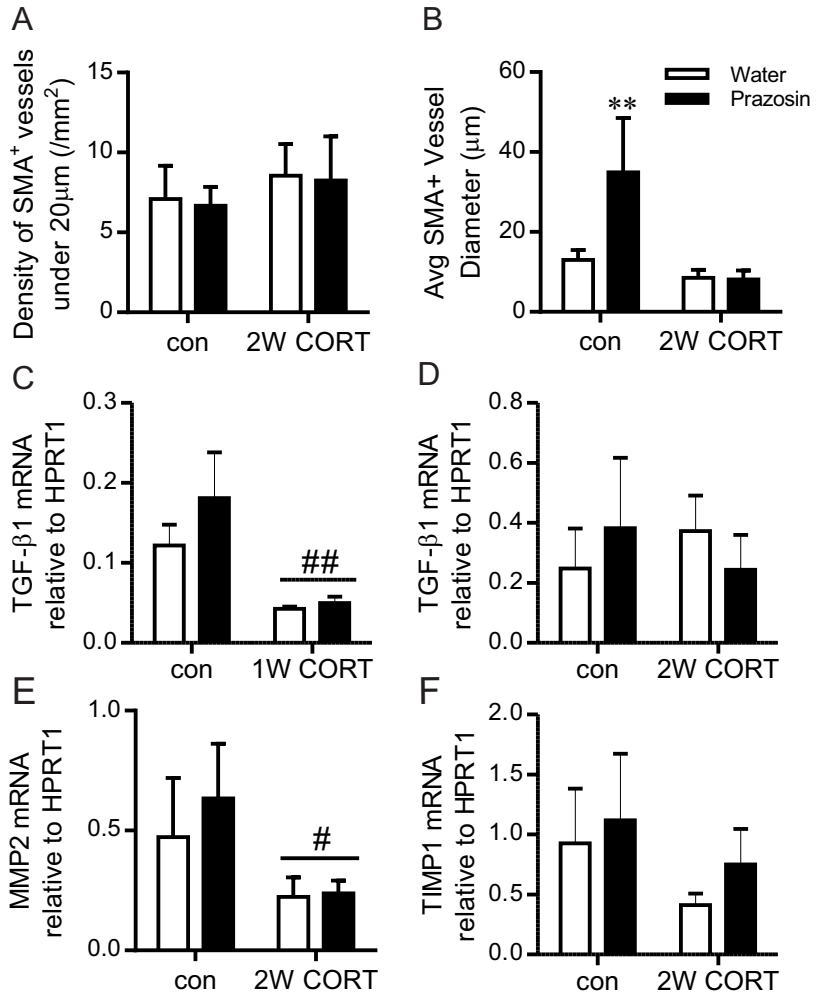

Figure 3.4: Alterations to flow induced arteriogenesis due to corticosterone treatment

Histological analysis of SMA positive vessels within the TA muscle post 2W treatment was calculated from 5 non-overlapping fields of view per rat. Two-way ANOVA and post hoc analysis was used to assess average SMA^+ density and average SMA^+ vessel diameter (n=5-13)A) Average SMA^+ density (per mm^2) was unaltered by CORT and/or prazosin treatment. B) Average SMA^+ vessel diameter was significantly elevated (** $P<0.05$ vs. corresponding water group) in control animals but not CORT-treated animals after 2W of concurrent prazosin treatment (n=5-9). Analysis of key arteriogenic factors occurred via mRNA isolation from the TA after 1W or 2W of CORT treatment with or without concurrent prazosin treatment. mRNA was quantified by Taqman qPCR, expressed as $2^{-\Delta Ct}$ and analyzed via two-way ANOVA. C) A CORT effect was detected on TGF-β1 mRNA expression within the 1W cohort of rats ($^{\#}$, $P<0.05$) which was absent at the 2W time-point (D). E) There was a significant CORT effect on MMP-2 expression within the 2W cohort ($^{\#}$ $P<0.05$). F) TIMP1 mRNA was unaltered by 2W of CORT-treatment.

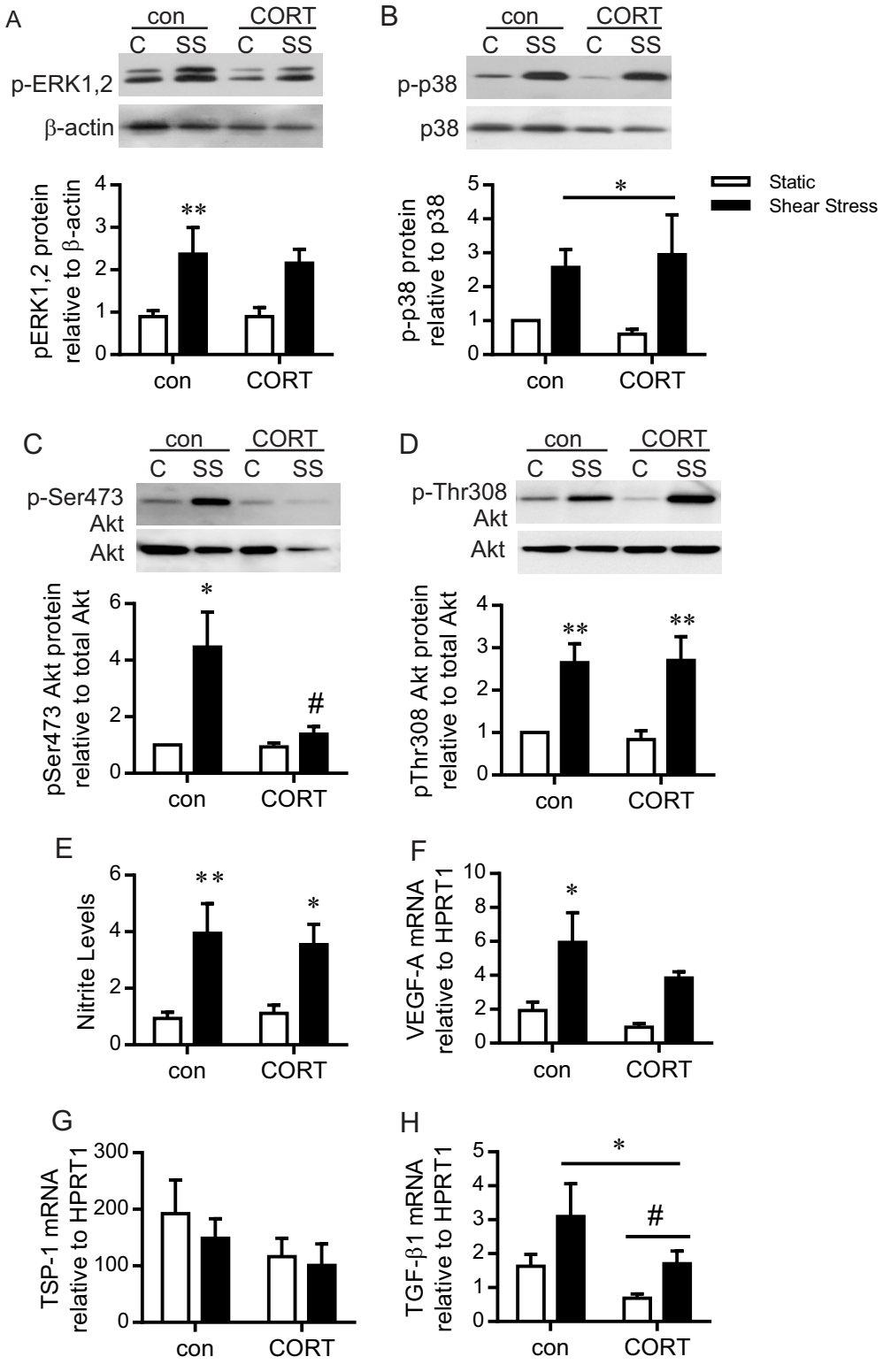
A
con
CORT
C SS C SS
p-ERK1,2
β-actin
pERK1,2 protein relative to β-actin
B
p-p38
p38
p-p38 protein relative to p38
Static
Shear Stress
C
p-Ser473 Akt
Akt
pSer473 Akt protein relative to total Akt
D
p-Thr308 Akt
pThr308 Akt protein relative to total Akt
E
Nitrite Levels
F
VEGF-A mRNA relative to HPRT1
G
TSP-1 mRNA relative to HPRT1
H
TGF-β1 mRNA relative to HPRT1

Figure 3.5: Influence of corticosterone on endothelial specific shear stress responsiveness

Cultured rat skeletal muscle endothelial cells were pre-treated with CORT (600 nM) for 48 hours prior to shear stress (15dynes/cm2), or were maintained in static conditions (C) for 2 hours. A-D: Whole cell lysates were analyzed by Western blotting. A) Phospho ERK1,2 protein level relative to b-actin. B) Phospho p38 protein level relative to total p38. C) Phospho-Ser473 Akt protein level relative to total Akt. D) Phospho-Thr308 Akt protein level relative to total Akt.
Two-way ANOVA indicated a significant shear effect for all kinases (pERK1,2- $P=0.007$; pp38- $P=0.02$; pSerAkt- $P=0.02$; pThrAkt- $P=0.0003$n=3-4). *, ** $P<0.05$, $P<0.01$ compared to respective static control, post hoc analysis. A significant interaction between shear stress and CORT was detected only for pAktSer473 (# $P=0.05$, n=3-4). E) Nitric oxide level was assessed indirectly by Griess assay. A main effect of shear stress was detected ($P=0.0006$; n=6). (*,**$P<0.05$ and $P<0.01$, relative to static controls as assessed via post hoc analysis). mRNA was isolated from skeletal muscle endothelial cells that were pre-treated for 48 hours with Cort (600nM) prior to 2 hr of elevated shear stress (15 dynes/cm2). mRNA was quantified by Taqman qPCR and expressed as 2-DCt. VEGF-A (F), TSP-1 (G) and TGF-b (H) mRNA levels were assessed relative to the housekeeping gene hypoxanthine-guanine phosphoribosyltransferase-1 (HPRT1). F) Two way ANOVA and post hoc test revealed a significant shear effect in control cells on VEGF-A mRNA expression (*$P<0.05$ compared to respective control group, n=6). G) No significant alterations were found in TSP-1 mRNA expression. H) There was an overall CORT and prazosin effect (* & # $P<0.05$ respectively) on TGF-b mRNA expression (n=4-6).

Supplementary Table 3.1: Body composition and plasma CORT levels of Control and CORT treated animals

	1 Week			
	Control-Water (n=5)	**Control-Prazosin (n=5)**	**CORT-Water (n=5)**	**CORT-Prazosin (n=5)**
Plasma corticosterone (ng/ml)	17.54±1.4	18.94±5.5	583.1±39.8#	485.5±72.3#
Body weight (kg)	0.36±0.01	0.36±0.008	0.26±0.006#	0.25±0.002#
TA relative weight (g/kg BW)	1.77±0.06	1.85±0.04	1.71±0.05	1.71±0.08
EDL relative weight (g/kg BW)	0.5±0.02	0.52±0.01	0.52±0.02	0.51±0.01
Plantaris relative weight (g/kg BW)	0.87±0.75	0.93±0.04	0.84±0.04	0.87±0.03
Soleus relative weight (g/kg BW)	0.41±0.01	0.38±0.02	0.49±0.01#	0.50±0.02#
Gastrocnemius relative weight (g/kg BW)	4.5±0.3	4.9±0.1	4.3±0.1	4.4±0.2
	2 Weeks			
	Control-Water (n=5)	**Control-Prazosin (n=5)**	**CORT-Water (n=9)**	**CORT-Prazosin (n=6)**
Plasma corticosterone (ng/ml)	16.21± 6.5	9.6 ±0.6	296.3±34.4#	284.7±34.2#
Body weight (kg)	0.37 ± 0.005	0.37±0.01	0.25±0.008#	0.25±0.009#
TA relative weight (g/kg BW)	1.88 ± 0.04	1.88±0.03	1.57±0.04#	1.58±0.05#
EDL relative weight (g/kg BW)	0.49 ± 0.01	0.52±0.01	0.48±0.02	0.47±0.02
Plantaris relative weight (g/kg BW)	0.91±0.04	0.92±0.02	0.82±0.03	0.81±0.03#
Soleus relative weight (g/kg BW)	0.45±0.009	0.40±0.02	0.54±0.02#	0.51±0.02#
Gastrocnemius relative weight (g/kg BW)	5.0±0.2	5.2±0.1	4.2±0.2#	4.3±0.1#

Values are expressed as mean ± standard error
c, main effect of CORT-treatment, Two-way ANOVA
#, significant difference compared to respective control group, Bonferroni post hoc analysis

Discussion:

The present study demonstrates that sustained exposure to elevated CORT results in a decrease in Ang-1 expression, which corresponds with the observed rarefaction of capillaries within skeletal muscle. A sustained elevation in skeletal muscle blood flow, induced by prazosin administration, prevents CORT-induced capillary rarefaction. However, both prazosin-induced angiogenesis and arteriogenesis are absent in CORT-treated animals. CORT does not interfere with several key endothelial cell shear stress signaling pathways including phosphorylation of ERK1/2 and p38 and the production of NO, but does reduce the magnitude of increase in the phosphorylation of Ser473Akt, and in VEGF-A and TGFβ1 mRNA, as compared to untreated cells. These findings highlight the broad influence of CORT on the microvasculature and indicate that sustained increases in blood flow can mitigate these deleterious effects.

The loss of capillaries in response to CORT treatment suggests the induction of endothelial cell apoptotic signaling or a loss of pro-survival signaling. Previously our group has shown that CORT does not induce apoptosis in cultured endothelial cells (Shikatani et al., 2012); therefore, in the current study we assessed several factors known to be associated with both endothelial cell survival and angiogenesis. Ang-1 is proposed to be important for the maintenance of a quiescent endothelium, structural integrity and endothelial cell survival through its activation of the Tie2 receptor (Brindle et al., 2006). The current study noted a decrease in Ang-1 after both 1W and 2W of CORT treatment, which paralleled CORT-mediated capillary rarefaction. In line with our observation, Ang-1 mRNA expression was shown to be down regulated and was postulated to contribute to the capillary rarefaction observed in hind-limb unloading (Wagatsuma,

2008), while 6 days of exposure to the synthetic GC, dexamethasone, reduced Ang-1 mRNA expression within the mouse adrenal gland (Féraud et al., 2003). However, Ang-1 expression was not altered by 48 hr. CORT treatment in cultured endothelial cells, suggesting that CORT does not exert direct transcriptional repression of Ang-1. *In vivo*, CORT may reduce the expression of Ang-1 mRNA from non-endothelial sources within the microenvironment (i.e. skeletal myocytes). Several of the cellular effects of Ang-1 are mediated through activation of the PI3K/Akt signaling pathway (Papapetropoulos, 2000). However, no change in the basal level of Akt phosphorylation (Ser473 or Thr308) was noted with CORT treatment. Thus, it is unlikely that a reduction in basal Akt activity underlies the CORT-induced capillary rarefaction, despite the established role of Akt in cell survival, proliferation and cell cycle progression (Cardone et al., 1998; Papapetropoulos, 2000; Manning and Cantley, 2007). Therefore, the mechanism through which reduced Ang-1 mRNA may contribute to GC-mediated capillary rarefaction remains to be established.

Endothelial cell derived VEGF-A has been shown to act as an important autocrine pro-survival signal (Lee et al., 2007). Although previous *in vitro* reports have demonstrated that GC treatment reduces VEGF-A mRNA in cultured endothelial cells (Shikatani et al., 2012), the current study found that CORT-repressive effects on VEGF-A were not sustained after 1 or 2 weeks of CORT treatment. Furthermore, the potent anti-angiogenic factor TSP-1 was not significantly increased by CORT treatment at any of the time points examined. A previous study reported a transient, but not sustained, GC-mediated increase in TSP-1 expression (Logie et al., 2010), and such an effect would have been missed in the time frame of our study. Thus, our data indicate that the

repression of Ang-1 expression, rather than alterations in VEGF-A or TSP-1, is the most plausible contributor to CORT-mediated capillary rarefaction. The apparent lack of direct influence of CORT on endothelial Ang-1 mRNA, when considered together with our prior finding that CORT treatment did not induce apoptosis in cultured microvascular endothelial cells (Shikatani et al., 2012), implies that CORT treatment evokes alterations within the skeletal muscle microenvironment that ultimately contributes to the loss of skeletal muscle capillaries.

Prazosin treatment was used as a tool to examine the impact of CORT on shear stress dependent remodeling within the skeletal muscle microvasculature, as it has been shown to induce angiogenesis and arteriogenesis within skeletal muscle of healthy rats (Skalak and Price, 1996; Zhou et al., 1998; Milkiewicz et al., 2001). While the expected angiogenic and arteriogenic responses occurred within control animals in the current study, they were absent in CORT-treated animals. Despite the lack of angiogenic response, 2W prazosin treatment effectively prevented the CORT-induced loss of capillaries. A partial recovery of Ang-1 mRNA level was detected at this time point. This effect is likely not a direct influence of blood flow on endothelial cell expression of Ang-1, since it was reported that shear stress does not modulate Ang-1 mRNA in cultured endothelial cells (Chlench et al., 2007). It is plausible that the prazosin-induced increase in blood flow stimulates the release of endothelial derived mediators, such as NO, which act as paracrine effectors of the expression of Ang-1 in neighboring cells. Nonetheless, the alteration in Ang-1 mRNA is modest with prazosin treatment and by itself, may not explain the lack of capillary rarefaction. It is likely that the concomitant restoration of

VEGF-A protein level in CORT-prazosin treated animals is an important contributor to the prevention of capillary rarefaction.

The absence of an angiogenic response to prazosin in CORT-treated animals could be attributed to impaired shear stress activation of angiogenic signals. Shear stress induced angiogenesis is mediated, in part, by an increase in pro-angiogenic signaling involving VEGF-A (Milkiewicz et al., 2001; Uchida et al., 2015) as well as NO production via Akt phosphorylation of eNOS (Hudlicka et al., 2006) and a down-regulation of anti-angiogenic factors such as TSP-1 (Bongrazio et al., 2008). In healthy rats, prazosin treatment has been reported to elicit an early increase in VEGF-A mRNA (within 2 days), preceding the increase in C:F (Milkiewicz et al., 2007). Thus, it is not surprising that we did not detect an increase in VEGF-A mRNA in control/prazosin treated animals, given the time points analyzed. Interestingly, VEGF-A mRNA increased after 2W of prazosin treatment within the CORT group, which may suggest that the angiogenic response to prazosin was delayed, but that it might have been detected if prazosin treatment continued beyond 2 weeks.

Elevated blood flow is known to induce the remodeling of arterioles (Skalak and Price, 1996). As expected, the current study noted that in healthy control animals, prazosin increased the average size of SMA^+ vessels, consistent with an outward remodeling response of arterioles to the sustained increase in blood flow. Prazosin induced arteriogenesis was absent in CORT-animals; this finding is corroborated by previous work that dexamethasone treatment impaired arteriogenesis in a mouse model of hind limb ischemia (Troidl et al., 2013). Arterial remodeling is regulated, in part, by TGFβ1 and MMP signaling (van Royen et al., 2002; Haas et al., 2007). In the current

study, *in vivo* CORT treatment transiently reduced the mRNA levels of TGFβ1 and a sustained reduction in MMP2 expression. Neither prazosin treatment nor *in vitro* shear stress was able to rescue the expression of TGFβ. Furthermore, in line with our findings, *in vitro* experiments have shown that MMP2 and 9 expression are significantly reduced by GCs (Burnham et al., 1991; Shikatani et al., 2012). While we did not detect changes in TIMP1 mRNA with CORT treatment, GC were reported to increase TIMP1 mRNA in cultured cerebral endothelial cells (Förster et al., 2007). Taken together, the reduction in TGFβ1 and MMP2 portray a scenario in which CORT alters the microvascular environment and represses flow-induced outward arteriolar remodeling by reducing the production of factors that can promote smooth muscle cell proliferation and extracellular matrix proteolysis.

Considering the lack of appropriate remodeling responses to prazosin treatment, *in vitro* endothelial cell culture experiments were employed to examine direct influences of CORT on endothelial cell shear stress responses. These data support the general conclusion that CORT-treated endothelial cells retain shear stress responsiveness of major cell signal pathways, such as pERK1/2 and p38MAPK. Interestingly, CORT did blunt pSer473 Akt phosphorylation in response to shear stress, both *in vitro* and *in vivo*. Evidence exists that phosphorylation at Thr308, and not Ser473, is required for Akt activation and the promotion of several downstream signaling pathways (Scheid and Woodgett, 2003), thus the functional consequence of reduced pSer473 Akt within the context of our study uncertain. Although we did not detect an alteration in shear stress induced NO production, a known downstream effector of Akt signaling (Dimmeler et al., 1999), we cannot exclude a possible influence on other Akt effectors that may have an

impact on capillary maintenance. It also is possible that CORT exerts influences through shear stress signaling pathways that were not assessed in the current study; however, CORT treatment did blunt the shear stress induced increases in both VEGF-A and TGFβ1 mRNA. Taken together these findings suggest that shear stress responsiveness is maintained although it is slightly blunted due to CORT pretreatment.

A limitation of the current study is that it did not include an assessment of muscle blood flow. The lack of angiogenesis and arteriolar remodeling within CORT-treated animals may reflect a failure to increase blood flow to the threshold level required for adaptive microvascular remodeling. CORT has been previously shown to elicit a reduction in blood flow within the temporal lobe (de Quervain et al., 2003). Thus, it is possible that prazosin treatment restored muscle blood flow within CORT-treated animals to normal baseline levels. As such, this level of shear stress was sufficient to prevent CORT-induced capillary rarefaction but not to induce further capillary growth.

The capillary network plays an important role in establishing the efficacy of insulin delivery to skeletal myocytes, thus having the potential to regulate insulin sensitivity and whole body metabolic homeostasis (Lillioja et al., 1987; Kusters and Barrett, 2015). Recently, the prazosin-induced increase in skeletal muscle capillary content was shown to improve insulin sensitivity and subsequent glucose disposal in healthy rats (Akerstrom et al., 2014). Our group has also found that C:F correlates positively with insulin sensitivity in CORT-treated animals (Dunford et al. 2016), indicating that the prevention of capillary rarefaction by prazosin can exert beneficial metabolic influences. These findings highlight the importance of assessing the molecular regulation of capillary rarefaction and potential ways of preventing it.

The current study demonstrates that CORT treatment evokes alterations within the skeletal muscle microenvironment that contributes to the loss of skeletal muscle capillaries. This may be due in part to sustained reduction in Ang-1 expression. Prazosin-induced augmentation in microvascular shear stress prevents CORT-induced capillary rarefaction, but is unable to elicit angiogenesis or arteriogenesis. Taken together these findings suggest that endothelial shear stress signaling is maintained, albeit slightly blunted, with prolonged CORT-treatment, thereby providing a tool for elevated muscle blood flow to prevent the deleterious effects of elevated levels of GCs.

Funding: This work was supported in part by Natural Science and Engineering Research Council of Canada Discovery Grants to TLH and MCR, and by a York University Faculty of Health minor research grant to TLH

Disclosures: None

Chapter 4:

Role of reactive oxygen species in glucocorticoid induced hypertension and capillary rarefaction

Erin R Mandel[1], Emily C. Dunford[1], Ghoncheh Abdifarkosh[1], Patrick Carson Turnbull[1], Christopher G. Perry[1], Michael C. Riddell[1] and Tara L. Haas[1,#]

School of Kinesiology and Health Science and Muscle Health Research Centre[1], York University, Toronto, ON Canada

Figures: 5
Tables: 2

I performed all of the experiments within this manuscript with the exception of Figure 4.2A & B, which was collected by Patrick Turnbull. Emily C. Dunford assisted with study design and animal conditioning. Ghoncheh Abdifarkosh assisted with animal care and systolic blood pressure collection.

Chapter Summary:

Sustained elevations in circulating glucocorticoids (GCs) induce hypertension and reduce skeletal muscle microvascular content, but little is known of the underlying mechanisms. We hypothesized that GC-mediated hypertension and capillary rarefaction would be prevented by treatment with Tempol, a reactive oxygen species (ROS) scavenger, as well as by prazosin, an α1 adrenergic receptor antagonist. Rats were implanted with corticosterone (CORT) or control pellets and subsequently treated for 2 weeks with Tempol (1 mmol/L) or prazosin (50mg/L). 2 weeks of CORT significantly elevated systolic blood pressure and reduced skeletal muscle blood flow. Reduced eNOS and increased endothelin-1 mRNA levels were detected after 1 week CORT, suggestive of GC-induced alterations in vascular tone. Protein carbonylation, an indicator of oxidative stress, was substantially increased in muscle after 1 week CORT. This was accompanied by a corresponding reduction in glutathione, ROS buffering, levels. While CORT reduced NADPH oxidase subunit expression within whole muscle, 600 nM CORT (48 hours) increased mRNA of NOX1 in cultured rat skeletal muscle endothelial cells. Tempol alleviated oxidative stress and was partially effective in attenuating hypertension, but exerted no rescue of skeletal muscle microvascular rarefaction. Conversely, prazosin ameliorated all of these deleterious effects of CORT and the reduction in systolic blood pressure was maintained upon drug cessation. Taken together, the current study demonstrates that CORT reduces muscle blood flow and increases systolic pressure, which involves both increases in oxidative stress and a shift to a vasoconstrictor profile. The capacity of prazosin but not Tempol to prevent CORT-induced microvascular

rarefaction highlights the importance of muscle blood flow in the maintenance of microvascular content, which in turn, will impact overall cardiovascular health.

Introduction:

Glucocorticoids (GCs) are steroid hormones that exert a strong angiostatic influence (Folkman, 1971; Small et al., 2005), induce skeletal muscle capillary rarefaction (Shikatani et al., 2012; Mandel et al., 2016) and hypertension (Vogt and Schmid-Schobein, 2001; Bachhav et al., 2011; van Raalte et al., 2013; Baum and Moe, 2008). While the precise mechanisms mediating the development of GC-induced hypertension are unclear, vascular alterations that are generally known to contribute to hypertension include excessive vasoconstriction (Yang and Zhang, 2004) and/or microvascular rarefaction (Humar et al., 2009). These alterations may occur due to changes in nitric oxide (NO) bioavailability (Watson et al., 2008), vessel perfusion (Humar et al., 2009) or reactive oxygen species (ROS) levels (Zhang et al., 2004; Staiculescu et al., 2014). Alteration to one or more of these factors due to GC excess could be an important contributor to GC-mediated hypertension.

Within the vasculature, moderate levels of ROS can regulate several cellular processes including cell growth, proliferation and apoptosis (Zhang and Gutterman, 2007). Cellular sources of ROS include mitochondrial respiration (Han et al., 2001), NADPH oxidase (Nauseef, 2008), xanthine oxidase (Garattini et al., 2003) and eNOS uncoupling (Marchesi et al., 2009). The excessive production of ROS and subsequent oxidative stress has been shown to play a pivotal role in the development of hypertension (Montezano and Touyz, 2014). ROS can impact the vasodilator /vasoconstrictor balance through reduced NO and increased endothelin-1 (ET-1) expression thereby increasing vascular tone (Kim et al., 2006; Montezano and Touyz, 2014). Elevated ROS also may induce endothelial cell apoptosis and skeletal muscle microvascular rarefaction

(Kobayashi et al., 2005). Tempol is a stable cell permeant piperidine nitroxide that acts as a superoxide dismutase mimetic (Wilcox and Pearlman, 2008). Tempol has been shown to reduce blood pressure in the spontaneously hypertensive rat model (Schnackenberg et al., 1998) and to protect lipids and proteins from oxidative damage (Damiani et al., 2000). Furthermore, dexamethasone-induced hypertensive rats experience a reduction in blood pressure with concurrent Tempol treatment (Zhang et al., 2004).

It has been recently established that skeletal muscle microvascular rarefaction is elicited by GC excess (Shikatani et al., 2012; Mandel et al., 2016). Alterations in skeletal muscle microvascular content are an important determinant of overall peripheral resistance (Greene et al., 1989), thus providing a mechanism through which microvascular rarefaction contributes to the development/exacerbation of hypertension (Greene et al., 1989; Humar et al., 2009). Furthermore, hypertension is a potent stimulus for microvascular rarefaction (Hansen-Smith et al., 1996) thereby creating a vicious and deleterious loop. While our group has established a role for GC excess in eliciting microvascular rarefaction, the instigating mechanisms are still unclear.

Therefore, the current study set out to examine the role of GC-induced increases in oxidative stress, which may contribute to the altered microvascular content, vascular tone and blood pressure regulation associated with GC excess. We hypothesized that both GC-mediated hypertension and capillary rarefaction are a consequence of increased oxidative stress and would be prevented with concurrent administration of Tempol. We compared the influence of Tempol to that of the anti-hypertensive drug prazosin, which is a selective α1-adrenergic receptor antagonist that induces skeletal muscle angiogenesis in

healthy animals (Ziada et al. 1989; Zhou et al. 1998; Rivilis et al. 2002; Gee et al. 2010) and prevents GC-induced capillary rarefaction (Mandel et al., 2016).

Materials and Methods:

All animal experiments were approved by York University Animal Care Committee and conducted in accordance with the Canadian Council for Animal Care Guidelines.

Animal Protocol

Male Sprague Dawley rats (initial weight 200 to 250g) were purchased from Charles River Laboratories (Montreal, QC, Canada). Rats were housed in the York University Vivarium in 12 hour light-dark cycle. After 7 days acclimation, animals were anesthetized by isoflurane inhalation and were implanted with four 100mg wax (control) or CORT pellets (C2505, Sigma-Aldrich, Oakville, Ontario, Canada) via subcutaneous incision in the mid-scapular region, as described previously (Shpilberg et al., 2012). Rats recovered in individual cages and were given ampicillin (20mg/kg body weight) in their drinking water for 2 days after which they were given regular water. All animals were fed a standard rodent chow diet (14% fat, 54% carbohydrate, 32% fat; 3.0 calories/g) *ad libitum*.

Protocol 1: The tibialis anterior (TA) and gastrocnemius muscles (N=10) from a previously conducted experiment (Mandel et al., 2016) were used for mRNA and glutathione assessments. This subset of animals, termed 1W CORT, was either control-water or CORT-water treated for 9 days prior to tissue collection.

Protocol 2: Control and CORT groups (N=8) given regular drinking water were used in this protocol to assess the degree of hypertension elicited by CORT treatment. The animals had BP taken on D0, prior to pellet implantation and on D4, 7, 14 and 16 post pellet implantation.

Protocol 3: Control and CORT groups (N=36) were given regular drinking water (CORT-water and con-water), drinking water containing prazosin (50 mg/L; P7791, Sigma Aldrich Canada) (CORT-prazosin and con-prazosin), or drinking water containing Tempol (1 mmol/L, 176141, Sigma Aldrich Canada) (CORT-Tempol, and con-Tempol). This dose of prazosin has previously been shown to prevent GC-mediated capillary rarefaction (Mandel et al., 2016) and this dose of Tempol has been previously shown to significantly reduce blood pressure in male Sprague Dawley rats treated with dexamethasone (Zhang et al., 2004). Prazosin or Tempol treatment began on day 2, and continued for 2 weeks. On day 15, drinking water containing prazosin or Tempol was replaced with untreated drinking water. Based on the pharmokinetics of both prazosin and Tempol, it was presumed that these drugs would no longer exert functional effects at the time of D16 measurements (Jaillon, 1980; Ueda et al., 2003).

Blood Pressure Assessment

Systolic blood pressure was assessed non-invasively via tail plethysmography (LE 5001 Pressure Meter, Harvard Apparatus) on days 0, 4, 7, 14 and 16 days while animals were lightly sedated (isoflurane inhalation) and body temperature was maintained. D16 blood pressure was assessed 18 hours after removal of prazosin or Tempol from the drinking water.

Hind-limb muscle blood flow

Skeletal muscle blood flow was assessed on D16, using a microsphere protocol modified from (Deveci and Egginton, 1999). Briefly, animals were anesthetized with isoflurane and fluorescent microspheres (500,000 spheres, 15μm in diameter, in 0.5 ml PBS) (Molecular Probes, FluoSpheres, #F8844) were injected directly into the left ventricle.

The brain, extensor digitorum longus (EDL) and soleus were immediately collected and flash frozen in liquid nitrogen. For analysis, tissue was incubated in 2M 0.5% tween ethanoic KOH for 24 hours at 37°C. After digestion, tubes were spun at 3000RPM for 15 minutes, followed by two ethanoic-tween washes. The microsphere pellet was re-suspended in xylene and the fluorescent signal was detected with a microplate reader (Cytation^{TM} 3, Biotek, Vermont USA). The normalized fluorescent intensity (FI) was calculated relative to tissue mass (FI/100g tissue). Relative blood flows were estimated by expressing the normalized FI of EDL and soleus muscles as a ratio to normalized brain FI, to discount the impact of artifacts associated with animal-to-animal variability in the microsphere injection. Muscle flow was normalized to the brain flow, with the assumption that brain blood flow would not be affected by GC treatment, as autoregulatory mechanisms maintain constant brain blood flow under a wide range of physiological and pathological conditions (Paulson et al., 1989; Strandgaard and Paulson, 1995).

Tissue Isolation

Hind-limb skeletal muscles were removed under isoflurane anesthesia. Muscles were weighed and snap frozen in liquid nitrogen for RNA and protein analyses or frozen in liquid nitrogen cooled isopentane for histology.

Bioinformatics search for glucocorticoid response elements within NADPH oxidase subunits

A bioinformatics search was conducted using the MultiTF function within ECR browser (Ovcharenko et al., 2004) to identify the multi-species (murine and human) conserved consensus glucocorticoid response elements (GRE), specifically examining the genes that

encode NADPH-oxidase subunits: NOX1, NOX2 ($gp91^{phox}$), NOX3, $p22^{phox}$, $p47^{phox}$, $p40^{phox}$ and $p67^{phox}$. The search focused on identification of putative GRE (with a predefined matrix similarity of 0.85 or greater) within the "start" region of these genes, which was defined as +/-3 kb relative to the first exon.

RNA extraction and Real Time qPCR

RNA was isolated from TA muscle using the Qiagen RNeasy Fibrous Tissue Mini Kit (74704, Qiagen, Toronto, ON Canada) as per the manufacturer's instructions. RNA was isolated from cultured endothelial cells using cells to cDNA lysis buffer (#AM8723, Invitrogen Canada; Burlington, ON Canada). RNA was reverse transcribed using MMLV reverse transcriptase (New England Biolabs, Whitby ON Canada). cDNA were analyzed by Taqman qPCR using qPCR mastermix (Invitrogen Canada) and Taqman probes for rat HPRT (Rn01527840), eNOS (Rn02132634), α-1 adrenergic receptor (Rn00567876), NOX1 (Rn00586652_m1), NOX2 ($gp91^{phox}$, Rn00576710_m1), NOX3 (Rn01430441_m1), $p47^{phox}$ (Rn00586945_m1) & ET-1 (Rn00561129_m1) using the ABI 7500 Fast PCR system (Invitrogen Canada). For each sample, the comparative Ct method was used to determine mRNA expression of target genes relative to the housekeeping gene HPRT and expressed as $2^{-\Delta Ct}$.

Muscle Histology and cell staining

10μm cryosections of TA muscle were fixed with 3.7% paraformaldehyde and stained with fluorescein isothiocyanate-conjugated *Griffonia simplicifolia* isolectin B4 (1:100; Vector Laboratories, Burlington ON, Canada) and anti-smooth muscle actin-Cy3 (1:300; C6198, Sigma Aldrich, Oakville ON, Canada). Sections were viewed using a Zeiss M200 inverted microscope with 20x objective. Images were captured using a cooled CCD

camera using Metamorph imaging software. Capillary-to-fiber (C:F) counts were averaged from 3 to 4 independent fields of view per rat by a blinded observer.

Skeletal muscle glutathione levels

Frozen muscle samples were homogenized in a 50mM Tris based buffer containing 20mM boric acid, 2mM L-serine, 20μM acivicin and 5mM N-ethylmaleimide. Muscle homogenate was acidified using trichloroacetic acid for reduced glutathione (GSH) determination, and 15% perchloric acid (PCA, Caledon Laboratories Ltd, Georgetown, Canada) for oxidized glutathione (GSSG). NEM irreversibly binds to GSH producing a GS-NEM conjugate, preventing auto-oxidation of glutathione during sample preparation. Samples were centrifuged at 20,000 RCF for 5 min (4^{o}C). The TCA-acidified muscle sample was then used for GSH analyses by HPLC (Agilent 1100) with column separation performed using a Zorbax high performance analytical 4.6x150mm 5μm column (Agilent, Santa Clara, USA). PCA-acidified muscle sample was diluted (1:5) in 0.5M NaOH. Samples were then incubated in the dark with 0.1% O-pthalymide (OPA, Sigma-Aldrich, Oakville, Canada) creating a GS-OPA conjugate and were then ready for GSSG quantification by HPLC as described above. Prior to acid deproteination, a sample of muscle homogenate was removed for protein concentration analysis using a Pierce BCA protein assay kit (Thermo, Fisher Scientific, Waltham, USA). All values were referenced to protein concentration and reported in μmol/g protein.

GSH was determined as previously described (Giustarini et al., 2013). Briefly, 0.25% glacial acetic acid with 6% acetonitrile was used for mobile phase at a flow rate of 1.25ml/min. GS-NEM conjugate was detected using a using a modular variable

wavelength detector at 265nm wavelength. Values were referenced to a standard curve of reduced glutathione (Sigma-Aldrich, Oakville, Canada) and expressed as μmol/g protein. Reduced glutathione was determined by separation by HPLC as previously described (Kand'ár et al., 2007). Briefly, 25mM Na_2HPO_4 in HPLC grade water with 15% methanol at 0.5ml/min was used for mobile phase separation at a flow rate 0.5ml/min. Following column separation, samples flowed through a flow-through cuvette (FireflySci 8830, New York, USA) in a PTI QuantaMaster 40 spectrofluorometer (Horiba, New Jersey, USA). GS-OPA conjugate was excited at 350nm and emission was detected at 420nm. Values were referenced to a standard curve of GSSG (Sigma-Aldrich, Oakville, Canada) and expressed as μmol/g protein.

Total glutathione was calculated as the sum of GSH and GSSG values.

Oxidative stress

Protein carbonylation was assessed as an indirect measure of accumulated oxidative stress (Davies et al., 1999) using a Protein Carbonyl Colorimetric Assay Kit (Caymen Chemical Company, # 10005020, Ann Arbor MI). Briefly, 100mg of tissue was extracted from the TA or gastrocnemius muscle in 1X PBS containing 1mM EDTA. Protein carbonyl content was assessed as per the manufacturer's instructions and was expressed as nmol/μg of total protein.

Cell culture experiments

Skeletal muscle microvascular endothelial cells were isolated from the TA muscle of male Sprague Dawley rats as described previously (Han et al., 2003). Cells were cultured with Dulbecco's Modified Eagle Medium (Invitrogen) supplemented with 10% heat denatured FBS, 1mM sodium pyruvate, 1mM Glutamax (Invitrogen), 50 units penicillin,

0.5mg/ml streptomycin and 1.25μg/ml Fungizone (Gibco). Cells were used for experiments between passages 4 to 6. Endothelial cells were plated on 12 well plates and subsequently treated with 600 nM CORT for 48 hours (Control or CORT), a dose that previously was shown to inhibit angiogenic behavior (Small et al., 2005; Shikatani et al., 2012). RNA was isolated from cultured endothelial cells using cells-to-cDNA lysis buffer (#AM8723, Invitrogen Canada; Burlington, ON Canada).

Statistical Analysis

All results were expressed as mean ± SEM and analyzed by one-way or two-way ANOVA with subsequent Bonferroni post hoc tests (Prism4; Graphpad software Inc; La Jolla, CA, USA). Systolic blood pressure was analyzed using a proc mixed of general linear model for a repeated measures analysis using SAS software, to account for repeated measures, the various conditions and treatment groups. $P < 0.05$ was considered statistically significant.

Results:

For full animal characteristics and details seen supplementary Table 4.1

CORT influence on blood pressure and skeletal muscle blood flow

Systolic blood pressure was significantly elevated after 4 days of CORT-treatment and remained elevated throughout the duration (D7 & 14) of the experiment (Figure 4.1A). After 2W of CORT treatment, systolic blood pressure was 78% higher than control animals (157±8 vs. 87±5 mmHg) (Figure 4.1A). CORT significantly decreased relative EDL blood flow (Figure 4.1B) but did not significantly alter relative soleus blood flow (35.1±16.5 vs. 19.2±11.2, $P>0.05$). eNOS mRNA was significantly reduced while ET-1 mRNA concurrently increased in TA muscle with 1W of CORT treatment (Figure 4.1C & D), suggesting an increase in vasoconstrictor signals. α1 adrenergic receptor mRNA expression was not significantly altered by 1W of CORT treatment (Figure 4.1E).

CORT induced oxidative stress

Augmented ROS levels are postulate to result in increased vascular tone (Staiculescu et al., 2014). ROS can accumulate due to increased ROS production and/or reduced ROS buffering. The glutathione system plays a critical role in protecting cells from ROS-mediated damage (Dringen, 2000). Both total glutathione and GSH (reduced glutathione) were significantly reduced with 1W of CORT treatment (Figure 4.2A & B), indicating a greatly diminished capacity for ROS buffering. Protein carbonylation was significantly increased in the CORT-treated muscles (Figure 4.2C).

NADPH oxidase is a major producer of cellular ROS (Siuda et al., 2014), thus an alteration in the expression of NADPH oxidase subunits may underlie the observed increased oxidative stress. A bioinformatics search revealed that several NADPH oxidase

subunits contained one or more conserved GC receptor-binding elements within their start region; NOX1 has 2 conserved sites, NOX2 has 4 conserved sites and NOX3 has 3 conserved sites within the start region (Figure 4.3A). $p47^{phox}$ was found to have 2 conserved sites, however these were located greater than 5 kb distal to the first exon. The subunits $p22^{phox}$, $p67^{phox}$ and $p40^{phox}$ did not have any conserved GRE sequences and thus were excluded from further analysis.

NOX1, NOX2 and $p47^{phox}$ mRNA were significantly reduced within whole muscle homogenates after 1W CORT (Figure 4.3B-D). NOX3 levels were below the level of detection. Conversely, NOX1 mRNA was significantly increased in cultured microvascular endothelial cells after 48 hours of CORT (Figure 4.3E). No significant changes in $p47^{phox}$ were seen (Figure 4.3F), and both NOX2 and NOX3 mRNA were undetectable in the cultured rat endothelial cells. These data indicate that CORT may repress whole muscle expression of NADPH oxidase subunits while increasing the level of NOX1 in endothelial cells.

Influence of Tempol or prazosin treatment on CORT-induced hypertension and capillary rarefaction

To investigate the role of oxidative stress on the development of CORT-induced hypertension and capillary rarefaction, we co-treated rats with the superoxide scavenger Tempol. We compared the influence of Tempol with that of the α1-adrenergic receptor antagonist prazosin, which has established influences both as an anti-hypertensive (Jaillon, 1980) as well as a preventer of GC-induced capillary rarefaction (Mandel et al., 2016). As anticipated, Tempol was effective in reducing CORT-induced oxidative stress, as evidenced by the significant reduction in protein carbonylation with 2W Tempol co-

treatment when compared to CORT alone (Figure 4.4A). Prazosin co-treatment also abolished the CORT-induced increase in protein carbonylation (Figure 4.4A).

GC treatment elicited substantive increases in systolic blood pressure after as little as 4 days (Figure 4.4B). Tempol and prazosin each significantly abrogated CORT-induced hypertension. The prazosin-induced reduction in systolic blood pressure was detectable at the 4 day time-point, whereas Tempol did not exert a significant reduction in systolic blood pressure until the 7 day time-point (Figure 4.4B). Neither Tempol nor prazosin significantly affected systolic blood pressure in control rats (Figure 4.4B & C). After 14 days, systolic blood pressure was 51% higher in CORT-water vs. control-water treated rats (Figure 4.4C). The percent increase in systolic blood pressure in both the CORT-prazosin and CORT-Tempol groups was significantly less than observed with CORT-water. However, only the CORT-prazosin group displayed a systolic blood pressure that was not significantly different from its respective control condition (Figure 4.4C). Alterations in heart rate over the course of the experiment see supplementary Figure 4.1.

The depressor influences of prazosin and Tempol may be a consequence of functional improvements, such as a reduction in ROS and a shift in the balance between vasodilators vs. vasoconstrictors, or may be associated with improved structural alterations in the vasculature, such as outward remodeling of small muscular arteries and arterioles. While functional alterations may depend on the continued presence of the drugs, structural remodeling should continue to exert a positive influence on systolic blood pressure without the drug being present. Thus, we reasoned that functional and structural influences could be distinguished from one another by reassessing blood

pressure after the removal and clearance of prazosin or Tempol. As expected, systolic blood pressure at day 16 remained consistently elevated in the CORT-water group, and systolic blood pressure remained unaltered compared to day 14 in all control groups (Figure 4.4D). Notably, systolic blood pressure in CORT-prazosin animals was not different at day 16 relative to day 14 values, and remained significantly lower than in the CORT-water group (Figure 4.4D). However, the removal of Tempol resulted in a significant increase in systolic blood pressure compared to the respective control group, such that systolic blood pressure in this group was no longer different from that of CORT-water animals (Figure 4.4D).

2W CORT caused a significant reduction in EDL C:F (Figure 5A &B), in line with previous reports (Mandel et al., 2016). CORT-mediated capillary rarefaction was prevented by concurrent prazosin but not Tempol treatment (Figure 4.5B &C). Furthermore, Tempol did not exert an angiogenic effect within control animals (Figure 4.5B & C). The lack of angiogenic influence of Tempol was confirmed by analysis of C:F in the TA muscle (control: 1.71±0.03; control-Tempol:1.73±0.03; CORT: 1.51±0.05; CORT-Tempol: 1.46±0.06).

A significant negative correlation between day 7 systolic blood pressure and day 16 skeletal muscle C:F was detected when comparing control with CORT (r= -0.84; Figure 4.5C) and CORT-water with CORT-prazosin (r=-0.77; Figure 4.5D). This may suggest that systolic blood pressure is a key determinant of C:F. However, this relationship was not maintained in the CORT-Tempol group (r=-0.16; Figure 4.5E). These findings highlight that alterations in systolic blood pressure are not solely

responsible for alterations in microvascular content and that additional factors may be important regulators of C:F in CORT-treated animals.

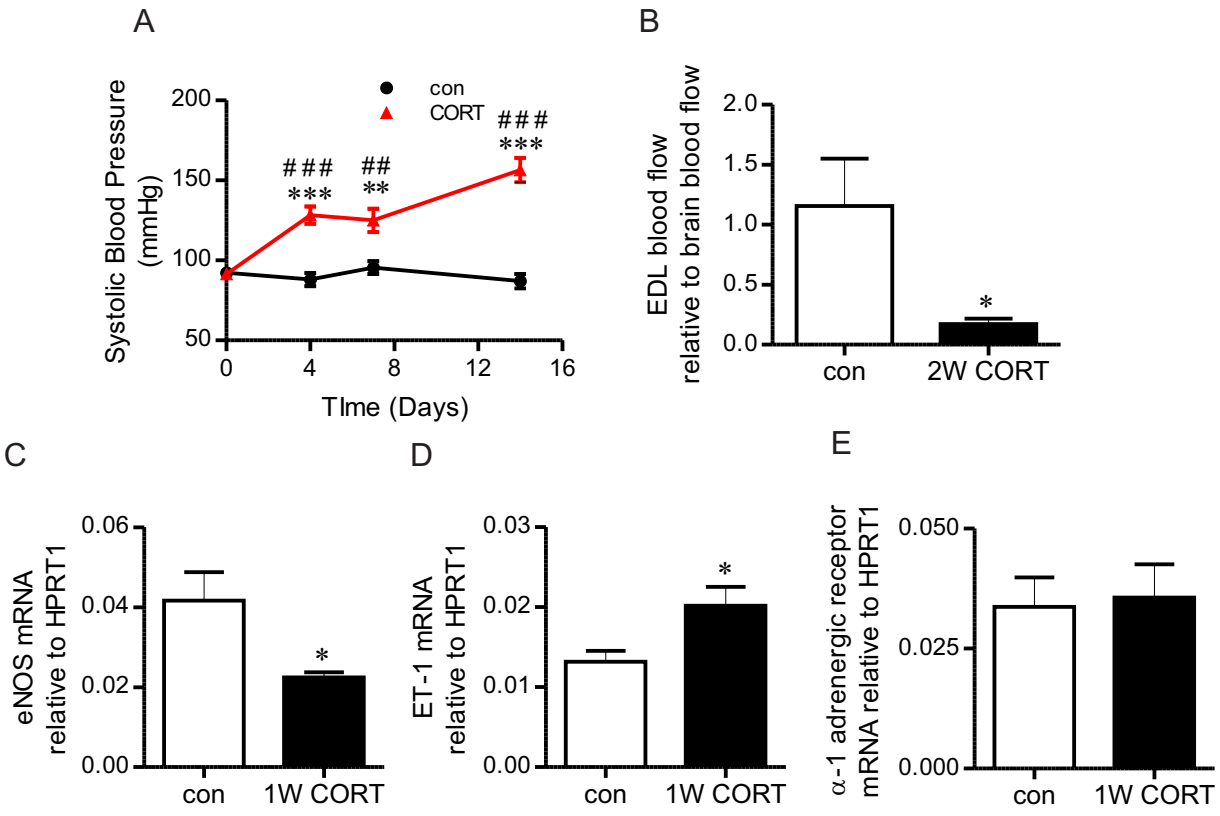

Figure 4.1: CORT induces hypertension and lowers skeletal muscle blood flow

A) Blood pressure was measured via tail plethysmography at D0, D4, D7 and D14. 1-way ANOVA and Tukey's multiple comparison post hoc tests were used to analyze the data. ** P=0.001 and *** P<0.0001 compared to respective D0 group; $^{\#\#}$ P<0.001 and $^{\#\#\#}$ P<0.0001 relative to control group (n=4).
B) Skeletal muscle blood flow was assessed using intra-ventricular infusion of fluorescent microspheres. Microsphere deposition in the muscle (Fluorescence AU/mg muscle) was normalized to that of the brain within each animal. The influence of CORT was analyzed via unpaired Student's t-test. *P<0.5 compared to 2W CORT (n=7-8).
C-E) RNA was isolated from the TA muscle after 1W of CORT treatment and quantified by Taqman qPCR to assess the relative expression eNOS (C), ET-1 (D) or α1-adrenergic receptor expression (E), expressed as $2^{-\Delta Ct}$ relative to the housekeeping gene hypoxanthine-guanine phosphoribosyltransferase-1 (HPRT1). The influence of CORT was assessed via unpaired t-test, * P<0.05 compared to controls (n=5).

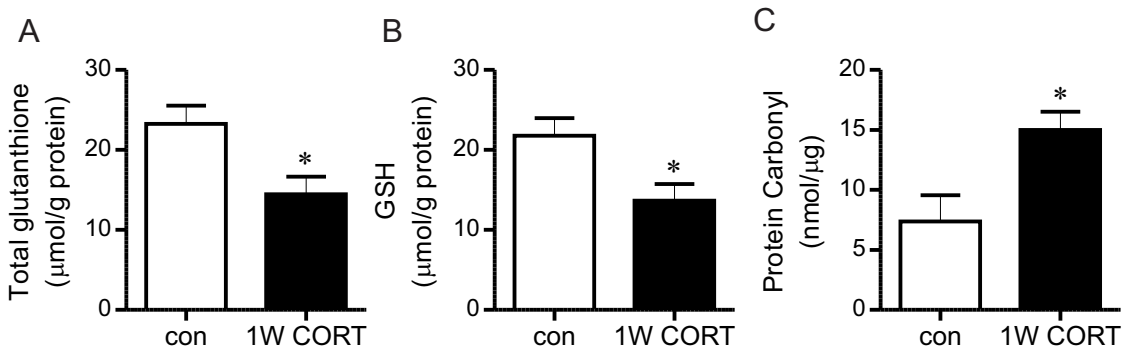

Figure 4.2: CORT reduces reactive oxygen species buffering and increases oxidative stress within skeletal muscle

Protein was extracted from the gastrocnemius muscle after 1W of CORT treatment to assess glutathione (A), reduced glutathione (GSH) (B) and protein carbonylation (C) levels, as a stable marker of oxidative stress. * $P<0.05$ relative to controls (n=5).

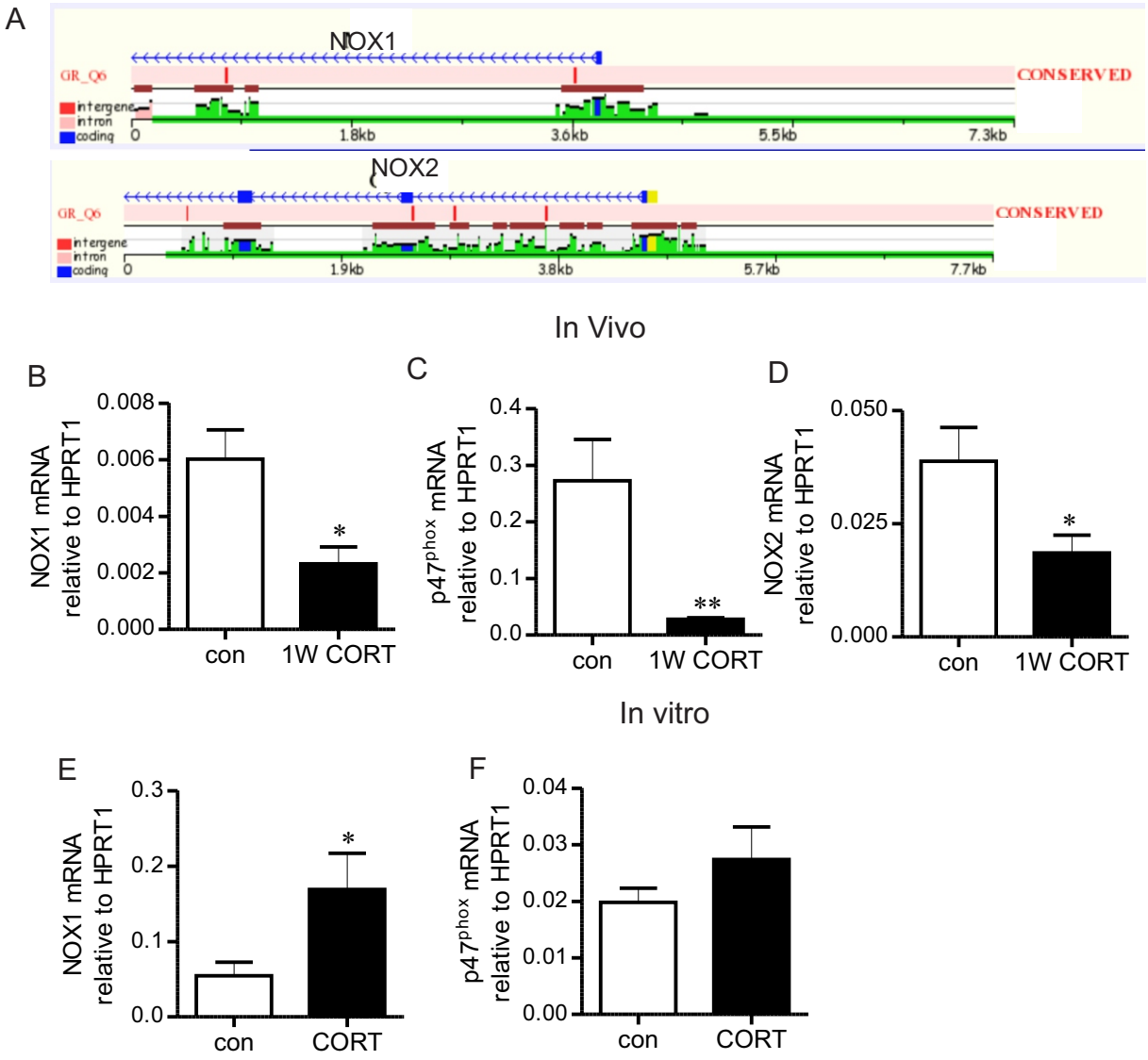

Figure 4.3: Effect of CORT treatment on NADPH oxidase mRNA expression

A) Representative image of the bioinformatics search result highlighting putative GRE within the "start" regions of NOX1 and NOX2 genes.
RNA was isolated from the TA muscle after 1W of CORT treatment, quantified by Taqman qPCR via $2^{-\Delta Ct}$ relative to the housekeeping gene HPRT1 to analyze the expression of NOX1 (B), NOX-2 (C) and in $p47^{phox}$ (D) mRNA after 1W of CORT treatment. Data was assessed via unpaired t-test, $*P<0.05$ relative to controls (n=5).
Rat skeletal muscle endothelial cells were pre-treated for 48 hours with CORT (600nM) followed by mRNA isolation and quantification by Taqman qPCR. mRNA expression of NOX1 (D) and $p47^{phox}$ (E), expressed as $2^{-\Delta Ct}$, relative to HPRT was assessed and analyzed via unpaired students unpaired t-test. $*P<0.05$ relative to control cells (n=5).

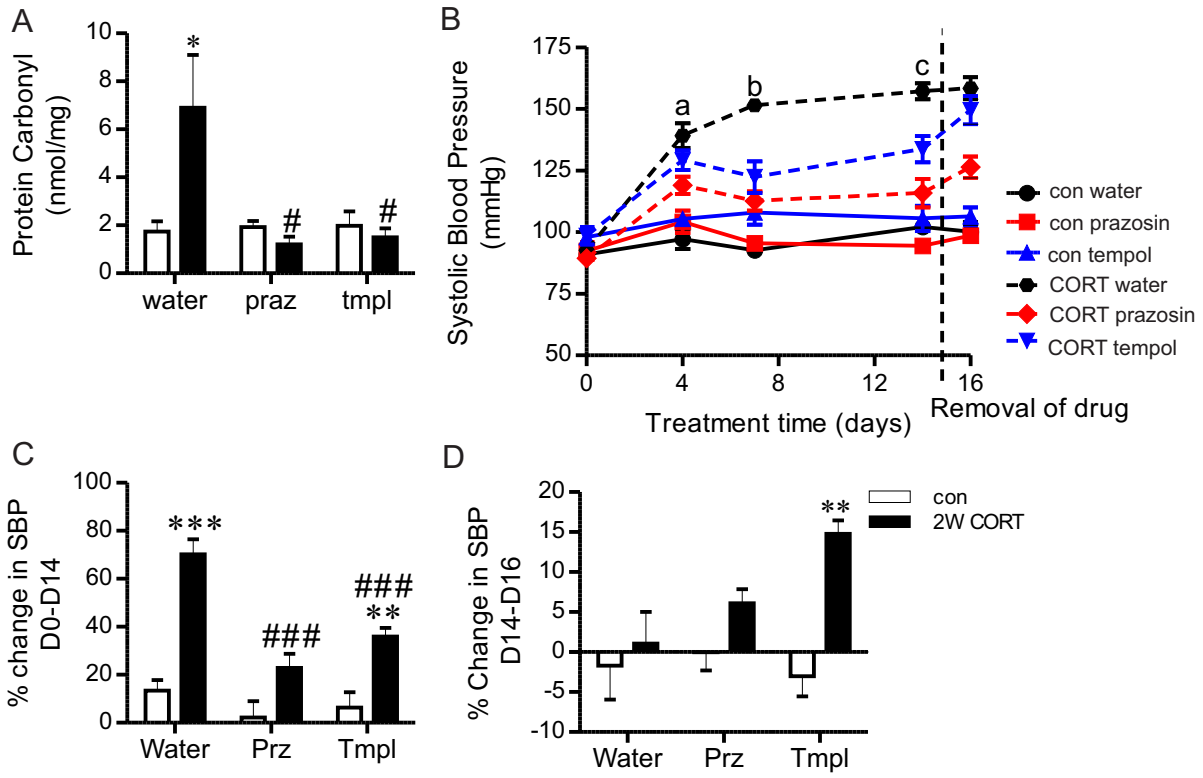

Figure 4.4:CORT-induced oxidative stress and hypertension is ameliorated by Tempol or prazosin co-treatment

A) Protein carbonyl content was assessed after 2W of CORT-treatment, with or without concurrent prazosin or Tempol treatment via two-way ANOVA. * $P<0.05$ relative to respective water group, # $P<0.05$ relative to corresponding control group (n=5-9).
Blood pressure was measured via tail plethsymography at D0, D4, D7, D14 and D16. B) A general linear model of repeated measures analysis was used to analyze the blood pressure data over days 0 to 14. D0 systolic blood pressure was not significantly different between the groups ($P=0.108$). Systolic blood pressure was not significantly different between the 3 control groups (con-water, con-prazosin, con-Tempol) at any time point, thus for all subsequent analyses, CORT-groups were compared to a composite of controls. a: D4 blood pressure CORT-water was significantly different from control groups ($P<0.0001$); CORT-water was significantly different compared to CORT-prazosin ($P=0.008$) but not CORT-Tempol ($P=0.15$). There was no significant difference between CORT-prazosin and CORT-Tempol ($P=0.08$). b: D7 blood pressure was significantly elevated in CORT-water compared to control animals ($P<0.0001$); both CORT-prazosin and CORT-Tempol were significantly different than CORT-water ($P<0.0001$ & $P<0.002$, respectively) but remained significantly elevated compared to control animals ($P<0.05$). c: D14 blood pressure was significantly elevated in CORT-water compared to control animals ($P<0.0001$), and this was significantly improved by both prazosin and Tempol treatments ($P<0.0001$ & $P=0.004$, respectively). Blood pressure was significantly different between CORT-prazosin and CORT-Tempol ($P=0.047$).
C) The percent change in blood pressure (delta systolic blood pressure) between day 0 and day 14 was assessed using two-way ANOVA and post hoc tests. ***$P<0.001$ compared to corresponding control group, $^{###}P<0.001$ compared to respective water group. (n=6)
D) Blood pressure was re-assessed on D16, 18 hours after removal of prazosin or Tempol. The percent change in blood pressure relative to D14 was determined for each treatment group. Data were analysed by two-way ANOVA and post-hoc tests; **$P<0.01$ vs corresponding control.

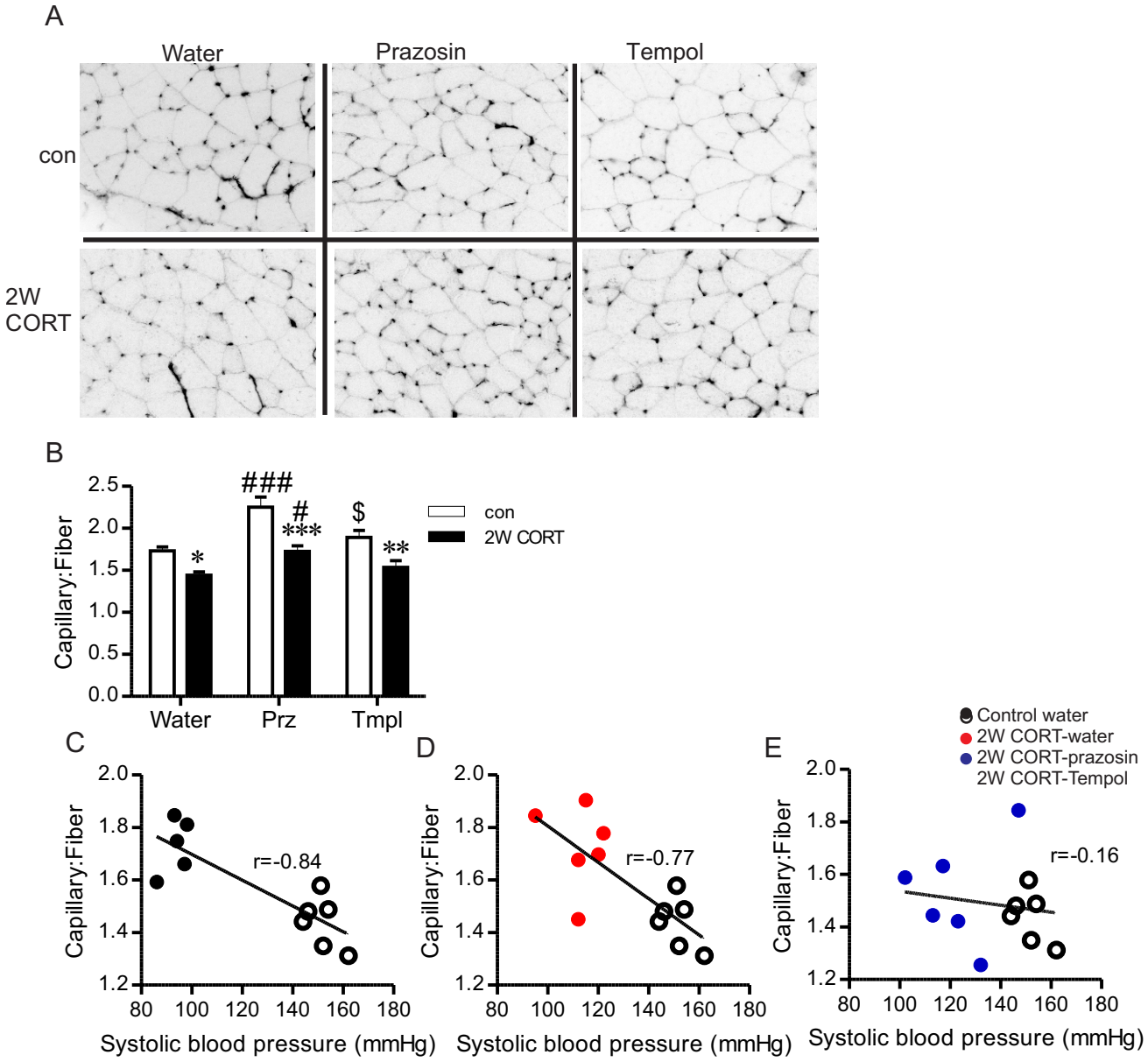

Figure 4.5: Microvascular rarefaction induced by sustained elevations in CORT is not reversed by reactive oxygen species scavenging.

A) Representative images of 2W EDL muscle stained for visualization of capillaries using *Griffonia Simplicifolia* isolectin-FITC. Inverted grey scale images are displayed to enhance visualization of individual muscle fibers. B) Capillary-to-fiber ratio from 3-4 non-overlapping fields of view was assessed by two way ANOVA and subsequent post hoc test. *, **, *** $P<0.05$, 0.01 and 0.001 compared to respective control group. $^{\#, \#\#\#}$ $P<0.05$ and 0.001 relative to corresponding water group; \$ $P<0.01$ relative to corresponding prazosin group (n=5-6). Correlation analysis was run between day 7 systolic blood pressure and day 16 C:F in control-water and CORT-water groups (C; r=-0.84; $P<0.05$), between CORT-water and CORT-prazosin groups (D, r=-0.77; $P<0.05$) and lastly between CORT-water and CORT-Tempol groups (E, r=-0.16; $P>0.05$, n=5-6).

Supplementary Table 4.1: Body composition of control or two week CORT-treated animals with or without concurrent Tempol or prazosin treatment

	control water (n=6)	**control prazosin (n=6)**	**control Tempol (n=6)**	**CORT water (n=6)**	**CORT prazosin (n=6)**	**CORT Tempol (n=6)**
Body Weight (g)	0.348±0.008	0.369±0.0046	0.358±0.01	0.22±0.004#	0.024± 0.007#	0.23± 0.009#
Absolute TA weight (g)	0.56±0.03	0.62 ±0.02	0.59 ±0.03	0.32 ±0.009#	0.39 ±0.03#	0.36± 0.02#
Relative TA weight (g/kg BW)	1.6 ±0.06	1.7± 0.06	1.7 ±0.05	1.5±0.05	1.6 ±0.1	1.6± 0.05
Absolute EDL weight (g)	0.16 ±0.004	0.17 ±0.004	0.17± 0.006	0.10 ±0.003#	0.10 ±0.01#	0.11 ±0.004#
Relative EDL weight (g/kg BW)	0.45 ±0.01	0.46± 0.01	0.47±0.007	0.48 ± 0.01	0.42 ± 0.05	0.49 ± 0.01
Abs Soleus weight (g)	0.13 ±0 01	0.14± 0.005	0.15 ± 0.008	0.11 ± 0.006#	0.092 ±0.01#	0.11±0.003#
Relative Soleus weight (g/kg BW)	0.39± 0.02	0.39 ± 0.01	0.41± 0.02	0.5± 0.03#	0.38 ±0.05	0.49± 0.02

Significant difference compared to respective control group

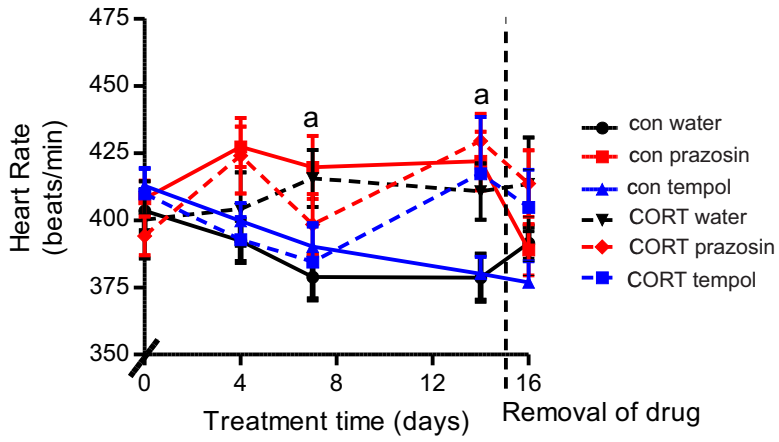

Supplementary Figure 4.1: Alterations in heart rate due to CORT treatment with or without concurrent Tempol or prazosin treatment

Heart rate was assessed during all systolic blood pressure assessments via tail plethysmography. Heart rate was recorded prior to pellet implantation (D0) and on days 4,7, 14 and 16 post pellet implantation. Animal administration of prazosin or Tempol began on D2.
Data analysed via two-way ANOVA and post hoc test. a indicates a significant different (P<0.05) between control water and control prazosin groups (n=6).

Discussion:

The current study demonstrated that both superoxide scavenging and α1 adrenergic receptor inhibition reduced GC-mediated oxidative stress and elevated systolic blood pressure. The elevation in systolic blood pressure preceded GC-induced capillary rarefaction suggestive of a role for elevated systolic blood pressure in skeletal muscle microvascular rarefaction. However, α1 adrenergic receptor inhibition, but not ROS-scavenging, prevented GC-mediated capillary rarefaction and maintained a reduction in systolic blood pressure upon drug cessation. These findings indicate that ROS contribute significantly to GC-mediated hypertension but that alleviation of oxidative stress is not sufficient to prevent capillary rarefaction. The prevention of capillary rarefaction by α1 adrenergic receptor inhibition points to the critical role for local skeletal muscle blood flow in the maintenance of microvascular content.

Relative basal blood flow to the glycolytic EDL muscle was significantly reduced after 2W CORT. Our data suggest a CORT-induced shift in vascular tone in favor of sustained vasoconstriction due to a decrease in eNOS with a concurrent increase in ET-1 mRNA. Previous studies have postulated that GCs modulate vascular tone through alterations in circulating hormones and/or potentiating the vasoconstrictor effects of catecholamines or angiotensin II (Ullian, 1999; Iuchi et al., 2003). We did not observe changes in α1 adrenergic receptor mRNA expression in CORT-treated animals. Rather, our results are consistent with the report that GC treatment reduced reactive hyperemia in humans, which was postulated to be a consequence of reduced NO production and/or bioavailability (Iuchi et al., 2003).

The current study found that oxidative stress was elevated after 1W and 2W of CORT treatment, as evidenced by increased protein carbonylation. CORT treatment significantly reduced total glutathione levels and increased endothelial cell NOX1 mRNA. These findings imply that CORT increases oxidative stress through both a reduction in ROS buffering capacity and increased vascular ROS production. Surprisingly, we found that 1W CORT treatment reduced the transcript levels of NADPH oxidase subunits, NOX1, NOX2 and $p47^{phox}$, in whole muscle lysates, which suggests that the GC influences on NOX expression may be cell type specific. Previous investigations are in support of the abovementioned findings. For example, increased nitrotyrosine levels were reported in the vasculature of patients with elevated GC (Iuchi et al., 2003). As well, rats treated with dexamethasone for 2 weeks had significant reductions in total glutathione levels within blood and skeletal muscle (Orzechowski et al., 2000). Lastly, GC treatment increased NOX2 protein levels in cultured endothelial cells (Muzaffar et al., 2005), but was reported to reduce NOX activity within cultured smooth muscle cells (Marumo et al 1998). An advantage of the current study is that we assessed both markers of vascular function as well as oxidative stress within the same animal model and that these observations were extended to consider their involvement in capillary rarefaction and augmented systolic blood pressure.

GC-mediated augmentation of ROS may play a direct role in the regulation of vascular tone. Dexamethasone induces the production of hydrogen peroxide, coinciding with reduced levels of NO, in cultured endothelial cells (Iuchi et al., 2003) This will impact NO-dependent vasodilation, and also will relieve the repressive influence of NO on NOX expression (Muzaffar et al., 2004). Therefore, the reduction in eNOS mRNA

detected in GC-treated animals combined with ROS-mediated reduction in NO bioavailability, may contribute to augment NOX subunit expression. Additionally, ROS can increase the generation or release of the vasoconstrictor ET-1 (Ruef et al., 2001). Thus, at the vascular level, the increased oxidative stress detected in the current study likely contributes to the alterations in the vasoconstrictor-vasodilator balance, thus influencing systolic arterial pressure.

Computational modeling experiments have suggested that microvascular rarefaction contributes to increased blood pressure (Greene et al., 1989), which is supported by studies in both hypertensive humans and in animal models (Hansen-Smith et al., 1996; Noon et al., 1997; Humar et al., 2009). In the current study, we reported an increase in systolic blood pressure after 4 days of CORT treatment, substantially prior to the occurrence of capillary rarefaction that is detected after 2W but not 1W of CORT-treatment (Mandel et al., 2016). The current study demonstrates a significant inverse correlation between augmented systolic blood pressure after 1W CORT and C:F after 2W CORT. Our study is more consistent with the postulation that augmented systolic blood pressure itself is a driving force behind capillary rarefaction (Hansen-Smith et al., 1996). Nonetheless, capillary rarefaction may in turn contribute to or further aggravate GC-induced hypertension.

Both Tempol and prazosin effectively reduced systolic blood pressure in GC-treated rats, in line with previous research (Jaillon, 1980; Schnackenberg and Wilcox, 1999; Sainz et al., 2005; Wilcox and Pearlman, 2008). This anti-hypertensive effect was moderately delayed in Tempol-treated rodents as compared to those administered prazosin. Additionally, the anti-hypertensive influence of Tempol was rapidly lost after

removal of the drug. These findings suggest that the superoxide scavenging effect of Tempol did not elicit sustained structural or functional adaptations within the skeletal muscle microvasculature.

In contrast to prazosin, 2W of Tempol treatment did not induce skeletal muscle angiogenesis in healthy rats, which may indicate that there is minimal superoxide generation under resting conditions in the vasculature of healthy animals. Surprisingly, Tempol failed to prevent capillary rarefaction in the GC-treated animals despite its depressor influence on systolic blood pressure, suggesting that superoxide scavenging by itself is an insufficient angiogenic stimulus. The dissimilar effects of Tempol and prazosin on capillary content may be due to the greater reduction in blood pressure achieved with prazosin, but it likely also reflects differences in the location/mode of action of prazosin compared to Tempol. Due to the high level of tonic sympathetic nerve activation (Korthuis, 2011) and the high density of alpha-adrenergic receptors (Stanfield, 2011) within the skeletal muscle under resting conditions, prazosin elicits vasodilation predominantly within the skeletal muscle that is associated with an approximately threefold increase in skeletal muscle blood flow (Williams et al., 2006). Conversely, the ROS-scavenging effects of Tempol occur throughout the entire vasculature, resulting in reduced resistance within many vascular beds. Therefore, the degree of influence on skeletal muscle blood flow is predicted to be more modest with Tempol compared to that of prazosin. In support of this idea, Tempol treatment was shown to reduce systemic blood pressure without improving skeletal muscle blood flow in rats with metabolic syndrome (Frisbee et al., 2011). A limitation of our experimental design is that we were not able to compare the extent of prazosin and Tempol-mediated alterations in skeletal

muscle blood flow because the end point of our experiment was 18 hours after removal of drugs. Nonetheless, the findings from our study point to the importance of improved skeletal muscle blood flow, rather than oxidative stress itself, in the preservation of capillary content. The maintenance of capillary content constitutes a structural adaptation that may have contributed to the maintenance of a reduced systolic blood pressure upon prazosin cessation.

GC-treatment also elicits skeletal muscle atrophy, with greatest reduction in fiber cross-sectional area occurring in type IIbx fibers in rodents (Beaudry et al., 2015; Dunford et al., 2016). Interestingly, relative soleus muscle weight is unaffected by CORT treatment, suggesting that oxidative muscles do not undergo extensive GC-mediated atrophy (Schakman et al., 2008; Shpilberg et al., 2012). Likewise, we found that 2W CORT-treatment reduced blood flow within the EDL but not the soleus muscle. These findings suggest a possible association between skeletal muscle atrophy and reduction in blood flow, which warrants further investigation.

In summary, the current study demonstrated that sustained elevations in GCs augmented oxidative stress, likely due to both increased ROS production and decreased ROS buffering. Oxidative stress may contribute to GC-mediated alterations in vascular tone and muscle blood flow. Although partially effective in attenuating the GC-mediated elevation in systolic blood pressure, Tempol alleviated oxidative stress but did not prevent skeletal muscle capillary rarefaction. Prazosin also attenuated oxidative stress and lowered systolic blood pressure. However, unlike Tempol, prazosin prevented capillary rarefaction and maintained a reduction in systolic blood pressure upon drug cessation. These findings suggest an important role for adrenergic control of muscle flow

and oxidative stress in the maintenance of microvascular content, which will in turn have an impact on overall cardiovascular health.

Funding: This work was supported in part by Natural Science and Engineering Research Council of Canada Discovery Grants to Dr. Tara L Haas and Dr. Michael C. Riddell. Dr. Tara L Haas also was the recipient of a York University Faculty of Health Internal Research Award.

Disclosures: None

Acknowledgements: We would like to thank Nora Zwingerman who conducted the statistical analysis of systolic blood pressure.

Chapter 5: Concluding remarks

In healthy adults, the skeletal muscle microvasculature responds, adapts and remodels to a multitude of stimuli. Microvascular remodeling results from the activation of signaling pathways and appropriate responses to said signals within the microenvironment. This involves communication between the different cell types within the microenvironment including skeletal myocytes, endothelial cells and smooth muscle cells. Additionally, vascular remodeling requires the coordinated balance between proteases and their inhibitors as well as the balance between pro-angiogenic and anti-angiogenic factors (Pepper, 2001). Thus, skeletal muscle microvascular remodeling is a highly regulated and complex process. However, as a result of a variety of diseases and other pathological conditions, the remodeling response can become impaired.

The current study set out to investigate signaling within the microenvironment in response to several different stimuli. Firstly, I used *Timp1*$^{-/-}$ mice with the intention of perturbing the proteolytic balance. The goal was to examine skeletal muscle microvascular remodeling due to alterations in flow in *Timp1*$^{-/-}$ compared to WT mice. Secondly, the deleterious effects of GCs on skeletal muscle capillarization have been documented (Shikatani et al., 2012); therefore, I examined factors that may be contributing to this phenotype and possible signaling pathways that can be altered to prevent its occurrence. Lastly, I further examined the GC model to determine how alterations to the skeletal muscle microvasculature may be impacting systolic blood pressure and which pathway(s) may be responsible. Employing these different animal models provided a comprehensive examination of different component/aspects of the

microvascular microenvironment, which mediates microvascular health and remodeling capabilities.

5.1: Summary of findings

The mouse model of TIMP1 deficiency was used to test the hypothesis that appropriate alterations in the proteolytic balance are integral for microvascular remodeling. While the loss of TIMP1 did not result in overt health complications, it impaired microvascular development. These findings are suggestive of impairments within the microenvironment of *Timp1*$^{-/-}$ mice, which negatively impacts normal blood vessel growth and/or maturation (Figure 5.1A). Contrary to our hypothesis, the deletion of TIMP1 did not appear to significantly increase proteolytic activity within the microenvironment thereby resulting in vascular remodeling (Figure 5.1A). Although the correct responses to altered flow (augmented VEGF-A and/or eNOS mRNA) occurred within the microenvironment of *Timp1*$^{-/-}$ mice, this was insufficient to elicit angiogenesis or arteriogenesis. These findings could imply an issue with signal transmission; i.e. the cells within the microenvironment can initiate but not respond to normal responses, thereby culminating in a lack of vascular remodeling. One likely possibility, which was not assessed in the current experiment, is alterations in the expression of specific VEGF isoforms, as different VEGF isoforms are known to have different cellular effects (Zhang et al., 2008). For example, altered $VEGF_{121}$ expression may have contributed to increased vascular permeability (Zhang et al., 2008) and subsequently the lack of remodeling in *Timp1*$^{-/-}$ mice. The results of the current study suggest that TIMP1 does not act as an anti-angiogenic factor, within skeletal muscle, but rather functions as a critical permissive factor for flow-induced microvascular remodeling (Figure 5.1A).

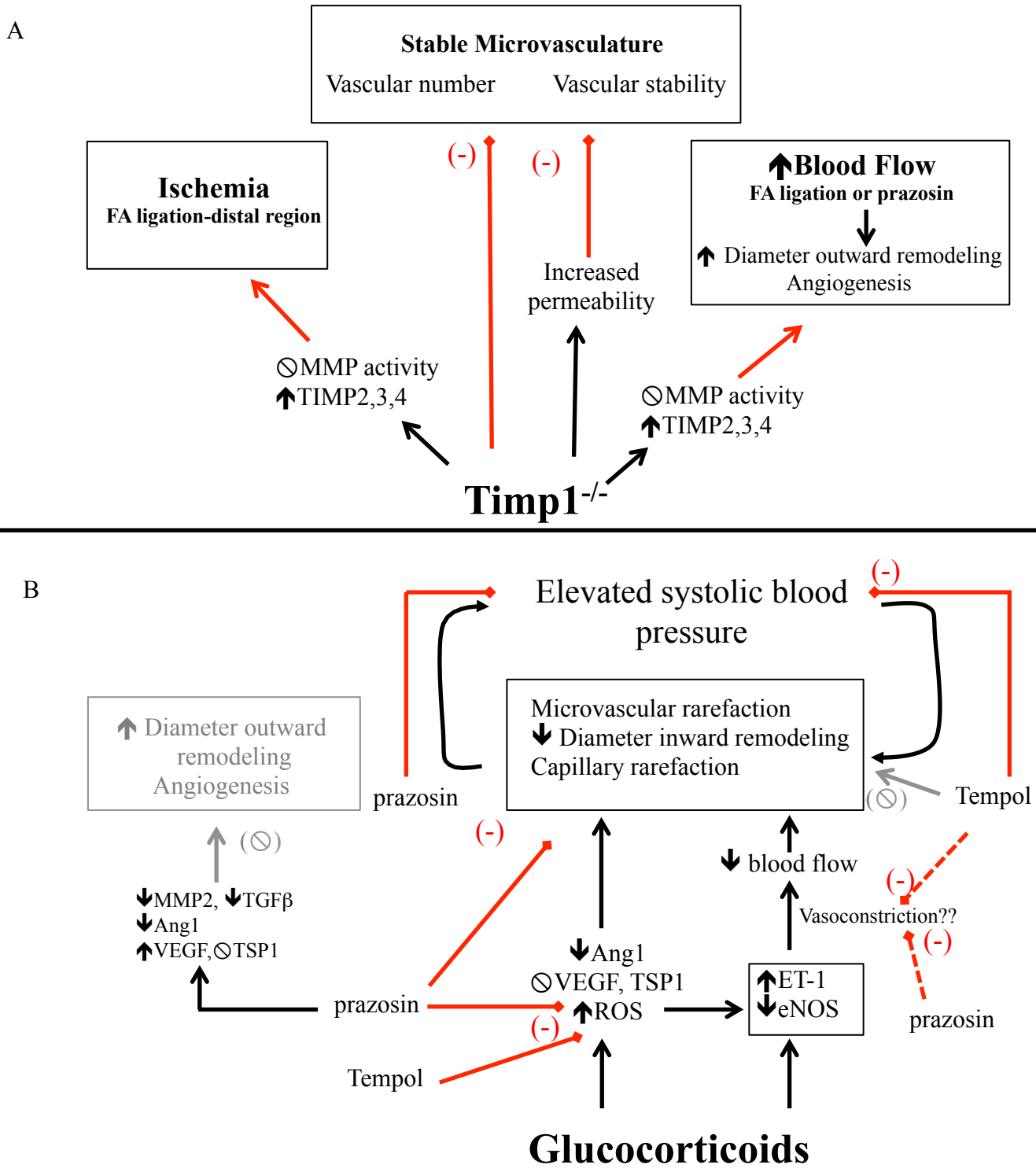

Figure 5.1: Summary of findings

A) The current study found that the loss of TIMP1 resulted in a reduction in microvascular stability. Contrary to our hypothesis the loss of TIMP1 did not increase MMP activity and in turn elicit an angiogenic response to FA ligation. In fact, *Timp1*$^{-/-}$ mice did not see any vascular remodeling responses to alterations in flow.
B) Excess levels of circulating GCs resulted in microvascular rarefaction, reduced skeletal muscle blood flow and elicited hypertension. Both Tempol and prazosin treatment had beneficial roles on one or more of the above-mentioned alterations.
Red arrow indicates inhibitor effect (-)
Black arrow indicates a stimulatory effect
Grey arrow indicates no effect (⃠)

The rodent model of GC excess was used as a tool to induce deleterious microvascular and metabolic effects. This model is pathologically relevant as it mimics the phenotype of several human conditions including Cushing's syndrome, prolonged GC treatment, metabolic syndrome and/or type 2 diabetes (Shpilberg et al., 2012). It was hypothesized that CORT treatment would inhibit endothelial mediated shear stress signaling and subsequently the angiogenic response to prazosin administration (Chapter 3). Skeletal muscle microvascular rarefaction was elicited through reduced Ang-1 levels and not significant blunting of VEGF expression or increased TSP-1 levels. Concurrent prazosin treatment abrogated rarefaction likely due to the maintenance of MAPK, NO and VEGF responsiveness to shear stress; however, in agreement with my hypothesis no angiogenic or arteriogenic response occurred. The present study demonstrates that the inhibition of α1-adrenergic receptors can prevent CORT-induced capillary rarefaction (Figure 5.1B), which could in turn have important benefits for overall skeletal muscle health and function and possibly ameliorate the animals' metabolic profile.

Based on our previous findings (Chapter 3), we continued using the rodent model of GC excess to examine the systemic influences of CORT (Chapter 4). This project was embarked upon to test the hypothesis that GC-mediated hypertension and capillary rarefaction would be prevented by concurrent treatment with the ROS scavenger Tempol. CORT-treatment elicited a significant increase in oxidative stress due in part to a reduction in ROS buffering and increased endothelial NADPH-oxidase levels. Furthermore, eNOS mRNA was significantly reduced, ET-1 mRNA was significantly elevated and relative EDL flow was significant reduced. The current study compared the structural and functional effects of Tempol to those seen with prazosin treatment. While

both drugs abrogated GC-mediated oxidative stress and hypertension, data from the current study suggests that α1-adrenergic receptor inhibition is more beneficial than superoxide scavenging alone. Prazosin, but not Tempol, prevented capillary rarefaction thereby allowing animals co-treated with prazosin to maintain a reduction in systolic blood pressure upon drug cessation. Furthermore, prazosin treated animals saw an earlier (day 4 compared to day 7) reduction in systolic blood pressure than Tempol treated animals. These findings highlight the important role for adrenergic control of muscle flow and oxidative stress in the prevention of the deleterious effects of GC excess (Figure 5.1B).

The findings from the abovementioned models (*Timp1*$^{-/-}$ and GC excess) highlight the intricacy of the microenvironment and the importance of proper communication between its various components. These studies demonstrate that although one or more cell types may be impacted by a given manipulation/situation, the microenvironment has tremendous plasticity, redundancy and resilience. These qualities enable the microenvironment to function, less than optimally, under pathological conditions.

5.2: Study limitations

There are a several limitations to the studies presented in this dissertation which should be mentioned. The first study (chapter 2) was carried out in mice, while later studies were performed on rats (Chapter 3, 4 & Appendix A). This was due to the ability to genetically manipulate TIMP1 levels in mice that is currently not possible in rats. Originally, I had proposed to generate a model of PAD in CORT-treated rats, in order to examine ischemia induced remodeling under pathological conditions; however, this model proved unviable due to complications in the animals' post surgery recovery (Appendix A).

I had hypothesized that an increase in C:F would occur only within *Timp1*$^{-/-}$ mice; however, no angiogenic response was seen in *Timp1*$^{-/-}$ or WT mice. The lack of an angiogenic response within *Timp1*$^{-/-}$ mice demonstrates no excessive increase in MMP-driven vascular remodeling. The lack of angiogenesis within WT mice may have been due to the inhibitory effects of FoxO proteins (Milkiewicz et al., 2011) or it had not yet developed. A previous report using a similar model reported an angiogenic response 35 days post unilateral iliac artery ligation (Milkiewicz et al., 2006).

For the CORT experiments (Chapters 3 & 4), male rats aged 8 to 9 weeks were used. At this age, rats are considered young and are still in a steady growth phase. As a healthy rat grows and develops, it stands to reason that skeletal muscle microvascular content will increase as well. However, it is possible that within CORT-treated young rats, normal capillary growth is blunted thus contributing to the lower C:F values reported. This issue could be addressed in future experiments by repeating the experimental design in adult age (7 to 8 month old) male Sprague Dawley rats.

In Chapter 4 hind-limb blood flow was assessed via a microsphere infusion protocol adapted from Deveci & Egginton (1999). An important limitation of the protocol I used is that unlike previous investigators, no arterial canulation was used to ensure direct microsphere injection or reference sample collection (Deveci and Egginton, 1999; Milkiewicz et al., 2006). Furthermore, brain blood flow was used to standardize limb blood flow, because brain blood flow should remain relatively constant (Paulson et al., 1989; Cipolla, 2009). However, previous reports have suggested that GCs can potentially affect cerebral blood flow (de Quervain et al., 2003). Care must be taken while interpreting the results of the current study as the animals were sedated at the time of flow determination, which in itself will reduce blood flow (Raisis, 2005). Furthermore, hind-limb basal blood flow can be very low, therefore it may be prudent to examine differences in hind-limb blood flow in response to a flow stimulus such as muscle contraction (Deveci and Egginton, 1999).

5.3: Future directions

Based on the results obtained from the current experiments, several important avenues are of interest for future examination. Within *Timp1*$^{-/-}$ mice it would be beneficial to assess the expression of various VEGF-A isoforms, specifically $VEGF_{165}$ and $VEGF_{121}$. It is possible that *Timp1*$^{-/-}$ mice have augmented MMP9 activity; the current study (Chapter 2) did not specifically measure MMP9 activity, only overall (MMP1-14) MMP-activity. If *Timp1*$^{-/-}$ mice have excessive MMP9 activity this could result in excessive cleavage of $VEGF_{165/185}$ (Hawinkels et al., 2008), thus allowing VEGF to diffuse away from the endothelium where VEGF typically exerts effects.

Within Chapter 3, I noted a significant increase in VEGF-A mRNA and protein expression after 14 days of concurrent prazosin and CORT treatment and maintenance of endothelial shear responsiveness. In healthy rats, augmented VEGF-A expression is seen prior to an increase in C:F (Milkiewicz et al., 2007). Therefore, future experiments could examine if an angiogenic response could be seen in CORT-prazosin animals if the experimental conditions were maintained for longer than 2 weeks. As well, it would be interesting to examine the health and functionality of the microvascular microenvironment in other disease models where skeletal muscle microvascular content is reduced, such as type-1 diabetes (Kivelä et al., 2006).

In Chapter 4, Tempol and prazosin were removed on day 15, 18 hours prior to the final systolic blood pressure recording in order to uncover potential structural and/or functional similarities/differences between these two drugs. However, this prevented assessments of Tempol and/or prazosin induced alterations/ameliorations in relative EDL flow. Future experiments would benefit from determining relative skeletal muscle blood

flow within CORT-Tempol and CORT-prazosin groups, while the drug is still being administered. This could help to uncover similarities/differences between prazosin and Tempol treatment and how these responses differ from control animals.

Previous investigations have reported an increased prevalence of PAD in patients with type-2 diabetes (Ziegler et al., 2010). Therefore, it would be useful to find a model of type-2 diabetes in which it is viability to examine PAD. Animal models of type 2 diabetes such as the *ob*/*ob* mouse or the ZDF rat are good candidates. These animal models have augmented GC levels (Alberts et al., 2005; Campbell et al., 2010), but not to the same extent as the levels reported in the current study. Therefore, either of these alternate animal models may be a more suitable model within which to examine PAD. This study used pathophysiological levels of CORT, i.e. GC levels were significantly greater than those seen in diabetic patients or those on exogenous GC treatment (Alberts et al., 2005; Campbell et al., 2010). It would therefore be beneficial to assess lower doses of GC, more within the 'typical' elevated range and determine the effects on the microvasculature and overall cardiovascular health.

Lastly, as discussed in Appendix B, further experimentation is warranted to refine our *in vitro* assessments of endothelial cell specific alterations to changes in shear stress. More specifically, more work is required on endothelial responses to sustained reductions in flow. In line with the finings of Appendix B, with elevated blood flow, it would be ideal to compare low shear stress (~1-2 dynes/cm^2) to normal capillary shear stress (5 dynes/cm^2).

In summary, the data presented in the current dissertation provide novel information regarding the plasticity, resilience and adaptability of the skeletal muscle

microvascular microenvironment. My dissertation highlights the importance for balance within the microenvironment between growth factors and inhibitors for ‘normal’ microvascular development and remodeling. As well, my dissertation points to the interconnectivity between skeletal muscle microvascular health and overall cardiovascular health.

Reference List:

Abid MR, Spokes KC, Shih S-C, Aird WC. 2007. NADPH oxidase activity selectively modulates vascular endothelial growth factor signaling pathways. J Biol Chem 282:35373–85.

Adair T, Montani J-P. 2011. *Angiogenesis* D. Granger & J. Granger, eds., Morgan & Claypool Life sciences.

Akerstrom T, Laub L, Vedel K, Brand CL, Pedersen BK, Kaufmann Lindqvist A, Wojtaszewski JFP, Hellsten Y. 2014. Increased skeletal muscle capillarization enhances insulin sensitivity. AJP Endocrinol Metab:ajpendo.00020.2014–.

Alberts P, Rönquist-Nii Y, Larsson C, Klingström G, Engblom L, Edling N, Lidell V, Berg I, Edlund P-O, Ashkzari M, Sahaf N, Norling S, Berggren V, Bergdahl K, Forsgren M, Abrahmsén L. 2005. Effect of high-fat diet on KKAy and ob/ob mouse liver and adipose tissue corticosterone and 11-dehydrocorticosterone concentrations. Horm Metab Res = Horm und Stoffwechselforsch = Horm métabolisme 37:402–7.

Alexander JS, Elrod JW. 2002. Extracellular matrix, junctional integrity and matrix metalloproteinase interactions in endothelial permeability regulation. J Anat 200:561–74.

Anderson EJ, Lustig ME, Boyle KE, Woodlief TL, Kane DA, Lin C-T, Price JW, Kang L, Rabinovitch PS, Szeto HH, Houmard JA, Cortright RN, Wasserman DH, Neufer PD. 2009. Mitochondrial H2O2 emission and cellular redox state link excess fat intake to insulin resistance in both rodents and humans. J Clin Invest 119:573–81.

Ando J, Yamamoto K. 2009. Vascular Mechanobiology. Circ J 73:1983–1992.

Arbiser JL, Petros J, Klafter R, Govindajaran B, McLaughlin ER, Brown LF, Cohen C, Moses M, Kilroy S, Arnold RS, Lambeth JD. 2002. Reactive oxygen generated by Nox1 triggers the angiogenic switch. Proc Natl Acad Sci U S A 99:715–20.

Armstrong LC, Björkblom B, Hankenson KD, Siadak AW, Stiles CE, Bornstein P. 2002. Thrombospondin 2 inhibits microvascular endothelial cell proliferation by a caspase-independent mechanism. Mol Biol Cell 13:1893–905.

Arras M, Ito WD, Scholz D, Winkler B, Schaper J, Schaper W. 1998. Monocyte activation in angiogenesis and collateral growth in the rabbit hindlimb. J Clin Invest 101:40–50.

Arsham AM, Plas DR, Thompson CB, Simon MC. 2002. Phosphatidylinositol 3-kinase/Akt signaling is neither required for hypoxic stabilization of HIF-1 alpha nor sufficient for HIF-1-dependent target gene transcription. J Biol Chem 277:15162–70.

Asahara T, Chen D, Takahashi T, Fujikawa K, Kearney M, Magner M, Yancopoulos GD, Isner JM. 1998. Tie2 Receptor Ligands, Angiopoietin-1 and Angiopoietin-2, Modulate VEGF-Induced Postnatal Neovascularization. Circ Res 83:233–240.

Bachhav SS, Patil SD, Bhutada MS, Surana SJ. 2011. Oleanolic acid prevents glucocorticoid-induced hypertension in rats. Phytother Res 25:1435–9.

Bagavandoss P, Wilks JW. 1990. Specific inhibition of endothelial cell proliferation by thrombospondin. Biochem Biophys Res Commun 170:867–72.

Barclay JL, Petersons CJ, Keshvari S, Sorbello J, Mangelsdorf BL, Thompson CH, Prins JB, Burt MG, Whitehead JP, Inder WJ. 2016. Thrombospondin-1 is a glucocorticoid responsive protein in humans. Eur J Endocrinol 174:193–201.

Barthes J, Özçelik H, Hindié M, Ndreu-Halili A, Hasan A, Vrana NE. 2014. Cell microenvironment engineering and monitoring for tissue engineering and regenerative medicine: the recent advances. Biomed Res Int 2014:921905.
Baum M, Moe OW. 2008. Glucocorticoid-mediated hypertension: does the vascular smooth muscle hold all the answers? J Am Soc Nephrol 19:1251–3.
Beaudry JL, Dunford EC, Leclair E, Mandel ER, Peckett AJ, Haas TL, Riddell MC. 2015. Voluntary exercise improves metabolic profile in high-fat fed glucocorticoid-treated rats. J Appl Physiol 118:1331–43.
Beaudry JL, Riddell MC. 2012. Effects of glucocorticoids and exercise on pancreatic β-cell function and diabetes development. Diabetes Metab Res Rev 28:560–73.
Benedict KF, Coffin GS, Barrett EJ, Skalak TC. 2011. Hemodynamic systems analysis of capillary network remodeling during the progression of type 2 diabetes. Microcirculation 18:63–73.
Bey L, Akunuri N, Zhao P, Hoffman EP, Hamilton DG, Hamilton MT. 2003. Patterns of global gene expression in rat skeletal muscle during unloading and low-intensity ambulatory activity. Physiol Genomics 13:157–67.
Bode W, Fernandez-Catalan C, Grams F, Gomis-Rüth FX, Nagase H, Tschesche H, Maskos K. 1999. Insights into MMP-TIMP interactions. Ann N Y Acad Sci 878:73–91.
Bongrazio M, Da Silva-Azevedo L, Bergmann EC, Baum O, Hinz B, Pries AR, Zakrzewicz A. 2008. Shear stress modulates the expression of thrombospondin-1 and CD36 in endothelial cells in vitro and during shear stress-induced angiogenesis in vivo. Int J Immunopathol Pharmacol 19:35–48.
Bonner JS, Lantier L, Hasenour CM, James FD, Bracy DP, Wasserman DH. 2013. Muscle-specific vascular endothelial growth factor deletion induces muscle capillary rarefaction creating muscle insulin resistance. Diabetes 62:572–80.
Boyd PJ, Doyle J, Gee E, Pallan S, Haas TL. 2005. MAPK signaling regulates endothelial cell assembly into networks and expression of MT1-MMP and MMP-2. Am J Physiol Cell Physiol 288:C659–68.
Breen E, Tang K, Olfert M, Knapp A, Wagner P. 2008. Skeletal muscle capillarity during hypoxia: VEGF and its activation. High Alt Med Biol 9:158–66.
Brevetti LS, Paek R, Brady SE, Hoffman JI, Sarkar R, Messina LM. 2001. Exercise-induced hyperemia unmasks regional blood flow deficit in experimental hindlimb ischemia. J Surg Res 98:21–6.
Brew K, Dinakarpandian D, Nagase H. 2000. Tissue inhibitors of metalloproteinases: evolution, structure and function. Biochim Biophys Acta 1477:267–83.
Brew K, Nagase H. 2010. The tissue inhibitors of metalloproteinases (TIMPs): an ancient family with structural and functional diversity. Biochim Biophys Acta 1803:55–71.
Brindle NPJ, Saharinen P, Alitalo K. 2006. Signaling and functions of angiopoietin-1 in vascular protection. Circ Res 98:1014–23.
Brown MD, Kent J, Kelsall CJ, Milkiewicz M, Hudlicka O. 2003. Remodeling in the microcirculation of rat skeletal muscle during chronic ischemia. Microcirculation 10:179–91.
Burnham JA, Wright RR, Dreisbach J, Murray RS. 1991. The effect of high-dose steroids on MRI gadolinium enhancement in acute demyelinating lesions. Neurology 41:1349–54.

Burridge K, Chrzanowska-Wodnicka M. 1996. Focal adhesions, contractility, and signaling. Annu Rev Cell Dev Biol 12:463–518.
Buschmann I, Heil M, Jost M, Schaper W. 2003. Influence of inflammatory cytokines on arteriogenesis. Microcirculation 10:371–9.
Byzova T V, Goldman CK, Pampori N, Thomas KA, Bett A, Shattil SJ, Plow EF. 2000. A mechanism for modulation of cellular responses to VEGF: activation of the integrins. Mol Cell 6:851–60.
Cai W, Schaper W. 2008. Mechanisms of arteriogenesis. Acta Biochim Biophys Sin (Shanghai) 40:681–92.
Cai W-J, Kocsis E, Luo X, Schaper W, Schaper J. 2004. Expression of endothelial nitric oxide synthase in the vascular wall during arteriogenesis. Mol Cell Biochem 264:193–200.
Campbell JE, Király MA, Atkinson DJ, D'souza AM, Vranic M, Riddell MC. 2010. Regular exercise prevents the development of hyperglucocorticoidemia via adaptations in the brain and adrenal glands in male Zucker diabetic fatty rats. Am J Physiol Regul Integr Comp Physiol 299:R168–76.
Cardone MH, Roy N, Stennicke HR, Salvesen GS, Franke TF, Stanbridge E, Frisch S, Reed JC. 1998. Regulation of cell death protease caspase-9 by phosphorylation. Science 282:1318–21.
Carmeliet P. 2000. Mechanisms of angiogenesis and arteriogenesis. Nat Med 6:389–95.
Carmeliet P, Ferreira V, Breier G, Pollefeyt S, Kieckens L, Gertsenstein M, Fahrig M, Vandenhoeck A, Harpal K, Eberhardt C, Declercq C, Pawling J, Moons L, Collen D, Risau W, Nagy A. 1996. Abnormal blood vessel development and lethality in embryos lacking a single VEGF allele. Nature 380:435–9.
Chalothorn D, Clayton JA, Zhang H, Pomp D, Faber JE. 2007. Collateral density, remodeling, and VEGF-A expression differ widely between mouse strains. Physiol Genomics 30:179–91.
Chen KD, Li YS, Kim M, Li S, Yuan S, Chien S, Shyy JY. 1999. Mechanotransduction in response to shear stress. Roles of receptor tyrosine kinases, integrins, and Shc. J Biol Chem 274:18393–400.
Cheng XW, Kuzuya M, Nakamura K, Maeda K, Tsuzuki M, Kim W, Sasaki T, Liu Z, Inoue N, Kondo T, Jin H, Numaguchi Y, Okumura K, Yokota M, Iguchi A, Murohara T. 2007. Mechanisms underlying the impairment of ischemia-induced neovascularization in matrix metalloproteinase 2-deficient mice. Circ Res 100:904–13.
Chien S. 2007. Mechanotransduction and endothelial cell homeostasis: the wisdom of the cell. Am J Physiol Heart Circ Physiol 292:H1209–24.
Chirco R, Liu X-W, Jung K-K, Kim H-RC. 2006. Novel functions of TIMPs in cell signaling. Cancer Metastasis Rev 25:99–113.
Chistiakov DA, Orekhov AN, Bobryshev Y V. 2015. Endothelial Barrier and Its Abnormalities in Cardiovascular Disease. Front Physiol 6:365.
Chlench S, Mecha Disassa N, Hohberg M, Hoffmann C, Pohlkamp T, Beyer G, Bongrazio M, Da Silva-Azevedo L, Baum O, Pries AR, Zakrzewicz A. 2007. Regulation of Foxo-1 and the angiopoietin-2/Tie2 system by shear stress. FEBS Lett 581:673–80.
Cipolla MJ. 2009. Control of Cerebral Blood Flow. In *The Cerebral Circulation*. Morgan

& Claypool Life Sciences.
Cotran RS, Majno G. 1964. The delayed and prolonged vascular leakage in inflammation. Topography of the leaking vessels after thermal injury. Am J Pathol 45:261–81.
Couffinhal T, Silver M, Zheng LP, Kearney M, Witzenbichler B, Isner JM. 1998. Mouse model of angiogenesis. Am J Pathol 152:1667–79.
Creemers EE, Cleutjens JP, Smits JF, Daemen MJ. 2001. Matrix metalloproteinase inhibition after myocardial infarction: a new approach to prevent heart failure? Circ Res 89:201–10.
Dai X, Faber JE. 2010. Endothelial nitric oxide synthase deficiency causes collateral vessel rarefaction and impairs activation of a cell cycle gene network during arteriogenesis. Circ Res 106:1870–81.
Daly C, Pasnikowski E, Burova E, Wong V, Aldrich TH, Griffiths J, Ioffe E, Daly TJ, Fandl JP, Papadopoulos N, McDonald DM, Thurston G, Yancopoulos GD, Rudge JS. 2006. Angiopoietin-2 functions as an autocrine protective factor in stressed endothelial cells. Proc Natl Acad Sci U S A 103:15491–6.
Damiani E, Carloni P, Biondi C, Greci L. 2000. Increased oxidative modification of albumin when illuminated in vitro in the presence of a common sunscreen ingredient: protection by nitroxide radicals. Free Radic Biol Med 28:193–201.
Darland DC, Massingham LJ, Smith SR, Piek E, Saint-Geniez M, D'Amore PA. 2003. Pericyte production of cell-associated VEGF is differentiation-dependent and is associated with endothelial survival. Dev Biol 264:275–88.
Davies MJ, Fu S, Wang H, Dean RT. 1999. Stable markers of oxidant damage to proteins and their application in the study of human disease. Free Radic Biol Med 27:1151–63.
Dawson JM, Hudlická O. 1989. The effects of long term administration of prazosin on the microcirculation in skeletal muscles. Cardiovasc Res 23:913–20.
Dehghanian F, Hojati Z, Kay M. 2014. New Insights into VEGF-A Alternative Splicing: Key Regulatory Switching in the Pathological Process. Avicenna J Med Biotechnol 6:192–9.
Dejana E. 2004. Endothelial cell-cell junctions: happy together. Nat Rev Mol Cell Biol 5:261–70.
Delavar H, Nogueira L, Wagner PD, Hogan MC, Metzger D, Breen EC. 2014. Skeletal myofiber VEGF is essential for the exercise training response in adult mice. Am J Physiol Regul Integr Comp Physiol 306:R586–95.
Desiniotis A, Kyprianou N. 2011. Advances in the design and synthesis of prazosin derivatives over the last ten years. Expert Opin Ther Targets 15:1405–18.
Deveci D, Egginton S. 1999. Development of the fluorescent microsphere technique for quantifying regional blood flow in small mammals. Exp Physiol 84:615–30.
Deveci D, Marshall JM, Egginton S, Gamboa JL, Andrade FH, Physiol AJ, Integr R, Physiol C, Scott GR, Egginton S, Richards JG, Milsom WK. 2001. Relationship between capillary angiogenesis , fiber type , and fiber size in chronic systemic hypoxia Relationship between capillary angiogenesis , fiber type , and fiber size in chronic systemic hypoxia. Am J Physiol Hear Circ Physiol 281:H241–H252.
Dimmeler S, Assmus B, Hermann C, Haendeler J, Zeiher AM. 1998. Fluid Shear Stress Stimulates Phosphorylation of Akt in Human Endothelial Cells : Involvement in Suppression of Apoptosis. Circ Res 83:334–341.

Dimmeler S, Fleming I, Fisslthaler B, Hermann C, Busse R, Zeiher AM. 1999. Activation of nitric oxide synthase in endothelial cells by Akt-dependent phosphorylation. Nature 399:601–5.
Dringen R. 2000. Metabolism and functions of glutathione in brain. Prog Neurobiol 62:649–71.
Dumont O, Kauffenstein G, Guihot A-L, Guérineau NC, Abraham P, Loufrani L, Henrion D. 2014. Time-related alteration in flow- (shear stress-) mediated remodeling in resistance arteries from spontaneously hypertensive rats. Int J Hypertens 2014:859793.
Dunford E, Mandel E, Mohajeri S, Haas T, Riddell M. 2016. The metabolic effects of prazosin on insulin resistance in glucocorticoid treated rats. Am J Physiol Regul Integr Comp Physiol Rev. In Review.
Egginton S, Brown MD, Hudlicka O. 2001. Unorthodox angiogenesis in skeletal muscle. Cardiovasc Res 49:634–646.
Egginton S, Gerritsen M. 2003. Lumen Formation. In vivo versus in vitro observations. Microcirculation 10:45–61.
Egginton S, Hudlicka O, Brown MD, Walter H, Weiss JB, Bate A. 1998. Capillary growth in relation to blood flow and performance in overloaded rat skeletal muscle. J Appl Physiol 85:2025–2032.
Egginton S, Zhou AL, Brown MD, Hudlická O. 2000. The role of pericytes in controlling angiogenesis in vivo. Adv Exp Med Biol 476:81–99.
Eskandari MK, Vijungco JD, Flores A, Borensztajn J, Shively V, Pearce WH. 2005. Enhanced abdominal aortic aneurysm in TIMP-1-deficient mice. J Surg Res 123:289–93.
Féraud O, Mallet C, Vilgrain I. 2003. Expressional regulation of the angiopoietin-1 and -2 and the endothelial-specific receptor tyrosine kinase Tie2 in adrenal atrophy: a study of adrenocorticotropin-induced repair. Endocrinology 144:4607–15.
Ferrara N. 2004. Vascular endothelial growth factor: basic science and clinical progress. Endocr Rev 25:581–611.
Ferrara N, Carver-Moore K, Chen H, Dowd M, Lu L, O'Shea KS, Powell-Braxton L, Hillan KJ, Moore MW. 1996. Heterozygous embryonic lethality induced by targeted inactivation of the VEGF gene. Nature 380:439–42.
Ferrara N, Gerber H-P, LeCouter J. 2003. The biology of VEGF and its receptors. Nat Med 9:669–76.
Ferrara N, Henzel WJ. 1989. Pituitary follicular cells secrete a novel heparin-binding growth factor specific for vascular endothelial cells. Biochem Biophys Res Commun 161:851–8.
Folkman J. 1971. Tumor angiogenesis: therapeutic implications. N Engl J Med 285:1182–6.
Folkman J, Langer R, Linhardt RJ, Haudenschild C, Taylor S. 1983. Angiogenesis inhibition and tumor regression caused by heparin or a heparin fragment in the presence of cortisone. Science 221:719–25.
Förster C, Kahles T, Kietz S, Drenckhahn D. 2007. Dexamethasone induces the expression of metalloproteinase inhibitor TIMP-1 in the murine cerebral vascular endothelial cell line cEND. J Physiol 580:937–49.
Forsythe JA, Jiang BH, Iyer N V, Agani F, Leung SW, Koos RD, Semenza GL. 1996.

Activation of vascular endothelial growth factor gene transcription by hypoxia-inducible factor 1. Mol Cell Biol 16:4604–13.
Frey RS, Ushio-Fukai M, Malik AB. 2009. NADPH oxidase-dependent signaling in endothelial cells: role in physiology and pathophysiology. Antioxid Redox Signal 11:791–810.
Frisbee JC, Goodwill AG, Butcher JT, Olfert IM. 2011. Divergence between arterial perfusion and fatigue resistance in skeletal muscle in the metabolic syndrome. Exp Physiol 96:369–83.
Fukuhara S, Sako K, Noda K, Zhang J, Minami M, Mochizuki N. 2010. Angiopoietin-1/Tie2 receptor signaling in vascular quiescence and angiogenesis. Histol Histopathol 25:387–96.
Fung E, Helisch A. 2012. Macrophages in collateral arteriogenesis. Front Physiol 3:353.
Furukawa S, Fujita T, Shimabukuro M, Iwaki M, Yamada Y, Nakajima Y, Nakayama O, Makishima M, Matsuda M, Shimomura I. 2004. Increased oxidative stress in obesity and its impact on metabolic syndrome. J Clin Invest 114:1752–1761.
Mac Gabhann F, Peirce SM. 2010. Collateral capillary arterialization following arteriolar ligation in murine skeletal muscle. Microcirculation 17:333–47.
Mac Gabhann F, Popel AS. 2007. Dimerization of VEGF receptors and implications for signal transduction: a computational study. Biophys Chem 128:125–39.
Galis ZS, Khatri JJ. 2002. Matrix metalloproteinases in vascular remodeling and atherogenesis: the good, the bad, and the ugly. Circ Res 90:251–62.
Garattini E, Mendel R, Romão MJ, Wright R, Terao M. 2003. Mammalian molybdo-flavoenzymes, an expanding family of proteins: structure, genetics, regulation, function and pathophysiology. Biochem J 372:15–32.
Gee E, Milkiewicz M, Haas TL. 2010. p38 MAPK activity is stimulated by vascular endothelial growth factor receptor 2 activation and is essential for shear stress-induced angiogenesis. J Cell Physiol 222:120–6.
Gerhardt H, Betsholtz C. 2003. Endothelial-pericyte interactions in angiogenesis. Cell Tissue Res 314:15–23.
Giustarini D, Dalle-Donne I, Milzani A, Fanti P, Rossi R. 2013. Analysis of GSH and GSSG after derivatization with N-ethylmaleimide. Nat Protoc 8:1660–9.
Good DJ, Polverini PJ, Rastinejad F, Le Beau MM, Lemons RS, Frazier WA, Bouck NP. 1990. A tumor suppressor-dependent inhibitor of angiogenesis is immunologically and functionally indistinguishable from a fragment of thrombospondin. Proc Natl Acad Sci U S A 87:6624–8.
Gorman JL, Liu STK, Slopack D, Shariati K, Hasanee A, Olenich S, Olfert IM, Haas TL. 2014. Angiotensin II evokes angiogenic signals within skeletal muscle through co-ordinated effects on skeletal myocytes and endothelial cells. PLoS One 9:e85537.
Greenaway J, Lawler J, Moorehead R, Bornstein P, Lamarre J, Petrik J. 2007. Thrombospondin-1 inhibits VEGF levels in the ovary directly by binding and internalization via the low density lipoprotein receptor-related protein-1 (LRP-1). J Cell Physiol 210:807–18.
Greene AS, Tonellato PJ, Lui J, Lombard JH, Cowley AW. 1989. Microvascular rarefaction and tissue vascular resistance in hypertension. Am J Physiol 256:H126–31.
Gustafsson T, Bodin K, Sylvén C, Gordon A, Tyni-Lenné R, Jansson E. 2001. Increased

expression of VEGF following exercise training in patients with heart failure. Eur J Clin Invest 31:362–6.
Gutterman DD, Chabowski DS, Kadlec AO, Durand MJ, Freed JK, Ait-Aissa K, Beyer AM. 2016. The Human Microcirculation. Circ Res 118:157–172.
Haas T. 2005. Endothelial cell regulation of matrix metalloproteinases. Can J Physiol Pharmacol 83:1–7.
Haas T, Davis SJ, Madri JA. 1998. Three-dimensional type I collagen lattices induce coordinate expression of matrix metalloproteinases MT1-MMP and MMP-2 in microvascular endothelial cells. J Biol Chem 273:3604–10.
Haas TL. 2002. Molecular control of capillary growth in skeletal muscle. Can J Appl Physiol 27:491–515.
Haas TL, Doyle JL, Distasi MR, Norton LE, Sheridan KM, Unthank JL. 2007. Involvement of MMPs in the outward remodeling of collateral mesenteric arteries. Am J Physiol Heart Circ Physiol 293:H2429–37.
Haas TL, Lloyd PG, Yang H, Terjung RL. 2012. Exercise Training and Peripheral Arterial Disease. 2:2933–3017.
Haas TL, Milkiewicz M, Davis SJ, Zhou AL, Egginton S, Brown MD, Madri JA, Hudlicka O. 2000. Matrix metalloproteinase activity is required for activity-induced angiogenesis in rat skeletal muscle. Am J Physiol Heart Circ Physiol 279:H1540–7.
Haber CA, Lam TKT, Yu Z, Gupta N, Goh T, Bogdanovic E, Giacca A, Fantus IG. 2003. N-acetylcysteine and taurine prevent hyperglycemia-induced insulin resistance in vivo: possible role of oxidative stress. Am J Physiol Endocrinol Metab 285:E744–53.
Han D, Williams E, Cadenas E. 2001. Mitochondrial respiratory chain-dependent generation of superoxide anion and its release into the intermembrane space. Biochem J 353:411–416.
Han X, Boyd PJ, Colgan S, Madri JA, Haas TL. 2003. Transcriptional up-regulation of endothelial cell matrix metalloproteinase-2 in response to extracellular cues involves GATA-2. J Biol Chem 278:47785–91.
Hanahan D. 1997. Cell biology: Signaling Vascular Morphogenesis and Maintenance. Science (80-) 277:48–50.
Hansen-Smith FM, Hudlicka O, Egginton S. 1996. In vivo angiogenesis in adult rat skeletal muscle: early changes in capillary network architecture and ultrastructure. Cell Tissue Res 286:123–36.
Hansen-Smith FM, Morris LW, Greene AS, Lombard JH. 1996. Rapid microvessel rarefaction with elevated salt intake and reduced renal mass hypertension in rats. Circ Res 79:324–30.
Hattori T, Murase T, Iwase E, Takahashi K, Ohtake M, Tsuboi K, Ohtake M, Miyachi M, Murohara T, Nagata K. 2013. Glucocorticoid-induced hypertension and cardiac injury: effects of mineralocorticoid and glucocorticoid receptor antagonism. Nagoya J Med Sci 75:81–92.
Haug C, Lenz C, Diaz F, Bachem M. 2004. Oxidized low-density lipoproteins stimulate extracellular matrix metalloproteinase Inducer (EMMPRIN) release by coronary smooth muscle cells. Arterioscler Thromb Vasc Biol 24:1823–1829.
Hawinkels LJAC, Zuidwijk K, Verspaget HW, de Jonge-Muller ESM, van Duijn W, Ferreira V, Fontijn RD, David G, Hommes DW, Lamers CBHW, Sier CFM. 2008.

VEGF release by MMP-9 mediated heparan sulphate cleavage induces colorectal cancer angiogenesis. Eur J Cancer 44:1904–13.
Heil M, Eitenmüller I, Schmitz-Rixen T, Schaper W. 2006. Arteriogenesis versus angiogenesis: similarities and differences. J Cell Mol Med 10:45–55.
Heilmann C. 2002. Collateral growth: cells arrive at the construction site. Cardiovasc Surg 10:570–578.
Helisch A, Schaper W. 2003. Arteriogenesis: the development and growth of collateral arteries. Microcirculation 10:83–97.
Hoeben A, Landuyt B, Highley MS, Wildiers H, Van Oosterom AT, De Bruijn EA. 2004. Vascular endothelial growth factor and angiogenesis. Pharmacol Rev 56:549–80.
Hoefer I. 2001. Time course of arteriogenesis following femoral artery occlusion in the rabbit. Cardiovasc Res 49:609–617.
Hogg PJ. 1994. Thrombospondin 1 as an enzyme inhibitor. Thromb Haemost 72:787–92.
Holmes DIR, Zachary I. 2005. The vascular endothelial growth factor (VEGF) family: angiogenic factors in health and disease. Genome Biol 6:209.
Houck KA, Leung DW, Rowland AM, Winer J, Ferrara N. 1992. Dual regulation of vascular endothelial growth factor bioavailability by genetic and proteolytic mechanisms. J Biol Chem 267:26031–7.
Houstis N, Rosen ED, Lander ES. 2006. Reactive oxygen species have a causal role in multiple forms of insulin resistance. Nature 440:944–8.
Huang PH, Chen YH, Wang CH, Chen JS, Tsai HY, Lin FY, Lo WY, Wu TC, Sata M, Chen JW, Lin SJ. 2009. Matrix metalloproteinase-9 is essential for ischemia-induced neovascularization by modulating bone marrow-derived endothelial progenitor Cells. Arterioscler Thromb Vasc Biol 29:1179–1184.
Hudlicka O, Brown MD. 2009. Adaptation of skeletal muscle microvasculature to increased or decreased blood flow: role of shear stress, nitric oxide and vascular endothelial growth factor. J Vasc Res 46:504–12.
Hudlicka O, Brown MD, Egginton S, Dawson JM. 1994. Effect of long-term electrical stimulation on vascular supply and fatigue in chronically ischemic muscles. J Appl Physiol 77:1317–24.
Hudlicka O, Brown MD, May S, Zakrzewicz A, Pries AR. 2006. Changes in capillary shear stress in skeletal muscles exposed to long-term activity: role of nitric oxide. Microcirculation 13:249–59.
Humar R, Zimmerli L, Battegay E. 2009. Angiogenesis and hypertension: an update. J Hum Hypertens 23:773–82.
Ichioka S, Shibata M, Kosaki K, Sato Y, Harii K, Kamiya A. 1998. In vivo measurement of morphometric and hemodynamic changes in the microcirculation during angiogenesis under chronic alpha1-adrenergic blocker treatment 1. Microvasc Res 55:165–174.
Ikonomidis JS, Hendrick JW, Parkhurst AM, Herron AR, Escobar PG, Dowdy KB, Stroud RE, Hapke E, Zile MR, Spinale FG. 2005. Accelerated LV remodeling after myocardial infarction in TIMP-1-deficient mice: effects of exogenous MMP inhibition. Am J Physiol Heart Circ Physiol 288:H149–H158.
Iruela-Arispe ML, Lombardo M, Krutzsch HC, Lawler J, Roberts DD. 1999. Inhibition of angiogenesis by thrombospondin-1 is mediated by 2 independent regions within the type 1 repeats. Circulation 100:1423–31.

Isenberg JS, Jia Y, Fukuyama J, Switzer CH, Wink DA, Roberts DD. 2007. Thrombospondin-1 inhibits nitric oxide signaling via CD36 by inhibiting myristic acid uptake. J Biol Chem 282:15404–15.
Ishida A, Murray J, Saito Y, Kanthou C, Benzakour O, Shibuya M, Wijelath ES. 2001. Expression of vascular endothelial growth factor receptors in smooth muscle cells. J Cell Physiol 188:359–68.
Ito WD, Arras M, Scholz D, Winkler B, Htun P, Schaper W. 1997. Angiogenesis but not collateral growth is associated with ischemia after femoral artery occlusion. Am J Physiol 273:H1255–65.
Iuchi T, Akaike M, Mitsui T, Ohshima Y, Shintani T, Azuma H, Matsumoto A. 2003. Glucocorticoid Excess Induces Superoxide Production in Vascular Endothelial Cells and Elicits Vascular Endothelial Dysfunction. Circ Res 92:81–87.
Ives CL, Eskin SG, McIntire L V. 1986. Mechanical effects on endothelial cell morphology: in vitro assessment. In Vitro Cell Dev Biol 22:500–7.
Jaillon P. 1980. Clinical pharmacokinetics of prazosin. Clin Pharmacokinet 5:365–76.
Ji JW, Tsoukias NM, Goldman D, Popel AS. 2006. A computational model of oxygen transport in skeletal muscle for sprouting and splitting modes of angiogenesis. J Theor Biol 241:94–108.
Jiménez B, Volpert O V, Crawford SE, Febbraio M, Silverstein RL, Bouck N. 2000. Signals leading to apoptosis-dependent inhibition of neovascularization by thrombospondin-1. Nat Med 6:41–8.
Jiménez B, Volpert O V, Reiher F, Chang L, Muñoz A, Karin M, Bouck N. 2001. c-Jun N-terminal kinase activation is required for the inhibition of neovascularization by thrombospondin-1. Oncogene 20:3443–8.
Jublanc C, Beaudeux JL, Aubart F, Raphael M, Chadarevian R, Chapman MJ, Bonnefont-Rousselot D, Bruckert E. 2011. Serum levels of adhesion molecules ICAM-1 and VCAM-1 and tissue inhibitor of metalloproteinases, TIMP-1, are elevated in patients with autoimmune thyroid disorders: relevance to vascular inflammation. Nutr Metab Cardiovasc Dis 21:817–22.
Jude EB, Eleftheriadou I, Tentolouris N. 2010. Peripheral arterial disease in diabetes--a review. Diabet Med 27:4–14.
Kadmiel M, Cidlowski JA. 2013. Glucocorticoid receptor signaling in health and disease. Trends Pharmacol Sci 34:518–30.
Kalebic T, Garbisa S, Glaser B, Liotta LA. 1983. Basement membrane collagen: degradation by migrating endothelial cells. Science 221:281–3.
Kallio PJ, Wilson WJ, O'Brien S, Makino Y, Poellinger L. 1999. Regulation of the hypoxia-inducible transcription factor 1alpha by the ubiquitin-proteasome pathway. J Biol Chem 274:6519–25.
Kand'ár R, Záková P, Lotková H, Kucera O, Cervinková Z. 2007. Determination of reduced and oxidized glutathione in biological samples using liquid chromatography with fluorimetric detection. J Pharm Biomed Anal 43:1382–7.
Kim H, Oda T, Lopez-Guisa J, Wing D, Edwards DR, Soloway PD, Eddy AA. 2001. TIMP-1 Deficiency Does Not Attenuate Interstitial Fibrosis in Obstructive Nephropathy. J Am Soc Nephrol 12:736–748.
Kim J, Montagnani M, Koh KK, Quon MJ. 2006. Reciprocal relationships between insulin resistance and endothelial dysfunction: molecular and pathophysiological

mechanisms. Circulation 113:1888–904.
Kim KH, Burkhart K, Chen P, Frevert CW, Randolph-Habecker J, Hackman RC, Soloway PD, Madtes DK. 2005. Tissue inhibitor of metalloproteinase-1 deficiency amplifies acute lung injury in bleomycin-exposed mice. Am J Respir Cell Mol Biol 33:271–279.
Kivelä R, Silvennoinen M, Touvra A-M, Lehti TM, Kainulainen H, Vihko V. 2006. Effects of experimental type 1 diabetes and exercise training on angiogenic gene expression and capillarization in skeletal muscle. FASEB J 20:1570–2.
Kobayashi N, DeLano FA, Schmid-Schönbein GW. 2005. Oxidative stress promotes endothelial cell apoptosis and loss of microvessels in the spontaneously hypertensive rats. Arterioscler Thromb Vasc Biol 25:2114–21.
Konttinen YT, Ainola M, Valleala H, Ma J, Ida H, Mandelin J, Kinne RW, Santavirta S, Sorsa T, López-Otín C, Takagi M. 1999. Analysis of 16 different matrix metalloproteinases (MMP-1 to MMP-20) in the synovial membrane: different profiles in trauma and rheumatoid arthritis. Ann Rheum Dis 58:691–7.
Korthuis RJ. 2011. Regulation of Vascular Tone in Skeletal Muscle. In *Skeletal muscle circulation*. Morgan & Claypool Life Sciences.
Krishna SM, Omer SM, Golledge J. 2016. Evaluation of the clinical relevance and limitations of current pre-clinical models of peripheral artery disease. Clin Sci (Lond) 130:127–50.
Kuchan MJ, Frangos JA. 1994. Role of calcium and calmodulin in flow-induced nitric oxide production in endothelial cells. Am J Physiol 266:C628–36.
Kuchan MJ, Jo H, Frangos JA. 1994. Role of G proteins in shear stress-mediated nitric oxide production by endothelial cells. Am J Physiol 267:C753–8.
Kusters YHAM, Barrett EJ. 2015. Muscle's microvasculature's structural and functional specializations facilitate muscle metabolism. Am J Physiol Endocrinol Metab 310:E379–380.
Kuzuya M, Iguchi A. 2003. Role of matrix metalloproteinases in vascular remodeling. J Atheroscler Thromb 10:275–82.
Lamalice L, Le Boeuf F, Huot J. 2007. Endothelial cell migration during angiogenesis. Circ Res 100:782–94.
Lambert E, Dassé E, Haye B, Petitfrère E. 2004. TIMPs as multifacial proteins. Crit Rev Oncol Hematol 49:187–98.
Lanahan AA, Hermans K, Claes F, Kerley-Hamilton JS, Zhuang ZW, Giordano FJ, Carmeliet P, Simons M. 2010. VEGF receptor 2 endocytic trafficking regulates arterial morphogenesis. Dev Cell 18:713–24.
Langille BL. 1996. Arterial remodeling : relation to hemodynamics. 841:834–841.
Lansang MC, Hustak LK. 2011. Glucocorticoid-induced diabetes and adrenal suppression: how to detect and manage them. Cleve Clin J Med 78:748–56.
Lawler JW, Slayter HS, Coligan JE. 1978. Isolation and characterization of a high molecular weight glycoprotein from human blood platelets. J Biol Chem 253:8609–16.
Lee S, Chen TT, Barber CL, Jordan MC, Murdock J, Desai S, Ferrara N, Nagy A, Roos KP, Iruela-Arispe ML. 2007. Autocrine VEGF signaling is required for vascular homeostasis. Cell 130:691–703.
Lee S, Jilani SM, Nikolova G V, Carpizo D, Iruela-Arispe ML. 2005. Processing of

VEGF-A by matrix metalloproteinases regulates bioavailability and vascular patterning in tumors. J Cell Biol 169:681–91.
Lenard A, Daetwyler S, Betz C, Ellertsdottir E, Belting H-G, Huisken J, Affolter M. 2015. Endothelial cell self-fusion during vascular pruning. PLoS Biol 13:e1002126.
Leren P. 1984. Effect of alpha- and beta-blocker therapy on blood lipids: European experience. Am J Med 76:67–71.
Lillioja S, Young AA, Culter CL, Ivy JL, Abbott WG, Zawadzki JK, Yki-Järvinen H, Christin L, Secomb TW, Bogardus C. 1987. Skeletal muscle capillary density and fiber type are possible determinants of in vivo insulin resistance in man. J Clin Invest 80:415–24.
Lindner V, Reidy MA. 1993. Expression of basic fibroblast growth factor and its receptor by smooth muscle cells and endothelium in injured rat arteries. An en face study. Circ Res 73:589–595.
Liu X-W, Taube ME, Jung K-K, Dong Z, Lee YJ, Roshy S, Sloane BF, Fridman R, Kim H-RC. 2005. Tissue inhibitor of metalloproteinase-1 protects human breast epithelial cells from extrinsic cell death: a potential oncogenic activity of tissue inhibitor of metalloproteinase-1. Cancer Res 65:898–906.
Lloyd PG, Prior BM, Li H, Yang HT, Terjung RL. 2005. VEGF receptor antagonism blocks arteriogenesis, but only partially inhibits angiogenesis, in skeletal muscle of exercise-trained rats. Am J Physiol Heart Circ Physiol 288:H759–68.
Logie JJ, Ali S, Marshall KM, Heck MMS, Walker BR, Hadoke PWF. 2010. Glucocorticoid-mediated inhibition of angiogenic changes in human endothelial cells is not caused by reductions in cell proliferation or migration. PLoS One 5:e14476.
Lotfi S, Patel AS, Mattock K, Egginton S, Smith A, Modarai B. 2013. Towards a more relevant hind limb model of muscle ischaemia. Atherosclerosis 227:1–8.
Lovell M, Harris K, Forbes T, Twillman G, Abramson B, Criqui MH, Schroeder P, Mohler ER, Hirsch AT. 2009. Peripheral arterial disease: lack of awareness in Canada. Can J Cardiol 25:39–45.
Malek MH, Olfert IM. 2009. Global deletion of thrombospondin-1 increases cardiac and skeletal muscle capillarity and exercise capacity in mice. Exp Physiol 94:749–60.
Mandel E, Dunford E, Trifonova A, Abdifarkoosh G, Tiech T, Riddell MC, Haas TL. 2016. Increase shear stress prevents the glucocorticoid-induced capillary rarefaction in rat skeletal muscle. Am J Physiol Regul Integr Comp Physiol Rev. In Review
Mandel E, Uchida C, Haas TL. 2013. Regulation of Proteases in Vascular Remodeling. In N. Dhalla & S. Chakraborti, eds. *Role of Proteases in Cellular Dysfunction*.
Manning BD, Cantley LC. 2007. AKT/PKB signaling: navigating downstream. Cell 129:1261–74.
Marchesi C, Ebrahimian T, Angulo O, Paradis P, Schiffrin EL. 2009. Endothelial Nitric Oxide Synthase Uncoupling and Perivascular Adipose Oxidative Stress and Inflammation Contribute to Vascular Dysfunction in a Rodent Model of Metabolic Syndrome. Hypertension 54:1384–1392.
Martin A, Komada MR, Sane DC. 2003. Abnormal angiogenesis in diabetes mellitus. Med Res Rev 23:117–45.
De Mey JGR, Schiffers PM, Hilgers RHP, Sanders MMW. 2005. Toward functional genomics of flow-induced outward remodeling of resistance arteries. Am J Physiol

Heart Circ Physiol 288:H1022–7.
Milkiewicz M, Brown MD, Egginton S, Hudlická O. 2001. Association between Shear Stress, Angiogenesis, and VEGF in Skeletal Muscles In Vivo. Microcirculation 8:229 – 241.
Milkiewicz M, Doyle JL, Fudalewski T, Ispanovic E, Aghasi M, Haas TL. 2007. HIF-1alpha and HIF-2alpha play a central role in stretch-induced but not shear-stress-induced angiogenesis in rat skeletal muscle. J Physiol 583:753–66.
Milkiewicz M, Hudlicka O, Shiner R, Egginton S, Brown MD. 2006. Vascular endothelial growth factor mRNA and protein do not change in parallel during non-inflammatory skeletal muscle ischaemia in rat. J Physiol 577:671–8.
Milkiewicz M, Kelland C, Colgan S, Haas TL. 2006. Nitric oxide and p38 MAP kinase mediate shear stress-dependent inhibition of MMP-2 production in microvascular endothelial cells. J Cell Physiol 208:229–37.
Milkiewicz M, Roudier E, Doyle JL, Trifonova A, Birot O, Haas TL. 2011. Identification of a Mechanism Underlying Regulation of the Anti-Angiogenic Forkhead Transcription Factor FoxO1 in Cultured Endothelial Cells and Ischemic Muscle. Am J Pathol 178:935–944.
Milkiewicz M, Uchida C, Gee E, Fudalewski T, Haas TL. 2008. Shear stress-induced Ets-1 modulates protease inhibitor expression in microvascular endothelial cells. J Cell Physiol 217:502–10.
Mondo CK, Yang W-S, Su J-Z, Huang T-G. 2009. Atorvastatin Prevented and Reversed Dexamethasone-Induced Hypertension in the Rat. Clin Exp Hypertens 28:499–509.
Montesano R, Pepper MS, Möhle-Steinlein U, Risau W, Wagner EF, Orci L. 1990. Increased proteolytic activity is responsible for the aberrant morphogenetic behavior of endothelial cells expressing the middle T oncogene. Cell 62:435–45.
Montezano AC, Touyz RM. 2014. Reactive oxygen species, vascular Noxs, and hypertension: focus on translational and clinical research. Antioxid Redox Signal 20:164–82.
Mosher DF. 1990. Physiology of thrombospondin. Annu Rev Med 41:85–97.
Mulvany MJ, Aalkjaer C. 1990. Structure and function of small arteries. Physiol Rev 70:921–61.
Murohara T, Asahara T, Silver M, Bauters C, Masuda H, Kalka C, Kearney M, Chen D, Symes JF, Fishman MC, Huang PL, Isner JM. 1998. Nitric oxide synthase modulates angiogenesis in response to tissue ischemia. J Clin Invest 101:2567–78.
Murphy-Ullrich JE, Höök M. 1989. Thrombospondin modulates focal adhesions in endothelial cells. J Cell Biol 109:1309–19.
Muzaffar S, Shukla N, Angelini G, Jeremy JY. 2004. Nitroaspirins and morpholinosydnonimine but not aspirin inhibit the formation of superoxide and the expression of gp91phox induced by endotoxin and cytokines in pig pulmonary artery vascular smooth muscle cells and endothelial cells. Circulation 110:1140–7.
Muzaffar S, Shukla N, Angelini GD, Jeremy JY. 2005. Prednisolone augments superoxide formation in porcine pulmonary artery endothelial cells through differential effects on the expression of nitric oxide synthase and NADPH oxidase. Br J Pharmacol 145:688–97.
Nascimento AR, Machado M, de Jesus N, Gomes F, Lessa MA, Bonomo IT, Tibiriçá E. 2013. Structural and functional microvascular alterations in a rat model of metabolic

syndrome induced by a high-fat diet. Obesity (Silver Spring) 21:2046–2054.
Nauli SM, Kawanabe Y, Kaminski JJ, Pearce WJ, Ingber DE, Zhou J. 2008. Endothelial cilia are fluid shear sensors that regulate calcium signaling and nitric oxide production through polycystin-1. Circulation 117:1161–71.
Nauseef WM. 2008. Biological roles for the NOX family NADPH oxidases. J Biol Chem 283:16961–5.
Neufeld G, Cohen T, Gengrinovitch S, Poltorak Z. 1999. Vascular endothelial growth factor (VEGF) and its receptors. FASEB J 13:9–22.
Noon JP, Walker BR, Webb DJ, Shore AC, Holton DW, Edwards H V, Watt GC. 1997. Impaired microvascular dilatation and capillary rarefaction in young adults with a predisposition to high blood pressure. J Clin Invest 99:1873–9.
Nör JE, Mitra RS, Sutorik MM, Mooney DJ, Castle VP, Polverini PJ. 2000. Thrombospondin-1 induces endothelial cell apoptosis and inhibits angiogenesis by activating the caspase death pathway. J Vasc Res 37:209–18.
Oakley RH, Cidlowski JA. 2011. Cellular processing of the glucocorticoid receptor gene and protein: new mechanisms for generating tissue-specific actions of glucocorticoids. J Biol Chem 286:3177–84.
Oganesian A, Armstrong LC, Migliorini MM, Strickland DK, Bornstein P. 2008. Thrombospondins use the VLDL receptor and a nonapoptotic pathway to inhibit cell division in microvascular endothelial cells. Mol Biol Cell 19:563–71.
Olfert IM. 2015. Physiological capillary regression is not dependent on reducing VEGF expression. Microcirculation 23:146–156.
Olfert IM, Birot O. 2011. Importance of anti-angiogenic factors in the regulation of skeletal muscle angiogenesis. Microcirculation 18:316–30.
Olfert IM, Howlett RA, Wagner PD, Breen EC. 2010. Myocyte vascular endothelial growth factor is required for exercise-induced skeletal muscle angiogenesis. Am J Physiol Regul Integr Comp Physiol 299:R1059–67.
Olsson A-K, Dimberg A, Kreuger J, Claesson-Welsh L. 2006. VEGF receptor signalling - in control of vascular function. Nat Rev Mol Cell Biol 7:359–71.
Ortega N, Hutchings H, Plouët J. 1999. Signal relays in the VEGF system. Front Biosci 4:D141–52.
Orzechowski A, Ostaszewski P, Brodnicka A, Wilczak J, Jank M, Balasińska B, Grzelkowska K, Ploszaj T, Olczak J, Mrówczyńska A. 2000. Excess of glucocorticoids impairs whole-body antioxidant status in young rats. relation to the effect of dexamethasone in soleus muscle and spleen. Horm Metab Res 32:174–80.
Osawa M, Masuda M, Kusano K, Fujiwara K. 2002. Evidence for a role of platelet endothelial cell adhesion molecule-1 in endothelial cell mechanosignal transduction: is it a mechanoresponsive molecule? J Cell Biol 158:773–85.
Ovcharenko I, Nobrega MA, Loots GG, Stubbs L. 2004. ECR Browser: a tool for visualizing and accessing data from comparisons of multiple vertebrate genomes, nucleic acide research. Nucleic Acids Res 32:W208–W286.
Papapetropoulos A. 2000. Angiopoietin-1 Inhibits Endothelial Cell Apoptosis via the Akt/Survivin Pathway. J Biol Chem 275:9102–9105.
Papapetropoulos A, García-Cardeña G, Madri JA, Sessa WC. 1997. Nitric oxide production contributes to the angiogenic properties of vascular endothelial growth factor in human endothelial cells. J Clin Invest 100:3131–9.

Paulson OB, Waldemar G, Schmidt JF, Strandgaard S. 1989. Cerebral circulation under normal and pathologic conditions. Am J Cardiol 63:C2–C5.
Pepper MS. 1997. Manipulating angiogenesis. From basic science to the bedside. Arterioscler Thromb Vasc Biol 17:605–19.
Pepper MS. 2001. Role of the matrix metalloproteinase and plasminogen activator-plasmin systems in angiogenesis. Arterioscler Thromb Vasc Biol 21:1104–17.
Pepper MS, Belin D, Montesano R, Orci L, Vassalli JD. 1990. Transforming growth factor-beta 1 modulates basic fibroblast growth factor-induced proteolytic and angiogenic properties of endothelial cells in vitro. J Cell Biol 111:743–55.
Piascik MT, Kusiak JW, Barron KW. 1990. α1-Adrenoceptor subtypes and the regulation of peripheral hemodynamics in the conscious rat. Eur J Pharmacol 186:273–278.
Pipp F. 2004. Elevated Fluid Shear Stress Enhances Postocclusive Collateral Artery Growth and Gene Expression in the Pig Hind Limb. Arterioscler Thromb Vasc Biol 24:1664–1668.
Pipp F, Heil M, Issbrücker K, Ziegelhoeffer T, Martin S, van den Heuvel J, Weich H, Fernandez B, Golomb G, Carmeliet P, Schaper W, Clauss M. 2003. VEGFR-1-selective VEGF homologue PlGF is arteriogenic: evidence for a monocyte-mediated mechanism. Circ Res 92:378–85.
Pollare T, Litgell H, Selinus I, Berne C. 1988. Application of prazosin is associated with an increase of insulin sensitivity in obese patients with hypertension. Diabetologia 31:415–420.
Potter RF, Groom AC. 1983. Capillary diameter and geometry in cardiac and skeletal muscle studied by means of corrosion casts. Microvasc Res 25:68–84.
Pourageaud F, De Mey JG. 1997. Structural properties of rat mesenteric small arteries after 4-wk exposure to elevated or reduced blood flow. Am J Physiol 273:H1699–706.
Powell RJ, Cronenwett JL, Fillinger MF, Wagner RJ, Sampson LN. 1996. Endothelial cell modulation of smooth muscle cell morphology and organizational growth pattern. Ann Vasc Surg 10:4–10.
Powell RJ, Hydowski J, Frank O, Bhargava J, Sumpio BE. 1997. Endothelial cell effect on smooth muscle cell collagen synthesis. J Surg Res 69:113–8.
Primo L, Ferrandi C, Roca C, Marchiò S, di Blasio L, Alessio M, Bussolino F. 2005. Identification of CD36 molecular features required for its in vitro angiostatic activity. FASEB J 19:1713–5.
de Quervain DJ-F, Henke K, Aerni A, Treyer V, McGaugh JL, Berthold T, Nitsch RM, Buck A, Roozendaal B, Hock C. 2003. Glucocorticoid-induced impairment of declarative memory retrieval is associated with reduced blood flow in the medial temporal lobe. Eur J Neurosci 17:1296–302.
Quinn TP, Peters KG, De Vries C, Ferrara N, Williams LT. 1993. Fetal liver kinase 1 is a receptor for vascular endothelial growth factor and is selectively expressed in vascular endothelium. Proc Natl Acad Sci U S A 90:7533–7.
van Raalte DH, Diamant M, Ouwens DM, Ijzerman RG, Linssen MML, Guigas B, Eringa EC, Serné EH. 2013. Glucocorticoid treatment impairs microvascular function in healthy men in association with its adverse effects on glucose metabolism and blood pressure: a randomised controlled trial. Diabetologia 56:2383–91.

Raisis AL. 2005. Skeletal muscle blood flow in anaesthetized horses. Part I: measurement techniques. Vet Anaesth Analg 32:324–30.
Ribatti D, Nico B, Crivellato E. 2011. The role of pericytes in angiogenesis. Int J Dev Biol 55:261–8.
Ries C. 2014. Cytokine functions of TIMP-1. Cell Mol Life Sci 71:659–72.
Risau W, Flamme I. 1995. Vasculogenesis. Annu Rev Cell Dev Biol 11:73–91.
Rivilis I, Milkiewicz M, Boyd P, Goldstein J, Brown MD, Egginton S, Hansen FM, Hudlicka O, Haas TL. 2002. Differential involvement of MMP-2 and VEGF during muscle stretch- versus shear stress-induced angiogenesis. Am J Physiol Heart Circ Physiol 283:H1430–8.
Rizzo V, Morton C, DePaola N, Schnitzer JE, Davies PF. 2003. Recruitment of endothelial caveolae into mechanotransduction pathways by flow conditioning in vitro. Am J Physiol Heart Circ Physiol 285:H1720–9.
Roberts DD, Isenberg JS, Ridnour LA, Wink DA. 2007. Nitric oxide and its gatekeeper thrombospondin-1 in tumor angiogenesis. Clin Cancer Res 13:795–8.
Rogers KM, Bonar CA, Estrella JL, Yang S. 2002. Inhibitory effect of glucocorticoid on coronary artery endothelial function. Am J Physiol Heart Circ Physiol 283:H1922–8.
Roskoski R. 2012. ERK1/2 MAP kinases: structure, function, and regulation. Pharmacol Res 66:105–43.
Roudier E, Chapados N, Decary S, Gineste C, Le Bel C, Lavoie J-M, Bergeron R, Birot O. 2009. Angiomotin p80/p130 ratio: a new indicator of exercise-induced angiogenic activity in skeletal muscles from obese and non-obese rats? J Physiol 587:4105–19.
Roudier E, Gineste C, Wazna A, Dehghan K, Desplanches D, Birot O. 2010. Angio-adaptation in unloaded skeletal muscle: new insights into an early and muscle type-specific dynamic process. J Physiol 588:4579–91.
Roudier E, Milkiewicz M, Birot O, Slopack D, Montelius A, Gustafsson T, Paik J, DePinho R, Casale G, Pipinos I, Haas T. 2013. Endothelial Fox01 is an intrinsic regulator of thrombospondin-1 expression that restrains angiogenesis in ischemic muscle. Angiogenesis 16:759–772.
van Royen N, Hoefer I, Buschmann I, Heil M, Kostin S, Deindl E, Vogel S, Korff T, Augustin H, Bode C, Piek JJ, Schaper W. 2002. Exogenous application of transforming growth factor beta 1 stimulates arteriogenesis in the peripheral circulation. FASEB J 16:432–4.
Rudic RD, Shesely EG, Maeda N, Smithies O, Segal SS, Sessa WC. 1998. Direct evidence for the importance of endothelium-derived nitric oxide in vascular remodeling. J Clin Invest 101:731–6.
Ruef J, Moser M, Kübler W, Bode C. 2001. Induction of endothelin-1 expression by oxidative stress in vascular smooth muscle cells. Cardiovasc Pathol 10:311–5.
Sainz J, Wangensteen R, Rodríguez Gómez I, Moreno JM, Chamorro V, Osuna A, Bueno P, Vargas F. 2005. Antioxidant enzymes and effects of tempol on the development of hypertension induced by nitric oxide inhibition. Am J Hypertens 18:871–7.
Schakman O, Gilson H, Thissen JP. 2008. Mechanisms of glucocorticoid-induced myopathy. J Endocrinol 197:1–10.
Schaper W. 2009. Collateral circulation: past and present. Basic Res Cardiol 104:5–21.
Scheid MP, Woodgett JR. 2003. Unravelling the activation mechanisms of protein kinase

B/Akt. FEBS Lett 546:108–112.
Schnackenberg C, Welch WJ, Wilcox CS. 1998. Normalization of Blood Pressure and Renal Vascular Resistance in SHR With a Membrane-Permeable Superoxide Dismutase Mimetic : Role of Nitric Oxide. Hypertension 32:59–64.
Schnackenberg CG, Welch WJ, Wilcox CS. 1998. Normalization of blood pressure and renal vascular resistance in SHR with a membrane-permeable superoxide dismutase mimetic: role of nitric oxide. Hypertension 32:59–64.
Schnackenberg CG, Wilcox CS. 1999. Two-week administration of tempol attenuates both hypertension and renal excretion of 8-Iso prostaglandin f2alpha. Hypertension 33:424–8.
Scholz D, Ito W, Fleming I, Deindl E, Sauer A, Wiesnet M, Busse R, Schaper J, Schaper W. 2000. Ultrastructure and molecular histology of rabbit hind-limb collateral artery growth (arteriogenesis). Virchows Arch 436:257–70.
Scholz D, Ziegelhoeffer T, Helisch A, Wagner S, Friedrich C, Podzuweit T, Schaper W. 2002. Contribution of arteriogenesis and angiogenesis to postocclusive hindlimb perfusion in mice. J Mol Cell Cardiol 34:775–87.
Senger DR, Galli SJ, Dvorak AM, Perruzzi CA, Harvey VS, Dvorak HF. 1983. Tumor cells secrete a vascular permeability factor that promotes accumulation of ascites fluid. Science 219:983–985.
Sessa WC. 2004. eNOS at a glance. J Cell Sci 117:2427–9.
Sherwood L, Kell R. 2010. *HUman Physiology- from cells to systems* First Cana. A. WIlliams, ed., Toronto ON: Nelso Education.
Shikatani E, Trifonova A, Mandel E, Liu S, Roudier E, Krylova A, Szigiato A, Beaudry J, Riddell M, Haas. 2012. Inhibition of proliferation, migration and proteolysis contribute to corticosterone-mediated inhibition of angiogenesis. PLoS One 7:e46625.
Shireman PK, Quinones MP. 2005. Differential necrosis despite similar perfusion in mouse strains after ischemia. J Surg Res 129:242–50.
Shofuda K, Hasenstab D, Kenagy R, Shofuda T, Li Z, Lieber A, CLowes A. 2001. Membrane-type matrix metalloproteinase-1 and -3 activity in primate smooth muscle cells. FASEB 15:2010–2020.
Shpilberg Y, Beaudry JL, D'Souza A, Campbell JE, Peckett A, Riddell MC. 2012. A rodent model of rapid-onset diabetes induced by glucocorticoids and high-fat feeding. Dis Model Mech 5:671–80.
Shweiki D, Itin A, Soffer D, Keshet E. 1992. Vascular endothelial growth factor induced by hypoxia may mediate hypoxia-initiated angiogenesis. Nature 359:843–5.
Sidibé A, Mannic T, Arboleas M, Subileau M, Gulino-Debrac D, Bouillet L, Jan M, Vandhuick T, Le Loët X, Vittecoq O, Vilgrain I. 2012. Soluble VE-cadherin in rheumatoid arthritis patients correlates with disease activity: evidence for tumor necrosis factor α-induced VE-cadherin cleavage. Arthritis Rheum 64:77–87.
Silvennoinen M, Rinnankoski-Tuikka R, Vuento M, Hulmi JJ, Torvinen S, Lehti M, Kivelä R, Kainulainen H. 2013. High-fat feeding induces angiogenesis in skeletal muscle and activates angiogenic pathways in capillaries. Angiogenesis 16:297–307.
Simantov R, Silverstein RL. 2003. CD36: a critical anti-angiogenic receptor. Front Biosci 8:s874–82.
Siuda D, Tobias S, Rus A, Xia N, Förstermann U, Li H. 2014. Dexamethasone

upregulates Nox1 expression in vascular smooth muscle cells. Pharmacology 94:13–20.
Skalak TC. 2005. Angiogenesis and microvascular remodeling: a brief history and future roadmap. Microcirculation 12:47–58.
Skalak TC, Price RJ. 1996. The role of mechanical stresses in microvascular remodeling. Microcirculation 3:143–65.
Slopack D, Roudier E, Liu STK, Nwadozi E, Birot O, Haas TL. 2014. Forkhead BoxO transcription factors restrain exercise-induced angiogenesis. J Physiol 592:4069–82.
Small GR, Hadoke PWF, Sharif I, Dover AR, Armour D, Kenyon CJ, Gray GA, Walker BR. 2005. Preventing local regeneration of glucocorticoids by 11beta-hydroxysteroid dehydrogenase type 1 enhances angiogenesis. Proc Natl Acad Sci U S A 102:12165–70.
Snoek-van Beurden PAM, Von den Hoff JW. 2005. Zymographic techniques for the analysis of matrix metalloproteinases and their inhibitors. Biotechniques 38:73–83.
Staiculescu MC, Foote C, Meininger GA, Martinez-Lemus LA. 2014. The role of reactive oxygen species in microvascular remodeling. Int J Mol Sci 15:23792–835.
Stanfield C. 2011. The nervous system: autonomic and motor systems. In *Principles of human physiology*. San Francisco, CA, pp. 303–321.
Strandgaard S, Paulson OB. 1995. Cerebral blood flow in untreated and treated hypertension. Neth J Med 47:180–4.
Sullivan CJ, Hoying JB. 2002. Flow-dependent remodeling in the carotid artery of fibroblast growth factor-2 knockout mice. Arterioscler Thromb Vasc Biol 22:1100–5.
Sumagin R, Kuebel JM, Sarelius IH. 2011. Leukocyte rolling and adhesion both contribute to regulation of microvascular permeability to albumin via ligation of ICAM-1. Am J Physiol Cell Physiol 301:C804–C813.
Swistocki ALM, Hoffman BB, W SH, Chen I, GM R. 1989. Effect of Prazosin Treatment on Carbohydrate and Lipoprotein Metabolism in Patients with Hypertension. Am J Med 86:14–18.
Tang GL, Chang DS, Sarkar R, Wang R, Messina LM. 2005. The effect of gradual or acute arterial occlusion on skeletal muscle blood flow, arteriogenesis, and inflammation in rat hindlimb ischemia. J Vasc Surg 41:312–20.
Tarbell JM, Pahakis MY. 2006. Mechanotransduction and the glycocalyx. J Intern Med 259:339–50.
Taube ME, Liu X-W, Fridman R, Kim H-RC. 2006. TIMP-1 regulation of cell cycle in human breast epithelial cells via stabilization of p27(KIP1) protein. Oncogene 25:3041–8.
Terman BI, Dougher-Vermazen M, Carrion ME, Dimitrov D, Armellino DC, Gospodarowicz D, Böhlen P. 1992. Identification of the KDR tyrosine kinase as a receptor for vascular endothelial cell growth factor. Biochem Biophys Res Commun 187:1579–86.
Tetlow LC, Adlam DJ, Woolley DE. 2001. Matrix metalloproteinase and proinflammatory cytokine production by chondrocytes of human osteoarthritic cartilage: associations with degenerative changes. Arthritis Rheum 44:585–94.
Triantafyllou A, Anyfanti P, Pyrpasopoulou A, Triantafyllou G, Aslanidis S, Douma S. 2015. Capillary rarefaction as an index for the microvascular assessment of

hypertensive patients. Curr Hypertens Rep 17:33.
Troidl C, Jung G, Troidl K, Hoffmann J, Mollmann H, Nef H, Schaper W, Hamm CW, Schmitz-Rixen T. 2013. The Temporal and Spatial Distribution of Macrophage Subpopulations During Arteriogenesis. Curr Vasc Pharmacol 11:5–12.
Tronc F, Mallat Z, Lehoux S, Wassef M, Esposito B, Tedgui A. 2000. Role of Matrix Metalloproteinases in Blood Flow-Induced Arterial Enlargement : Interaction With NO. Arterioscler Thromb Vasc Biol 20:e120–e126.
Tronc F, Wassef M, Esposito B, Henrion D, Glagov S, Tedgui A. 1996. Role of NO in flow-induced remodeling of the rabbit common carotid artery. Arterioscler Thromb Vasc Biol 16:1256–62.
Tuttle JL, Nachreiner RD, Bhuller AS, Condict KW, Connors BA, Herring BP, Dalsing MC, Unthank JL. 2001. Shear level influences resistance artery remodeling: wall dimensions, cell density, and eNOS expression. Am J Physiol Hear Circ Physiol 281:H1380–1389.
Tzima E, Irani-Tehrani M, Kiosses WB, Dejana E, Schultz DA, Engelhardt B, Cao G, DeLisser H, Schwartz MA. 2005. A mechanosensory complex that mediates the endothelial cell response to fluid shear stress. Nature 437:426–31.
Uchida C, Gee E, Ispanovic E, Haas TL. 2008. JNK as a positive regulator of angiogenic potential in endothelial cells. Cell Biol Int 32:769–76.
Uchida C, Haas TL. 2014. Endothelial cell TIMP-1 is upregulated by shear stress via Sp-1 and the TGFβ1 signaling pathways. Biochem Cell Biol 92:77–83.
Uchida C, Nwadozi E, Hasanee A, Olenich S, Olfert IM, Haas TL. 2015. Muscle-derived vascular endothelial growth factor regulates microvascular remodelling in response to increased shear stress in mice. Acta Physiol 214:349–360.
Ueda A, Nagase S, Yokoyama H, Tada M, Noda H, Ohya H, Kamada H, Hirayama A, Koyama A. 2003. Importance of renal mitochondria in the reduction of TEMPOL, a nitroxide radical. Mol Cell Biochem 244:119–24.
Ullian M. 1999. The role of corticosteroids in the regulation of vascular tone. Cardiovasc Res 41:55–64.
Vempati P, Popel AS, Mac Gabhann F. 2014. Extracellular regulation of VEGF: isoforms, proteolysis, and vascular patterning. Cytokine Growth Factor Rev 25:1–19.
Vogt CJ, Schmid-Schobein GW. 2001. Microvascular Endothelial Cell Death and Rarefaction in the Glucocorticoid-Induced Hypertensive Rat. Microcirculation 8:129–139.
de Vries C, Escobedo JA, Ueno H, Houck K, Ferrara N, Williams LT. 1992. The fms-like tyrosine kinase, a receptor for vascular endothelial growth factor. Science 255:989–91.
Wagatsuma A. 2008. Effect of hindlimb unweighting on expression of hypoxia-inducible factor-1alpha vascular endothelial growth factor, angiopoietin, and their receptors in mouse skeletal muscle. Physiol Res 57:613–20.
Wang S, Park JK, Duh EJ. 2012. Novel targets against retinal angiogenesis in diabetic retinopathy. Curr Diab Rep 12:355–63.
Wang Y, Chang J, Li Y-C, Li Y-S, Shyy JY-J, Chien S. 2004. Shear stress and VEGF activate IKK via the Flk-1/Cbl/Akt signaling pathway. Am J Physiol Heart Circ Physiol 286:H685–92.

Wang Y, Miao H, Li S, Chen K-D, Li Y-S, Yuan S, Shyy JY-J, Chien S. 2002. Interplay between integrins and FLK-1 in shear stress-induced signaling. Am J Physiol Cell Physiol 283:C1540–7.
Watson T, Goon PKY, Lip GYH. 2008. Endothelial progenitor cells, endothelial dysfunction, inflammation, and oxidative stress in hypertension. Antioxid Redox Signal 10:1079–88.
Weinbaum S, Zhang X, Han Y, Vink H, Cowin SC. 2003. Mechanotransduction and flow across the endothelial glycocalyx. Proc Natl Acad Sci U S A 100:7988–95.
Weinstein RS, Wan C, Liu Q, Wang Y, Almeida M, O'Brien CA, Thostenson J, Roberson PK, Boskey AL, Clemens TL, Manolagas SC. 2010. Endogenous glucocorticoids decrease skeletal angiogenesis, vascularity, hydration, and strength in aged mice. Aging Cell 9:147–61.
Westvik TS, Fitzgerald TN, Muto A, Maloney SP, Pimiento JM, Fancher TT, Magri D, Westvik HH, Nishibe T, Velazquez OC, Dardik A. 2009. Limb ischemia after iliac ligation in aged mice stimulates angiogenesis without arteriogenesis. J Vasc Surg 49:464–73.
Whitworth JA, Mangos GJ, Kelly JJ. 2000. Cushing, Cortisol, and Cardiovascular Disease. Hypertension 36:912–916.
Wilcox CS, Pearlman A. 2008. Chemistry and antihypertensive effects of tempol and other nitroxides. Pharmacol Rev 60:418–69.
Williams JL, Cartland D, Hussain A, Egginton S. 2006. A differential role for nitric oxide in two forms of physiological angiogenesis in mouse. J Physiol 570:445–54.
Williams JL, Cartland D, Rudge JS, Egginton S. 2006b. VEGF trap abolishes shear stress- and overload-dependent angiogenesis in skeletal muscle. Microcirculation 13:499–509.
Williams JL, Weichert A, Zakrzewicz A, Da Silva-Azevedo L, Pries AR, Baum O, Egginton S. 2006. Differential gene and protein expression in abluminal sprouting and intraluminal splitting forms of angiogenesis. Clin Sci 110:587–95.
Wu L-W. 2000. VRAP Is an Adaptor Protein That Binds KDR, a Receptor for Vascular Endothelial Cell Growth Factor. J Biol Chem 275:6059–6062.
Yang S, Zhang L. 2004. Glucocorticoids and vascular reactivity. Curr Vasc Pharmacol 2:1–12.
Yano K, Brown LF, Lawler J, Miyakawa T, Detmar M. 2003. Thrombospondin-1 plays a critical role in the induction of hair follicle involution and vascular regression during the catagen phase. J Invest Dermatol 120:14–9.
Yuen KCJ, Chong LE, Riddle MC. 2013. Influence of glucocorticoids and growth hormone on insulin sensitivity in humans. Diabet Med 30:651–63.
Zachary I. 2003. VEGF signalling: integration and multi-tasking in endothelial cell biology. Biochem Soc Trans 31:1171–1177.
Zhang DX, Gutterman DD. 2007. Mitochondrial reactive oxygen species-mediated signaling in endothelial cells. Am J Physiol Heart Circ Physiol 292:H2023–31.
Zhang X, Lawler J. 2007. Thrombospondin-based antiangiogenic therapy. Microvasc Res 74:90–9.
Zhang Y, Croft KD, Mori TA, Schyvens CG, McKenzie KUS, Whitworth JA. 2004. The antioxidant tempol prevents and partially reverses dexamethasone-induced hypertension in the rat. Am J Hypertens 17:260–5.

Zhang Y, Furumura M, Morita E. 2008. Distinct signaling pathways confer different vascular responses to VEGF 121 and VEGF 165. Growth Factors 26:125–31.
Zhou A, Egginton S, Hudlická O, Brown MD. 1998. Internal division of capillaries in rat skeletal muscle in response to chronic vasodilator treatment with alpha1-antagonist prazosin. Cell Tissue Res 293:293–303.
Zhu W, Smart EJ. 2005. Myristic acid stimulates endothelial nitric-oxide synthase in a CD36- and an AMP kinase-dependent manner. J Biol Chem 280:29543–50.
Zhuang ZW, Shi J, Rhodes JM, Tsapakos MJ, Simons M. 2011. Challenging the surgical rodent hindlimb ischemia model with the miniinterventional technique. J Vasc Interv Radiol 22:1437–46.
Ziada A, Hudlicka O, Tyler KR. 1989. The effect of long-term administration of alpha 1-blocker prazosin on capillary density in cardiac and skeletal muscle. Pflugers Arch 415:355–60.
Ziegler MA, Distasi MR, Bills RG, Miller SJ, Alloosh M, Murphy MP, George Akingba A, Sturek M, Dalsing MC, Unthank JL. 2010. Marvels, mysteries, and misconceptions of vascular compensation to peripheral artery occlusion. Microcirculation 17:3–20.

Appendix A:

The effect of high fat diet on CORT-induced microcirculatory phenotype

Introduction:

Glucocorticoids (GC) are steroid hormones known to be elevated in type-2 diabetes and Cushing's syndrome (Lansang and Hustak, 2011; Beaudry and Riddell, 2012). The addition of a high fat diet (HF) to rats treated with corticosterone (CORT) more accurately represents the human population with type 2 diabetes and/or metabolic syndrome (Shpilberg et al., 2012). Furthermore, the additional of a HF diet exacerbates the negative effects of GC excess alone (Shpilberg et al., 2012).

Augmented GC levels results in hypertension (Whitworth et al., 2000; Jude et al., 2010), microvascular rarefaction (Shikatani et al., 2012) and increased risk of developing peripheral artery disease (PAD) (Ziegler et al., 2010). PAD is the occlusion of a major conduit artery, typically those of lower extremity, which limits oxygen and nutrient supply to distal tissues. PAD is commonly studied via femoral or iliac artery ligation of small mammals (Lotfi et al., 2013; Krishna et al., 2016). Blood flow recovery depends on vascular remodeling, arteriogenesis and/or angiogenesis, within the affected limb (Lotfi et al., 2013). Asides from the known anti-hypertensive effects of prazosin (Desiniotis and Kyprianou, 2011), it can be used as a tool to study endothelial shear stress responsiveness.

The current study set out to assess the usefulness of the CORT-HF model as a model for PAD with concurrent diabetes. We wanted to determine if a) this model is viable for testing the influence of hind limb ischemia and b) to examine the effectiveness of prazosin in ameliorating the vascular complications seen within this model. It was

hypothesized that recovery from femoral artery (FA) ligation would be severely impaired and hypertension would develop in CORT-treated animals and this would be improved with concurrent prazosin treatment.

Material and Methods:

All animal experiments were approved by York University Animal Care Committee and conducted in accordance with the Canadian Council for Animal Care Guidelines.

Animal Protocol

Male Sprague Dawley rats (N=13; initial weight 200 to 250g) were purchased from Charles River Laboratories (Montreal, QC, Canada). For further description see methods section chapter 3.

In the current study all animals were fed a high fat rodent chow diet (5.1kcal/g food) *ad libitum*. Animals were implanted on day negative seven with either wax (control) or CORT pellets. 1 week post pellet implantation animals underwent unilateral FA ligation, the contralateral limb acting as the control (D0). Subsequently, rodents recovered in individual cages and were given ampicillin (20mg/kg body weight) or ampicillin and prazosin for the next 2 weeks; see Figure A.1 for full study design.

Femoral Artery Ligation and hind limb blood flow assessment

For further detail see methods section chapter 2.

Briefly, flow assessments were made prior to surgery (Pre), immediately post-surgery (D0) and on days 4, 7 and 14 (D4, D7, D14) post-surgery, via laser Doppler imager (PeriMed, Stockholm, Sweden). On day 14 post surgery, FA blood flow distal to the ligation site and collateral reintegration was assessed using needle laser Doppler probe (mooreVMS-LDF2 laser Doppler monitor, Moor Instruments, Delaware USA).

Blood Glucose Assessment

Blood glucose was assessed after on D0, 7 and 14 via hand held glucometer (Contour blood glucose meter, Bayer, Toronto, ON).

Blood Pressure Assessment

Systolic blood pressure was assessed on D0, 4, 7, and 14. See methods section chapter 4 for more information.

Tissue Isolation and Muscle Histology

See chapter 3 for complete details.

At the end point, hind-limb skeletal muscles were excised, weighed and subsequently snap frozen in liquid nitrogen cooled isopentane.

Statistical analysis

Results were expressed as mean $\pm$ SEM.

Results:

The current study started with 13 animals, with an n of 3 to 4 per group. However, due to poor wound healing post FA ligation, a subset of animals (n=5) needed to be euthanized early (on day 13 post pellet implantation). Therefore, there were not enough animals left to run statistical analysis.

Systemic effects of sustained elevations in CORT

There was a trend for a CORT mediated reduction in body weight and relative skeletal muscle mass of the TA and EDL, but not the slow twitch soleus (Table A.1). Additionally, there is a trend towards greater caloric consumption within the CORT- animals as compared to control animals. All of the above mentioned morphological

measurements were unaffected by prazosin co-treatment. Blood glucose was assessed after 2 weeks of concurrent prazosin treatment, and was shown to be lower in CORT-prazosin animals as compared to CORT-water group. The same trend was seen after one week of concurrent prazosin treatment (data not shown).

Glucocorticoid mediated capillary rarefaction was not abrogated by prazosin treatment

As expected CORT-treatment induced capillary rarefaction; however, there was no evidence of prevention due to prazosin administration. As well, within control animals, no angiogenesis was noted in response to prazosin treatment (Figure A.2A & B). Ligation did not appear to alter C:F within any group. C:F was significantly higher in control animals fed a HF diet compared to those on a standard chow diet (Figure A.2C & D).

Glucocorticoid mediated cardiovascular and microvascular complications

Systolic blood pressure was elevated with CORT-treatment (Figure A.3A). Prazosin lowered systolic blood pressure in CORT treated animals, while eliciting only a minor reduction in control animals (Figure A.3A).

FA ligation reduced relative hind-limb blood flow to approximately 45% compared to pre-ligation levels; furthermore, there were no discernable differences in flow recovery between groups (Figure A.3B). Needle Doppler assessments of FA flow showed a trend for increased flow in the control-prazosin group compared to water group. As well, femoral artery blood flow was lower with CORT-treatment, compared to control animals, regardless of prazosin being present (Figure A.3C).

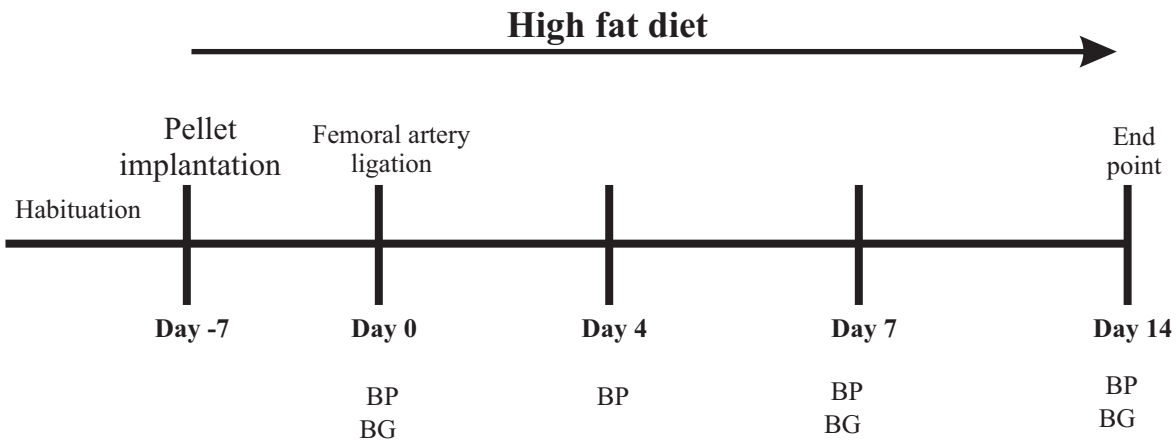

Figure A.1: Experimental protocol time-line

Animals were allowed to acclimate to their environment for 7 days prior to pellet implantation. From day -7 onwards animals were fed a high fat diet. On day 0 animals underwent unilateral femoral artery ligation. Blood glucose was assessed on D0, D7 and D14. As well, blood pressure was assessed on D0, D4, D7 and 14. Tissue was harvested on day14.

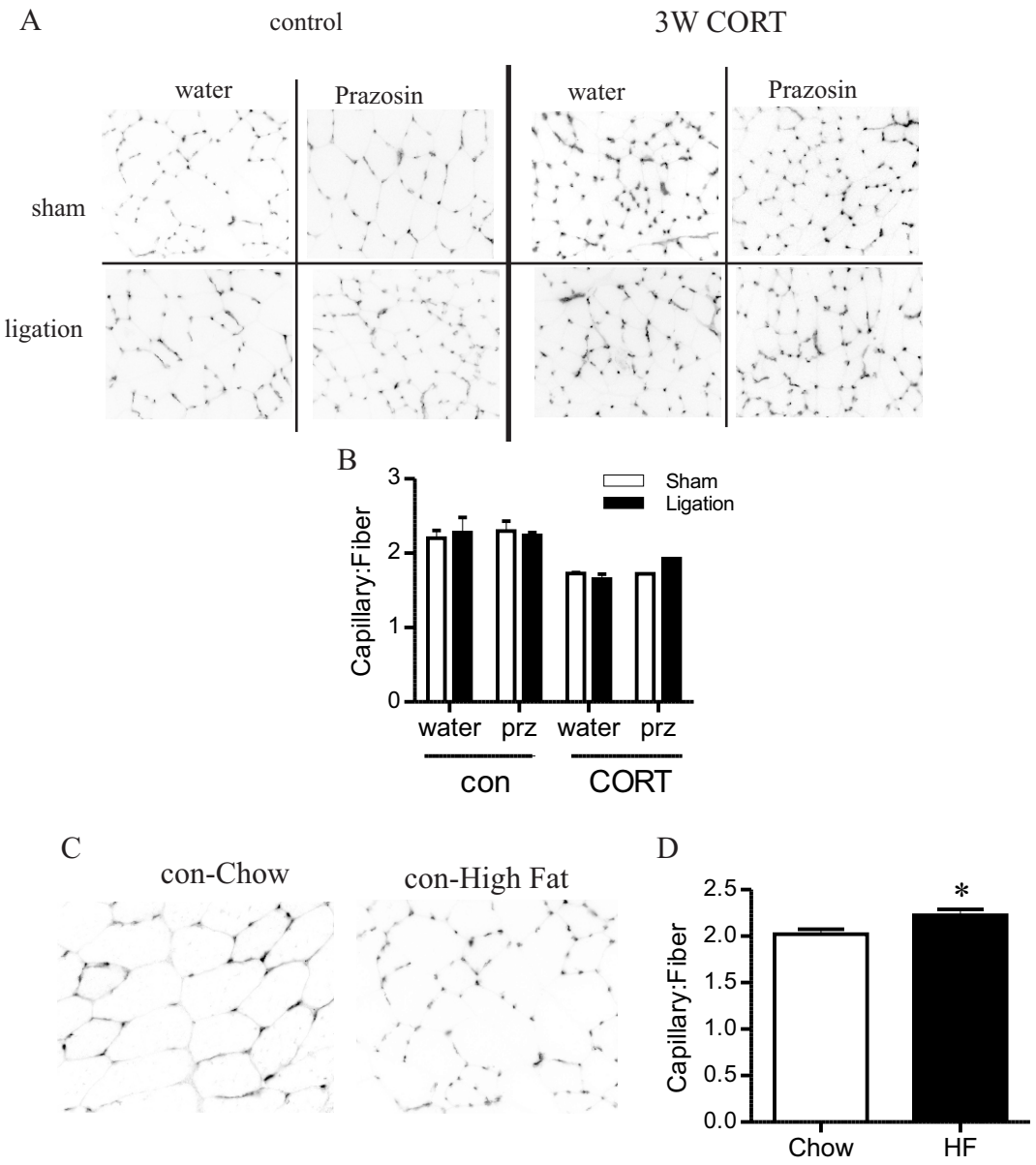

Figure A.2: Microvascular alterations due to CORT and/or high fat diet

The TA muscle was sectioned and stained for capillaries using *Griffonia Simplicifolia* isolectin-fluorescein and Cy3-anti–α smooth muscle actin. Images were captured from both control and ligated legs and inverted to grey scale images for improved visualization. A) Representative images 3-weeks (3W) post pellet implantation. B) There was a trend towards a reduction in C:F with CORT-treatment. No apparent benefits of concurrent prazosin-treatment was seen in control or CORT treated animals (n=1-3). C) Representative images after 2-weeks of a high-fat diet or standard chow diet in control animals D) Capillary-to-fiber ratio was analysed via unpaired t-test was used to analyse data, * $P<0.05$ compared to chow animals (n=11-14)

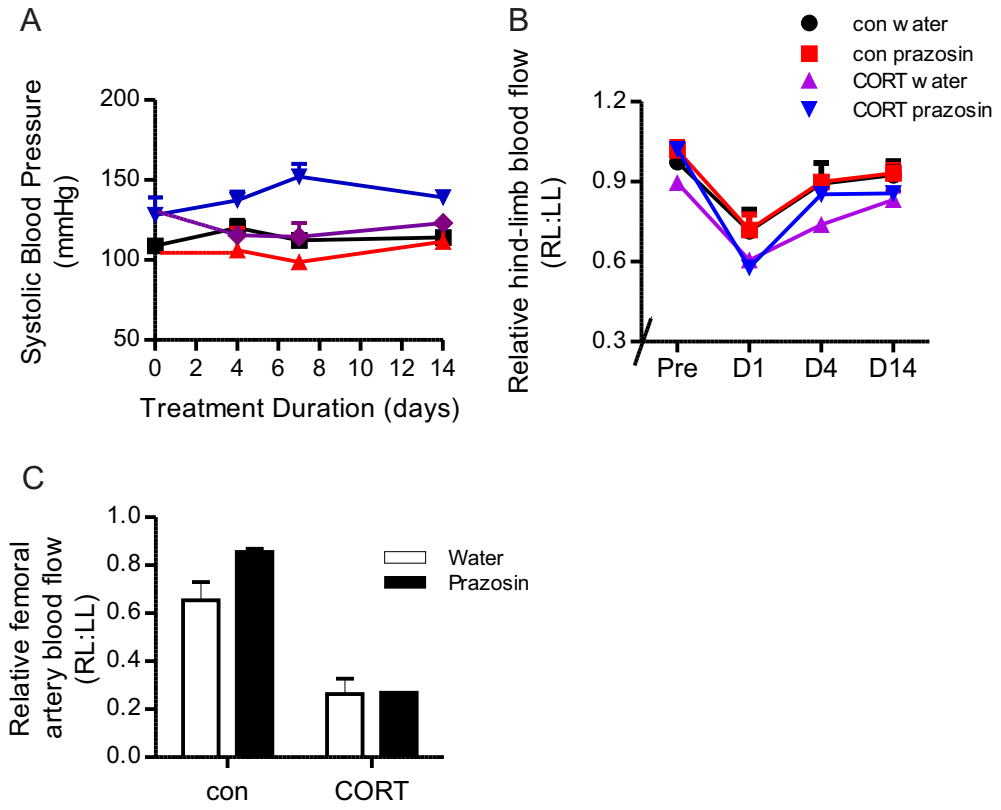

Figure A.3: CORT-induced alterations in blood pressure and ishcemia induced blood flow recovery

A) Blood pressure was measured via venous tail plethysmography at D0, 4, 7 and 14. There was trend towards an elevation in systolic blood pressure with CORT-treatment, which was prevented with concurrent prazosin treatment
B) Hind-limb blood flow was assessed via Laser Doppler, and quantified as the ratio of the ligated to the non-ligated leg. There is an approximate 45% reduction in hind-limb blood flow with femoral artery ligation; however, no other discernable differences in recovery between groups were noted. C) Needle probe Doppler assessment of femoral artery flow 14 days after ligation, expressed as the ratio of the ligated o non-ligated leg. Recovery appeared improved with prazosin treatment within control animals and impaired within CORT-HF animals as compared to control-water animals (n=1-3).

Table A.1: Animal characteristics after 3 weeks of CORT treatment with or without 2 weeks of prazosin co-treatment

	Control Water (n=2)	Control Prazosin (n=2)	CORT Water (n=3)	CORT Prazosin (n=1)
Body weight (g)	419.1	410±20.75	272.4±14.9	292.9
Blood Glucose (mmol/L)	6.1	5.6±0.5	21.6±1.3	5.9
TA relative weight (g/kg BW)	1.64	1.72±0.02	1.35±0.15	1.43
EDL relative weight (g/kg BW)	0.46	0.49±0.001	0.39 ±0.05	0.422
Soleus relative weight (g/kg BW)	0.43±0.005	0.44 ±0.01	0.47±0.007	0.551
Heart relative weight (G/kg BW)	1.28±0.17	1.13±0.1	0.90±0.05	0.90
Food consumption (kcal/g BW)	0.275±0.02	0.26±0.03	0.35±0.03	0.36
Average water consumption (ml/day)	40.88±15.5	34.04±11.1	58.2±13.1	40.56

Discussion:

The current study utilized the addition of hind-limb ischemia to the CORT-HF model to study intermittent claudication within the context of type-2 diabetes. However, the immunosuppressive effects of Cort resulted in poor wound healing making this an unsuitable model.

In line with results seen in chapter 3, CORT-HF treatment elicited skeletal muscle capillary rarefaction. However, this was not prevented with concurrent prazosin treatment. Unexpectedly, the current study noted no angiogenic effects of prazosin within control animals, which may be due to the concurrent consumption of a high-fat diet. Previous research has reported that a high fat diet will increase C:F (Silvennoinen et al., 2013), which is in line with findings from the current study. In the current study, control-chow animals (used in chapter 3) were pooled with current and previous control-HF animals; this data revealed that short term HF-diet significantly increased C:F. Therefore a basal increase in C:F, due to the HF-diet, may have prevented prazosin from exerting further angiogenic effects.

As expected (Mondo et al., 2009; Bachhav et al., 2011; Hattori et al., 2013), CORT-treatment elicited hypertension, which was prevented with concurrent prazosin treatment. Therefore the vasodilatory benefits of prazosin, while insufficient to prevent rarefaction could prevent CORT-induced hypertension. Direct assessment of FA flow, distal to the ligation site, revealed a possible benefit of prazosin treatment within control animals. Interestingly, FA flow was noticeably reduced within CORT-treated animals regardless of prazosin co-treatment, which is suggestive of impaired arteriogenesis. This is in line with a recent report that dexamethasone-treatment impaired arteriogenesis in a

mouse model of hind limb ischemia (Troidl et al., 2013). Unexpectedly the current study noted an apparent abolishment of CORT-mediated hyperglycemia with concurrent prazosin treatment, which was not seen previously in CORT-chow animals (Dunford et al., 2016). Therefore, care should be taken when drawing conclusions, as they may simply be sample issues or a result of being a fed assessment.

Although the current project proved nonviable it provided valuable information that aided in chapter 4's study design.

Appendix B:

Effect of basal versus elevated shear stress on endothelial cell shear responsiveness

Introduction:

The effects of alterations in shear stress, the frictional force exerted by blood as it flows past the vessel wall, is commonly investigated *in vitro* via parallel flow chamber. Endothelial cells are plated on a cover slip placed on the bottom of a rectangular channel with a uniform height along the length of the flow path. The flow of media is generated using a mechanical pump at the desired shear stress intensity (Ives et al., 1986; Chien, 2007). After exposing the endothelial cells to a shear stimulus for a set period of time the cells can be lysed and subsequently analyzed for changes in protein and/or mRNA expression.

An *in vitro* shear stress intensity of 15 dynes/cm^2 mimics the intensity seen *in vivo* due to prazosin administration (Milkiewicz et al., 2001). Traditionally, assessments of "elevated" shear stress are made relative to static control. However within a healthy capillary bed, basal shear stress is not 0 dynes/cm^2 but rather 5 dynes/cm^2 (Hudlicka et al., 2006). Therefore, the current study set out to examine differences in the expression of two key angiogenic factors, VEGF-A and MMP2, under static, 5 and 15 dynes/cm^2 of shear stress. It was hypothesized that comparing "elevated" to "normal" shear stress will provide the most accurate representation of alterations in endothelial cell shear responsiveness.

Materials & Methods:

Cell culture and shear stress stimulation

Skeletal muscle microvascular endothelial cells were isolated from extensor digitorum longus (EDL) muscle of male Sprague Dawley rats as described previously (Han et al., 2003). Shear stress experiments were conducted as previously described (Milkiewicz et al., 2006). Briefly, cells were subjected to 5 or 15 dynes/cm^2 shear stress for 24 hours using a parallel plate flow system (Bioptechs), or remained under static conditions, as described in Chapter 2 and 3.

RNA extraction and Real Time qPCR

RNA was isolated from endothelial cells using Cell-to-cDNA lysis buffer (Ambion, AM8723) as per the manufacturer's instructions. RNA was reverse transcribed using MMLV reverse transcriptase (New England Biolabs, Whitby ON Canada). cDNA were analyzed by Taqman qPCR using qPCR mastermix (#4444963; Invitrogen Canada) and Taqman probes for mouse VEGF (Mm00437306), MMP2 (Mm00439498) or GAPDH (Mm99999915).

Statistical Analysis

Results were expressed as mean ± SEM and analyzed by one-way ANOVA with subsequent Bonferroni post hoc tests where appropriate (Prism4; Graphpad software Inc; La Jolla, CA, USA). $P < 0.05$ was considered statistically significant.

Results:

5 dynes/cm^2 of shear stress did not significantly alter VEGF-A mRNA compared to static control. 15 dynes/cm^2 elicited a significant increase in VEGF-A mRNA compared to both static (*** P<0.001), and 5 dynes/cm^2 (## P<0.01) (Figure B.1A).

Both 5 and 15 dynes/cm^2 of shear stress significantly reduced MMP2 mRNA (*,** P<0.05 and 0.01 respectively) as compared to static controls. No significant differences in MMP2 mRNA expression between 5 and 15 dynes/cm^2 of shear stress were noted (Figure B.1B).

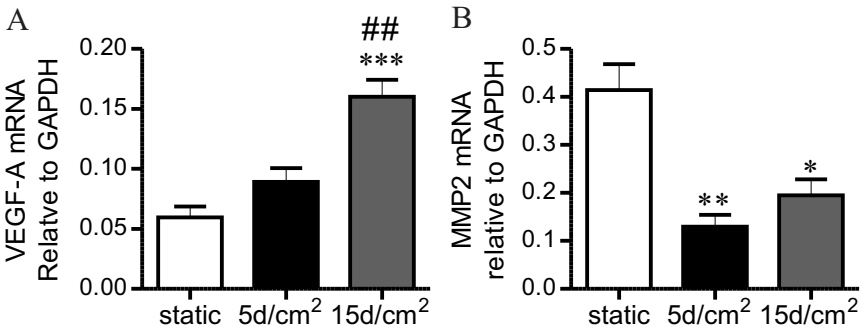

Figure B.1: Endothelial alterations to VEGF-A and MMP2 mRNA in response to elevated shear stress

RNA was extracted from rat skeletal muscle endothelial cells after exposure to elevated shear stress (5 or 15 dynes/cm^2) or remaining under static conditions for 24 hours. mRNA was quantified by Taqman qPCR and data was analyzed via one-way ANOVA (n=4-9). A) Comparison of VEGF-A mRNA under static, 5dynes/cm^2 and 15dynes/cm^2 of shear stress. *** $P<0.001$ compared to static controls, ## $P<0.01$ compared to 5dynes/cm^2. B) Comparison of MMP2 mRNA mRNA under static, 5dynes/cm^2 and 15dynes/cm^2 of shear stress, *, ** $P<0.05$ and 0.01 respectively relative to static controls.

Discussion:

The results from the current study demonstrate that comparing "elevated" (~15 dynes/cm^2) to "normal" (~5 dynes/cm^2) shear stress conditions *in vitro* may more closely mimic *in vivo* conditions. The alterations in VEGF-A mRNA to elevated shear stress was the same when comparing elevated shear stress to static or normal shear stress conditions. However, the expected reduction in MMP2 due to elevated shear stress (Rivilis et al., 2002) was abolished when comparing elevated shear stress or normal conditions. Thus comparing the 15 dynes/cm^2 to 5 dynes/cm^2 provides different information than comparing 15 dynes/cm^2 to static controls.

This study is merely preliminary work; however, these findings suggest that it may be ideal to compare alterations in shear stress to normal (5 dynes/cm^2) shear stress rather than static controls. Doing so will likely provide a more accurate *in vitro* model of how elevated shear stress is impacting endothelial production of pro or anti-angiogenic factors. More work is needed to evaluate this model in greater detail and analyze additional factors that are altered by elevated shear stress.

Appendix C
Summary of publications

Published:

Shikatani EA, Trifonova A, **Mandel ER**, Liu ST, Roudier E, Krylova A, Szigiato A, Beaudry J, Riddell MC, Haas TL. 2012. Inhibition of proliferation, migration and proteolysis contribute to corticosterone-mediated inhibition of angiogenesis. PLoS One 7:e46625.

Mandel ER, Uchida C, Haas TL. 2013. Regulation of Proteases in Vascular Remodeling. In *Role of Proteases in Cellular Dysfunction*. N. Dhalla & S. Chakraborti, eds.

Beaudry JL, Dunford EC, Leclair E, **Mandel ER**, Peckett AJ, Haas TL, Riddell MC. 2015. Voluntary exercise improves metabolic profile in high-fat fed glucocorticoid-treated rats. J Appl Physiol 118:1331–43.

In Review:

Mandel ER, Dunford EC, Trifonova A, Abdifarkoosh G, Tiech T, Riddell MC, Haas TL. 2016. Increase shear stress prevents the glucocorticoid-induced capillary rarefaction in rat skeletal muscle. Am J Physiol Regul Integr Comp Physiol. In Review.

Dunford EC, **Mandel ER**, Sepideh M, Haas TL, Riddell MC. 2016. The metabolic effects of prazosin on insulin resistance in glucocorticoid treated rats. Am J Physiol Regul Integr Comp Physiol. In Review.

Mandel ER, Uchida C, Nwadozi E, Haas TL. 2016. Tissue inhibitor of metalloproteinase 1 influences vascular adaptionals to chronic alterations in blood flow. J Cell Physiol. In Rewiew

Manuscripts in Prerpation:

Mandel ER, Dunford EC, Ghoncheh A, Turnbull PC, Perry CG, Riddell, MC, Haas TL. 2016. Role of reactive oxygen species in glucocorticoid induced hypertension and capillary rarefaction.

Dunford EC, LeClair E, Aiken J, **Mandel ER**, Birot O, Haas TL, Riddell MC. The effects of voluntary exercise and prazosin on skeletal muscle capillary rarefaction and metabolism in streptozotocin-induced diabetic rats.